# Stony Brook University

# Phospholipase $C\beta_1$ and Its Interactions With Members of the $G\alpha_q$ Signaling Pathway: *in vitro* and *in vivo* implications for a self-scaffolding model

A Dissertation Presented

by

**Louisa Marie Dowal**

to

The Graduate School

in Partial fulfillment of the

Requirements

for the Degree of

**Doctor of Philosophy**

**in**

**Physiology and Biophysics**

Stony Brook University

August 2007

Stony Brook University

The Graduate School

**Louisa Marie Dowal**

We, the dissertation committee for the above candidate

for the Doctor of Philosophy degree in Physiology and Biophysics,

Hereby recommend acceptance of this dissertation.

**Dissertation Advisor – Dr. Suzanne Scarlata**
Professor, Physiology and Biophysics

**Chairperson of Defense – Dr. Peter Brink**
Professor, Physiology and Biophysics

**Dr. James Konopka**
Professor, Molecular Genetics and Microbiology

**Dr. Richard Lin**
Associate Professor, Medicine and Physiology and Biophysics

**Dr. Mario Rebecchi**
Associate Professor, Research - Anesthesiology

**Dr. Catherine Berlot**
Geisinger Institute – Staff Scientist

This dissertation is accepted by the Graduate School.

Lawrence Martin
**Dean of the Graduate School**

Abstract of the Dissertation

# Phospholipase $C\beta_1$ and Its Interactions With Members of the $G\alpha_q$ Signaling Pathway: *in vitro* and *in vivo* implications for a self-scaffolding model

By

**Louisa Marie Dowal**

**Doctor of Philosophy Degree**

**in**

**Physiology and Biophysics**

Stony Brook University

2007

Signaling through G protein coupled receptors, coupled to $G\alpha_q$, occurs through a classical, well-known pathway. Activation of the receptor promotes the exchange of GTP for GDP on the $G\alpha_q$ subunit, which in the basal state, is bound to $G\beta\gamma$ subunit. GTP bound $G\alpha_q$ has a weaker affinity for $G\beta\gamma$ and they then separately activate their effectors. The main effector of $G\alpha_q$ is Phospholipase $C\beta_1$ ($PLC\beta_1$). $PLC\beta_1$ hydrolyzes phosphatidylinositol(4,5)-bisphosphate into two important second messengers, which leads to the activation of Protein Kinase C and an increase in intracellular calcium. Cessation of the signal occurs when GTP is hydrolyzed back to GDP on the $G\alpha_q$ subunit via GTPase accelerating proteins (GAPs) promoting reassociation with $G\beta\gamma$. Current dogma states that upon $G\alpha_q$ activation, $PLC\beta_1$ will have greater affinity for the G protein and this greater affinity will promote association. Using purified proteins reconstituted on model membranes, we measured the binding affinities between $G\alpha_q$, $G\beta\gamma$, $PLC\beta_1$, and

Regulator of G protein Signaling 4 (RGS4). Our *in vitro* results suggest that weakly associating, ternary complexes can form between these proteins. RGS4 is also a GAP for $G\alpha_q$, and the ability of these proteins to self-scaffold would promote rapid signaling. Using GFP fusion proteins and an *in vivo* Fluorescence Resonance Energy Transfer technique, we next asked whether we could observe these complexes in living cells. We find, surprisingly, $PLC\beta_1$ and $G\alpha_q$ are preassociated in living cells in the basal state. In addition, we find that the nature of this association is unchanged upon stimulation and is not dependent upon the activation state of $G\alpha_q$. Taken together, our data leads to a model in which activation does not depend on diffusion and association; rather activation of effectors takes place by changes in intramolecular interactions between proteins and thus places limitations on the speed of the signal to generation and diffusion of second messengers. Preassociated complexes between $G\alpha_q$ and $PLC\beta_1$ would provide spatial localization of the signal and direct the signal along a specific pathway.

This work is dedicated to my loving husband, Robb
and our soon to be born baby, Madeline.

# Table of Contents

# List of Figures and Tables

# Acknowledgements

Over the past seven years, I have been extremely fortunate to be under the direction and guidance of my thesis advisor, Dr. Suzanne Scarlata. Her constant support and advice has been invaluable, and without her encouragement, I would have never become a graduate student or thought that I was capable of working toward a PhD. And, even though there have been times when I doubted myself and aspects of my project, there has never been any doubt in my mind about my decision to work with Suzanne. As a scientist and a mother, she has provided an excellent role model – a model that I hope I will be able to follow and maintain throughout my own career. When I first came to Suzanne's lab as her technician, I had just completed my undergraduate degree and didn't know anything – not even how to make a buffer. I could pipet, and that was about it. I never understood why she decided to hire me. I was very lucky that she did. Thank you so much for everything you have done for me and giving me a chance to be part of your lab group.

I am also indebted to my committee whose understanding and patience I have greatly appreciated. I have had many great conversations with Dr. Peter Brink, and his advice about my project and my life outside of my project has been very helpful. I always knew that I could go to him with any problems and talk to him about anything that was troubling me. Dr. Mario Rebecchi has been a constant source of support and guidance throughout my time at Stony Brook. He has always taken the time to help me with the technical aspects of my experiments, and he was the first person to show me

how to use an epifluorescence microscope. Mario has been very generous with his time and with his reagents. I had the opportunity to do a rotation in the laboratory of Dr. James Konopka and enjoyed my time in his lab very much. I was very happy when Jamie agreed to be on my committee as my project has benefited from his insight and advice during my committee meetings. Dr. Richard Lin has also been very helpful. After my thesis proposal, he encouraged me to think in more global terms about my project and where I fit in the literature, which is something I have since always tried to keep in mind. And, finally, I am very, very grateful for my outside reader, Dr. Catherine Berlot. Not only did she provide the constructs I need for my experiments, but she also let Suzanne and I run some experiments in her lab which helped shape the direction and focus of this work. I am very fortunate that she agreed to read my thesis and am in her debt. For some reason, I was very nervous to tell my committee when I became pregnant, and I soon came to realize that my nervousness was completely unfounded as they all have been extremely supportive. Thank you for your advice and guidance over the past few years.

I am also very thankful for the guidance and friendship of Dr. Raafat El-Maghrabi. When I was looking for someone to do my first rotation with, I asked Raafat, and he said that he didn't know if he had anything to teach me. From Raafat, I have learned so much and continued to seek his advice long after my rotation was over. Over the years, I have constantly bothered him with questions and have always gone to him for reassurance that I was thinking and going about things in the right way. Raafat has always, always made time for me and stopped whatever he was doing when I needed to talk to him. Raafat gave me a very special necklace that he brought back from Egypt – it

is a symbol that wards off the evil eye. I have worn it for almost every presentation and talk I have ever given – I know that it brings me a lot of luck.

There are also many other faculty and staff who have helped along the way. I am thankful for the encouragement and advice of Dr. Stuart McLaughlin, Dr. Irene Solomon, and Dr. Roger Johnson. Also, Mel has made sure that I have dotted all i's and crossed all t's. I appreciate her always taking care of everything and making sure and double checking that everything was alright.

Being part of Suzanne's group has enabled me to work with a wonderful group of people. Dr. John Elliot and Dr. Tieli Wang were very helpful when I first joined the lab. They taught me everything from making buffers to protein purification to using the fluorometer. I was also fortunate to be put on a couple of Tieli's papers which really inspired me. I am also very thankful for the friendship of Dr. Vijaya Narayanan. Viji and I would often have long talks, and even though she moved on from the lab many years ago, I still miss her terribly and have often wished she were here. Dr. Yuanjian Guo has also given me a lot of help and advice. Jean always knew everything, and I didn't realize how much I depended on her, until she left the lab, and I was constantly going downstairs to the 5$^{th}$ floor to ask her questions. Dr. Marjorie BonHomme is a great friend and a wonderful person. I love Marge and miss her. She is so much fun, and I always enjoyed sharing a bottle of wine with her. Without Dr. Paxton Provitera, this work would not have been possible. Basically, whenever you see a picture of a cell that has had any analysis done to it that was Paxton. He wrote the FRET program I needed to analyze my data, and without that program, I don't know what I would have done. He spent two years refining the program to my specifications and needs at the expense of his

own work. Paxton is also a very close friend and confidant and has always supported me and been there when I needed him. To say that I have missed him since he moved on from the lab would be a gross understatement. Paxton, thank you so much for everything you have done for me – I truly treasure our friendship. Dr. Finly Philip also became a close friend, and for awhile, it was just the two of us in lab which was really fun. When Finly left, I felt like I was abandoned – the only one left from the old Scarlata lab. And, I was. However, Jing Ting, Steve, Omoz, and Parijat and Urszula have been great and very helpful these last few months. Urszula has been a good friend since the start of my graduate work, and I am very grateful for her friendship. And, even though he isn't part of the Scarlata lab, Dwan Gerido has been a great friend and a good person to know.

My freshman year of college I was given a lab partner in Honors Lab for General Biology. Since then, Julianna LeMeiux has been a wonderful friend and a constant source of support. After that initial pairing, we were lab partners for every class and suffered endless hours of organic chemistry lab together and studied for every exam together. I can't imagine what college would have been like without Julie – how important she is to me still – how happy I am she is still my closest and most dear friend. Our lives always seem to be running parallel – graduate school, marriage, and motherhood. How lucky I am to experience life and share its changes with Julie.

My husband, Robb, is my best friend. When we first met, I never thought that someone as intelligent and handsome as Robb would ever want to be with me. I am so lucky to be able to share my life and my work with him. His interest in my project, his constant support and encouragement has given me the strength to finish and push on to the end. I know that we are going to have the most beautiful baby, and that he is going to

be a wonderful father. I cannot express in words how much I love you Robb. Thank you for helping me to believe that I could do anything that I wanted to. I'm so looking forward to starting this next chapter in our lives – welcoming baby Madeline Barbara into the world and our move back North.

And, finally, I must thank my wonderful family. My mom, my dad, my sisters, Kara and Sarah, Robb's parents, Jay and Sharon have given me so much love and support throughout my life and over the past years. Thank you so much for your encouragement and help. Even after all this time on Long Island, it never truly became our home, and I think in large part it was because all of you were still in New Hampshire. I love you all very much.

## Chapter 1: General Introduction

Signaling through a group of proteins known as Phospholipase C (PLC) mediates a very important response in the cell, a rise in cytoplasmic $Ca^{2+}$. $Ca^{2+}$ is a universal second messenger and is responsible for a variety of cellular outcomes via the activation of many different $Ca^{2+}$ dependent proteins. One important aspect of $Ca^{2+}$ signaling is that it is temporal. Examples of responses that are brought about by brief spikes of $Ca^{2+}$ or $Ca^{2+}$ waves are muscle fiber contraction, release of neurotransmitters, and the activation of transcription factors which regulate gene transcription for cell differentiation and proliferation (1). As such, the regulation of cytoplasmic $Ca^{2+}$ levels and its mobilization are tightly controlled.

Classically, the activation of PLC family members results in the hydrolysis of phosphatidylinositol(4,5)bisphosphate ($PI(4,5)P_2$). PLCs catalyze the cleavage of the head group of $PI(4,5)P_2$ generating the second messengers diacylglycerol (DAG), which is responsible for protein kinsase C (PKC) activation, and inositol triphosphate ($IP_3$) which diffuses through the cytoplasm to the endoplasmic reticulum where it binds to its receptor causing the release of $Ca^{2+}$ from intracellular stores (2).

An important pathway for mobilization of $Ca^{2+}$ centers on the activation of G protein coupled receptors (GPCR). This family of receptors is characterized by seven transmembrane domains, and is activated by numerous stimuli such as neurotransmitters, hormones, and sensory stimuli. They are coupled to certain members of the PLC family (most notably, PLCβ) via the action of G protein subunits, Gα and Gβγ. Recent research

has focused on the interplay between GPCRs, G proteins subunits, and their PLCβ effectors, and main questions in the field revolve around how external signals at the cell surface are transduced to internal signals inside the cell.

*The Phospholipase C family*

The Phospholipase C family (PLC) is currently made up of five family members (see figure 1.1) (3). There are also recent reports of a sixth family member, PLCη, which has a similar domain organization to the PLCβ family ((4) and (5)). PLCs have similar domain organization (see figure 1.1) even though their amino acid sequences are fairly nonconserved. Differences between family members are reflected in their regulation and cellular distribution.

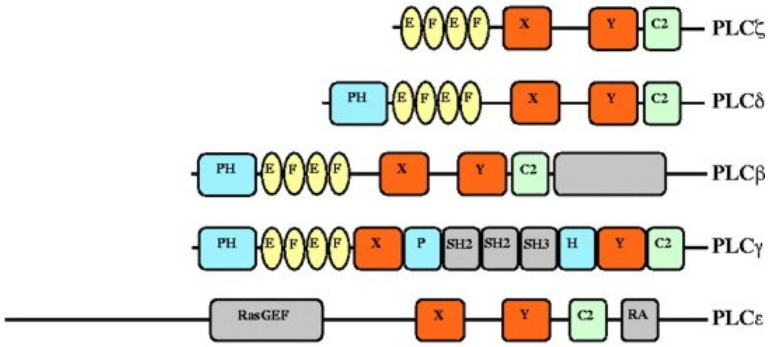


**Figure1.1**: Domain organization of PLC family members. Adapted from Saunders *et al.* (2002) (3).

With the exception of PLCζ and PLCε, the other PLC family members have pleckstrin homology (PH) domains at their N-termini. PH domains are found in hundreds of signaling proteins and some PH domains are known to bind to phosphoinositides and aid in membrane targeting (6). The elongation factor (EF hand) domain has been shown to bind Ca2+ in PLCδ (7) and is found in all family members except PLCε. The two

most different family members are PLCγ which has an additional PH domain which is spilt by two SH2 and one SH3 domain and PLCε which has a Ras guanine nucleotide exchange factor (RasGEF) and Ras binding (RA) domain. All PLCs possess an X and Y domain which is the region responsible for their catalytic activity. The catalytic region is 40-60% conserved among family members (8). In addition, all family members have a C2 domain which, for PLCδ, has been shown to bind $Ca^{2+}$ and lipids (9). Unlike the other family members, PLCβ has a C-terminal extension which is important for its regulation and cellular localization (see below) (for a comprehensive review see (2)).

As stated previously, differences in the domain organization of PLC family members results in differing mechanisms of regulation and activation. The most recently described family member, PLCη, may be downstream of GPCR signaling and may be regulated by Gβγ subunits (4). PLCζ is found only in sperm and its activity seems to be important in triggering the $Ca^{2+}$ oscillations required for egg activation (3). The activation and regulation of PLCδ is still relatively unknown, and which receptor(s) it is coupled too is also unclear; however, there are reports that it may be regulated by a member of the PLCβ family, $PLC\beta_2$ (10). The PLCβ family has been established to be regulated by the activation of GPCRs which is mediated by the G protein subunits Gα and Gβγ. PLCγ activation is established to occur via receptor and nonreceptor tyrosine kinases (2), and it is thought that PLCε activation occurs via Ras and $G\alpha_{12}$ and Gβγ subunits (11).

*The PLC substrate Phosphatidylinositol(4,5)-bisphosphate*

Phosphatidylinositol lipids (PI) are an important component of the inner leaflet of the plasma membrane. Its structure is a D-myo-inositol-1-phosphate ring linked to a 1-stearoyl, 2 arachidonoyl diacylglycerol moiety via its phosphate group. Phosphorylation of the inositol ring at one or more of the 3,4, or 5 positions give phosphorylated derivatives which play a variety of roles within the cell (12).

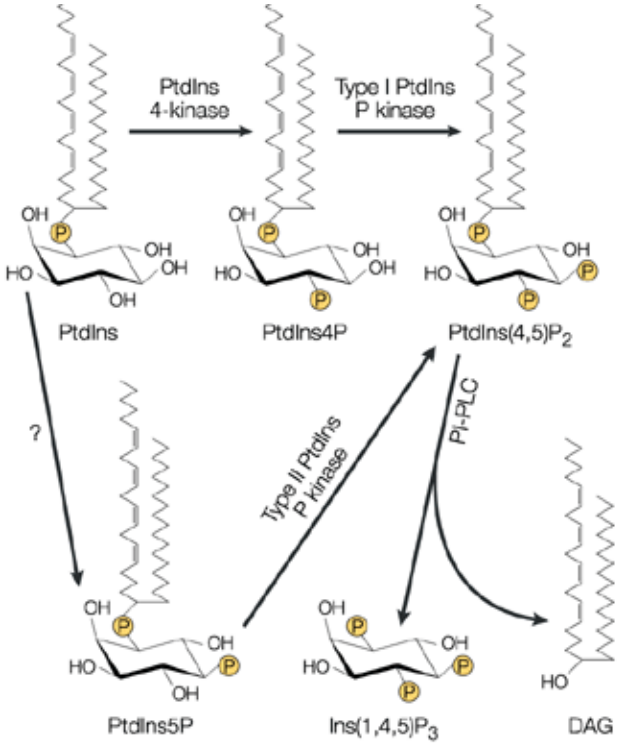


**Figure 1.2:** Phosphoinositide metabolism. Figure adapted from Robin F. Irvine *Nature Reviews Molecular Cell Biology*. (2003). 4: 349-361.

Phosphatidylinositol(4,5)-bisphosphate ($PI(4,5)P_2$) is the major phosphoinositide lipid in mammalian cells. It is involved in a variety of cellular processes such as endo- and exocytososis, membrane/cytoskeletal interactions, targeting of proteins to the plasma membrane, enzyme activation, regulation of ion channels, anchoring sites for scaffolding

proteins and cell signaling by directing a very important pathway through the generation of the second messengers, $IP_3$ and DAG, from its hydrolysis (13).

$PI(4,5)P_2$ is an ideal signaling molecule because its synthesis and breakdown are very rapid, and it appears to exist in discrete micro-domains (14). As such, $PI(4,5)P_2$ production is highly regulated and occurs via two routes (see figure 1.2). In the "classical PI cycle," $PI(4,5)P_2$ is generated by the action of Type I PIP kinases on PI(4)P. In the other pathway, Type II PIP kinases phosphorylate PI(5)P. Type I and Type II kinases have different localizations in the cell; Type I are found at the plasma membrane where they are thought to regulate actin rearrangement, secretion and endocytosis, and Type II are found in the cytosol, nucleus, endoplasmic reticulum, and also at actin-cytoskeleton junctions (15).

$PI(4,5)P_2$ is not distributed symmetrically within the plasma membrane and exists in what can be thought of as "pools." This uneven distribution gives way to spatial localization of signaling events as do rapid changes in its concentration at the plasma membrane (for a short review see (16)). For example, $PI(4,5)P_2$ has been found concentrated in membrane ruffles and sites of active membrane rearrangement (14). It follows that there would be mechanisms in place to allow the cell to rapidly turn over its "pools" of $PI(4,5)P_2$ upon stimulation. Changes in $PI(4,5)P_2$ concentration would be dependent on the enzymatic activity of PLC versus that of the lateral diffusion of the lipid. Indeed, in a study by Varnai *et al*, they found that upon stimulation, the localization of the PH domain of PLCδ fused to GFP would change – moving from the plasma membrane to the cytosol. This movement correlated with a decease in the $PI(4,5)P_2$ levels and could be reversed with $Ca^{2+}$chelation. In this study, the authors also

discussed previous reports of the heterogeneity of $PI(4,5)P_2$ pools – these pools are synthesized by different PI kinases and may be subjected to different regulation upon agonist stimulation (17). Compartmentalized $Ca^{2+}$ signaling through microdomains would allow for temporal and spatial control upon receptor activation and enable the cell to segregate functional responses to different hormones and neuromodulators.

*G proteins and Their Interaction with the Phospholipase Cβ family*

Heterotrimeric G proteins are composed of 3 subunits, an α, β, and γ. To date 21 α, 5 β, and 12 γ subunits have been described, and while not all subunit combinations are possible, many are, making the number of potential combinations very large. Further complexity is added to the system due to the promiscuity of certain subunits in coupling to different receptors and visa versa (for recent reviews see (18) and (19)). Furthermore, Gα subunits are broken down into four families $G\alpha_s$, $G\alpha_{i/o}$, $G\alpha_{q/11}$, and $G\alpha_{12/13}$, and each family has a distinct role in the cell. $G\alpha_s$ and $G\alpha_{i/o}$ activate and inhibit adenylyl cyclase, respectively, $G\alpha_{q/11}$ activates phospholipase Cβ, and $G\alpha_{12/13}$ regulates Rho guanine nucleotide exchange factors.

Gβγ subunits do not simply function as a regulatory binding partner for Gα subunits – promoting reassociation upon Gα deactivation and suppression of Gα signaling. Indeed, Gβγ subunits possess a range of effectors in their own right including PLCβs, adenylyl cyclases, and $K^+$(GIRK) and $Ca^{2+}$ channels (20).

The PLCβ family is composed of four isoforms ($PLC\beta_{1\text{-}4}$). These isoforms vary in their tissue distribution and their sensitivity to activation by G protein subunits (see below). Although both $G\alpha_q$ subfamily members and Gβγ subunits activate PLCβs, the

site of the interaction for activation is different. $G\alpha_q$ interacts with the long, C-terminal extension of PLCβ and Gβγ interacts with the XY catalytic region (8) and PH domain (21).

The C-terminal extension of the PLCβ family is essential for its cellular localization and activation. Although deletion of the C-terminus does not affect the catalytic activity of the enzyme, it does result in the loss of the ability to be activated by $G\alpha_q$ (22). Additional studies by Kim *et al* also revealed the importance of the C-terminus of $PLC\beta_1$. In this study, deletion of the C-terminus not only abolished activation by $G\alpha_q$ but affected its localization as well as a C-terminal truncation mutant no longer associated with the particulate fraction or localized to the nucleus. The C-terminus of $PLC\beta_1$ is predicted to have three helical regions with clusters of highly conserved basic residues (23). The crystal structure of the C-terminus of $PLC\beta_1$ shows that it forms an intertwined helical dimmer, but it is not clear whether this occurs in nature (24). Additionally, Kim and colleagues found that two of the alpha helical regions seemed to be essential for activation via $G\alpha_q$. Mutations of the basic residues in regions one and two resulted in a reduction in the sensitivity to $G\alpha_q$ activation while mutations in region three did not. However, mutations in all 3 regions resulted in a reduction in association to the particulate fraction (23).

$PLC\beta_1$ exists as two alternately spliced isoforms ($PLC\beta_1a$ and $PLC\beta_1b$). The 1b variant (140 kDa) and 1a variant (150 kDa) differ in their carboxy terminus. Although there is some dissension in the literature, it is generally accepted that the 1b form is found predominately in the nucleus, and the 1a form predominately in the cytosol (25). There is, in the nucleus, a separate and distinct inositol signaling pathway from that which

occurs at the plasma membrane. Via the MAP kinase pathway, PLC$\beta_1$ in the nucleus is activated. Termination of PLC$\beta_1$ signaling occurs when PKC$\alpha$, attracted to the nucleus by increasing levels of DAG, phosphorylates PLC$\beta_1$ and inactivates it (26).

It is important to note, of the Gq subfamily, all four ($\alpha_q$, $\alpha_{11}$, $\alpha_{14}$, and $\alpha_{16}$) activate the PLC$\beta$ family but not PLC$\gamma$, -$\delta$, or –$\varepsilon$. In terms of sensitivity to G$\alpha_q$ activation, PLC$\beta_1$ is greater or equal to $\beta_3$ which is greater than $\beta_2$. PLC$\beta_4$ is also activated by G$\alpha_q$ subunits, but the extent of this activation is unclear. With the exception of PLC$\beta_4$, PLC$\beta$ isotypes are also activated by G$\beta\gamma$ subunits, and sensitivity to G$\beta\gamma$ activation is as follows, PLC$\beta_2$ is greater than $\beta_3$ and is much greater than PLC$\beta_1$(8).

G proteins transduce extracellular signals from a seven transmembrane GPCRs to the inside of the cell. In the basal or resting state, GDP is bound the G$\alpha$ subunit which is in a complex with the G$\beta\gamma$ subunit and receptor. Activation of a GPCR promotes the exchange of GTP for GDP on the G$\alpha$ subunit allowing both G$\alpha$ and G$\beta\gamma$ to activate their downstream effectors such as enzymes and ion channels. Cessation of this signaling cascade occurs when GTP is hydrolyzed to GDP on the G$\alpha$ subunit which has intrinsic GTPase ability. Numerous stimuli, such as neurotransmitters and hormones, can activate GPCRs, and thus, activation of G protein signaling can have a variety of outcomes inside the cell.

In recent years, there has been a wealth of research into the termination of G protein signaling, as it was discovered that the intrinsic rate of GTPase activity of the G$\alpha$ subunit is not fast enough given physiological constraints (27). There were marked contrasts in the rates obtained for *in vitro* and *in vivo* data, and *in vitro* studies using purified G$\alpha$ subunits produced GTP hydrolysis rates that were not on a time scale

required for rapid deactivation in a cellular context. Thus, it was thought that there must be "accelerators" for this process; factors that enhance the rate of GTP hydrolysis which would allow for rapid signaling. Indeed, such factors do exist, and they are termed GTPase Accelerating Proteins (GAPs). Interestingly, PLC$\beta_1$ is a GAP for the $G_q$ subfamily and not for $G_i$, $G_o$, $G_s$, or $G_z$ (28), and as a result of this activity, it is responsible for the termination of its own signaling.

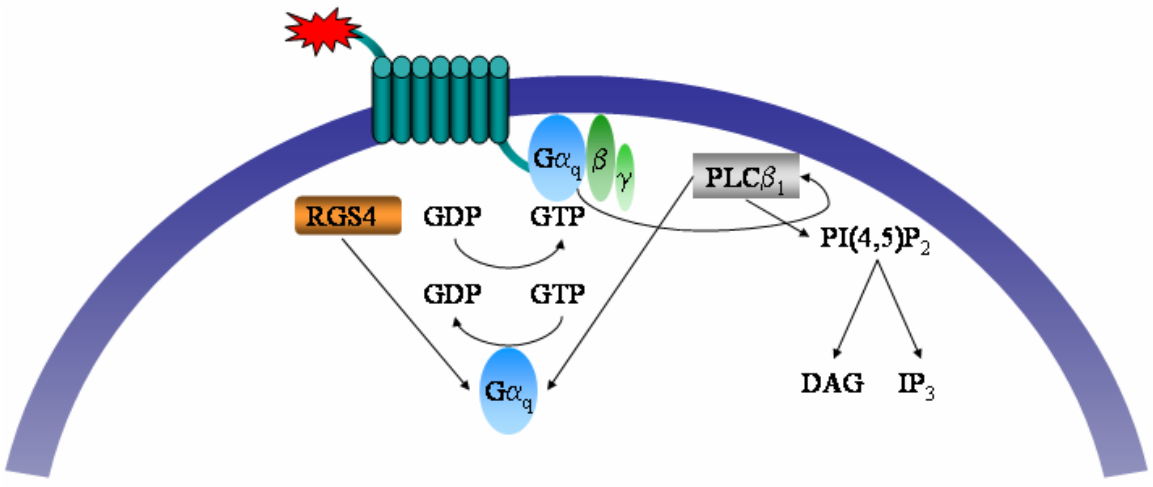


**Figure 1.3:** Cartoon depicting $G\alpha_q$ signaling pathway. Upon binding of a ligand to a seven transmembrane receptor, the exchange of GDP for GTP is favored on the $G\alpha$ subunit. Activated $G\alpha_q$ then goes on to activate its effector PLC$\beta_1$ which hydrolyzes PI(4,5)$P_2$ into the two important second messengers DAG and $IP_3$. Termination of the signal occurs when GTP is hydrolyzed back to GDP on the $G\alpha$ subunit by the GAP activity of PLC$\beta_1$ or RGS4.

Another important class of GAPs for $G\alpha$ subunits are known as regulators of G protein signaling (RGS proteins) which, in some cases, can accelerate the rate of GTP hydrolysis about 1000-fold (29) (see figure 1.3 for model).

*Regulators of G Protein Signaling*

There have been 30 mammalian RGS and RGS-like family members identified all of which share a homologous 130 amino acid core or RGS domain which is responsible

for their GAP activity. Studies and crystal structures suggest that RGS proteins bound to the Gα subunit stabilize the GTP to GDP transition state lowering the energy required for hydrolysis ((30), (31), and (32)). Thus, RGS proteins are negative regulators of Gα subunits; however, they may have other roles as well (for review see (33)).

RGS proteins can be divided into 9 subfamilies based on the alignment of their RGS domains (see figure 1.4) (34). Flanking the RGS domain or box are variable regions that confer specificity of action to the protein which gives a wide range of diversity and function between family membranes. Also, besides their homologous RGS domain, family members vary widely in amino acid homology and size. The simplest families are A/RZ and B/R4 which are mostly made up of the RGS domain (see figure adapted from (34)). The other seven families have a more complex domain structure which would allow them to function outside of being simple GAPs and are most likely multi-functional. In addition, differing domains would alter the subcellular localization of the proteins and target family members to the plasma membrane and/or protein partners. For example, the presence of a PH domain would allow for plasma membrane targeting. Again, this gives a great diversity of function to the RGS family extending from simple modulators of G proteins to more complex interactions as integrators of cell signaling pathways (35). However, even the simple family members may participate in multiple protein-protein interactions and serve in scaffolding complexes (36).

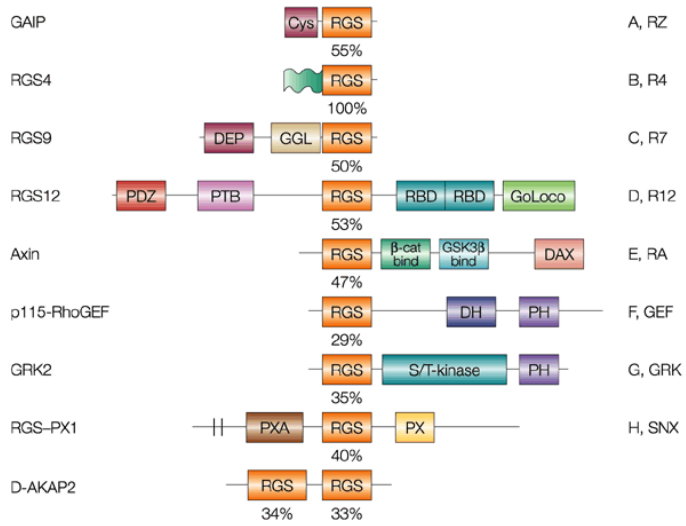


**Figure1.4:** Alignment of RGS domains of RGS family members. Adapted from Neubig, R. et al. *Nature Reviews Drug Discovery*. (2002). 1(3): 187-197.

Of all RGS proteins RGS4 is the most widely studied, and it was one of the first RGS proteins to be described (35). It is a member of the B/R4 family which unlike other family members (except for 2 members of the A/RZ family) has an N-terminal amphipathic helix (37). RGS4 is a GAP for $G\alpha_{i/o}$ and $G\alpha_q$ family members (38). In this study, Hepler and colleagues found that RGS4 and GAIP accelerated the rate of GTP hydrolysis for $G\alpha_q$ and interfered with $G\alpha_q$ activation of PLCβ leading the authors to speculate that RGS4 occluded the binding site between $G\alpha_q$ and PLCβ and was unrelated to its GAP activity.

In addition to having specific interactions with G proteins, RGS4 may have interactions with other proteins as well such as GPCRs. In a cell study, Roy and colleagues, attempted to address the question of what targets RGS4 to the plasma membrane, and whether there even needs to be stable membrane association for RGS4 since its actions are catalytic. They found, when they co-expressed RGS4-GFP or RGS2-GFP with either $G\alpha_s$, $G\alpha_{i2}$, or, $G\alpha_q$ that the GFP fusion proteins were selectively

recruited to the plasma membrane. In addition, co-expressing RGS4 or RGS2 with corresponding receptors, β2-adrenergic receptor, M2 muscarinic receptor or $AT_{1A}$ angiotensin II receptor resulted in the same expression pattern of the RGS fusion proteins when co-expressed with the receptors cognate G proteins. They also found that recruitment of RGS4 and RGS2 to the plasma membrane was not dependent on the activation state of the G protein, as agonist stimulation, constitutively active or poorly activated G protein mutants produced similar results (39).

What is the nature of the interaction between RGS4 and membranes? And, do its flanking regions play a role in membrane targeting? Current data suggests that the N-terminal region of RGS4 is required for plasma membrane targeting and its activity. RGS4 is also palmitoylated most likely at cysteine residue(s) 2 and/or 12 (40). However, in this study, deletion of these residues did not affect plasma membrane targeting of RGS4 in yeast. Deletion of the first 33 residues of RGS4 resulted in a loss in plasma membrane localization and activity. When they fused residues 1-33 to GFP and looked at cellular localization, these residues were sufficient to localize the fusion protein to the plasma membrane leading the authors to speculate that there was something else about the first 33 residues other than palmitoylation that enabled plasma membrane targeting. Further studies revealed an answer. In the presence of anionic lipids, a peptide corresponding to the first 31 amino acids of RGS4 was in an α-helical conformation (37). Upon mutating the positive charges on the hydrophilic portion of the helix or substituting the polar residues on the hydrophobic portion, binding to anionic membranes was disrupted as was the formation of the α-helix. This suggests that the secondary structure of the N-terminal flanking region is required for membrane targeting. Additional studies

by Ross and colleagues imply that proper orientation on the plasma membrane is a prerequisite for RGS4 GAP activity (41), and that after binding to the membrane, RGS4 must either reorient itself on the plasma membrane or undergo a conformational change for proper interaction with receptor and G protein. Again, this process is dependent on the N-terminal domain of RGS4.

Certainly, RGS4 cannot have unrestricted GAP activity within the cell; it must be regulated. Within the RGS domain of RGS4 is a cluster of positively charged residues which are on the opposite side from the portion of the domain which interacts with Gα subunits (42). A physiological role for these residues was suggested in a study where the GAP activity of RGS4 was inhibited by $PI(3,4,5)P_3$ in cardiac myocytes but was recovered upon activation of $Ca^{2+}$/calmodulin presumably through competitive binding. This inhibition by $PI(3,4,5)P_3$ would provide control of RGS4 GAP activity which, in order for G protein activation to occur, can not be unrestricted. A direct interaction between RGS4 and $Ca^{2+}$/calmodulin was demonstrated in a FRET based assay where, upon stimulation, the FRET between eCFP-$Ca^{2+}$/calmodulin and eYFP-RGS4 increased indicating the interaction between these two proteins was Ca2+ dependent. Furthermore, depletion of cholesterol from the plasma membrane with methyl-β-cyclodextrin decreased the FRET efficiency between this pair suggesting the involvement of lipid rafts in the physiological control of RGS4 GAP activity (43).

*Evidence for a self-scaffolding model*

Signaling speed and specificity of the signal would be greatly enhanced if members of a signaling pathway were held together in a scaffold. What is the nature of

this scaffold? How is it organized? Are protein-protein interactions within the scaffold "permanent," or are they more transient in nature? Certainly, the fluid-mosaic model (44) of the plasma membrane wherein proteins are freely diffusing is too simple, and now, there are many studies which support compartmentalization of signaling components as lipid rafts (for review see (45)) and caveolae (for review see (46) have been implicated in sequestering signaling components.

Higher order complexes between receptors, G proteins and effectors would greatly accelerate the rate of effector activation because activation would not longer be dependent upon diffusion and association. And, there is evidence in the literature for the formation of signaling complexes. Studies by Ross and co-workers give rates for the activation and deactivation of Gq mediated signaling. Since PLC$\beta_1$ is a GAP for G$\alpha_q$, the opposing action of the receptor and PLC$\beta_1$ would control the amplitude and rate of GTP exchange. In these studies, the authors used a reconstituted system in which they added purified PLC$\beta_1$ to phospholipid vesicles containing PI(4,5)$P_2$, purified M1 muscarinic receptor, and purified G$\alpha_q$. When they stimulated the system with carbachol and GTP, there was a large (90-fold) increase in PLC$\beta_1$ activity and a substantial increase in its GTPase activity as well. Even in light of this rapid GTP hydrolysis, the receptor was able to maintain greater than 10% of the G$\alpha_q$ population in the GTP bound state. This led them to conclude that there must be a complex between the three proteins over multiple cycles of GTP hydrolysis and that dissociation of G$\alpha_q$ from its receptor would not be probable given the rapid rate of G$\alpha_q$-PLC$\beta_1$ signaling (28).

There is also evidence in cells for the formation of receptor-G$\alpha$ subunit complexes upon stimulation. In smooth muscle cells, association of receptors coupled to

$G\alpha_q$ and $G\alpha_i$ has been observed with bradykinin stimulation. Co-enrichment in density gradients, immunoelectron microscopy and co-immunoprecipitation studies indicated that, when these cells are stimulated, the occupied receptor and receptors coupled to $G\alpha_q$ and $G\alpha_i$ are recruited and sequestered into caveloe. In addition, their work also suggested the presence of PLCβ in caveloe as well leading the authors to speculate that sequestering of signaling components would be a mechanism for signal amplification (47).

Other systems provide evidence for signaling complexes as well. In *Drosophila*, a higher order signaling complex termed a "transducisome" has been described. In this complex, PDZ domains of the *ina*D gene product serve as a scaffold for phototransduction machinery which involves light-activated ion channels, and PLCβ and PKC homologues. Interestingly, the G-protein coupled signaling cascade that occurs during phototransduction in *Drosophila* is the fastest known (48).

It has been the focus of this dissertation to study the interactions between members of the $G\alpha_q$ mediated signaling cascade. These studies began as *in vitro* studies using purified proteins, and it was during this time that we began to define the interactions between RGS4, G proteins, and $PLC\beta_1$ on membrane surfaces. The most interesting aspect of this study was the result that RGS4 not only had an interaction with activated and deactivated $G\alpha_q$, which was expected, but it also had affinity to $G\beta\gamma$ and $PLC\beta_1$ as well. These results indicated that weakly associating, ternary complexes could form between these proteins. These secondary interactions would enable signaling proteins to remain in close proximity to one another perhaps in preformed complexes enabling rapid initiation and termination of signaling processes (49).

There is dissension in the literature as to whether or not Gα and Gβγ physically dissociate upon activation or remain bound in a complex. Classically, biochemical studies indicated subunit dissociation (for review see (50) and below). However, two relatively recent studies are of note as they highlight these two opposing views and were also conducted in living cells. In *Dictyostelium discoideum*, Devreotes and colleagues found that upon receptor activation, rapid dissociation of the G Protein heterotrimer occurred (51). In these studies, FRET-based assays were preformed in which CFP was on the Gα subunit and YFP on the Gβγ subunit. Addition of a chemoattractant to the cells resulted in a loss of FRET indicating that the heterotrimer was coming apart. Removal of the chemoattractant resulted in reassociation of the Gα and Gβγ subunits.

Conversely, another group found that $G\alpha_i$ and Gβγ subunits do not dissociate in living cells upon activation (52); rather, they undergo a rearrangement. This group also utilized a FRET-based assay, and instead of observing a loss in fluorescence upon stimulation between YFP-$G\alpha_i$ and CFP-Gβγ, they observed an increase in FRET indicating that the $G\alpha_i$ and Gβγ subunits were moving closer together and undergoing molecular rearrangement. The authors of the second study speculated that differences in the Gα subunit used ($G\alpha_i$ versus $G\alpha_s$) could account for the contradicting results. Furthermore, these authors suggested that the heterotrimer would serve as a perfect scaffold for effectors independent of the activation state of the G protein.

The following two chapters detail work wherein, we moved from an *in vitro* to a cell based system to look at these protein-protein interactions hoping to observe higher order complexes *in vivo*. To do this, we utilized an *in vivo* fluorescence resonance energy technique which allowed us to look at the interaction between two proteins in living cells

in the basal and stimulated states (53). Although kinetic data argued against it, current dogma (50) invoked a model wherein activation of $G\alpha_q$ promoted dissociation of the G protein from its receptor and $G\beta\gamma$, and it would diffuse along the plasma membrane, find $PLC\beta_1$, associate with it and activate it. This dogma came from early biochemical work. Studies of the crystal structures of the G protein heterotrimer, transducin, implied that upon activation the $G\beta\gamma$ subunit dissociated from the $G\alpha$ subunit (54) and (55). These studies describe the conformational changes the $G\alpha$ subunit undergoes upon GTP for GDP exchange which results in the release and activation of the $G\beta\gamma$ subunit. Based on these crystal structures, it has been argued (50) that the regions involved in the interaction between $G\alpha$ and $G\beta\gamma$ overlap that of the interaction sites for effectors which would indicate that, in order to activate their effectors, $G\alpha$ and $G\beta\gamma$ subunits have to physically dissociate. In addition, G protein purification schemes were based on the dissociation of $G\alpha$ from $G\beta\gamma$ (56) as one would purify the heterotrimer and release the $G\alpha$ subunit from the resin bound $G\beta\gamma$ subunit by activating it with aluminum floride.

Prior to the crystallization studies mentioned above, studies of adenylate cyclase activation by β-adrenergic receptors in reconstituted membrane systems resulted in a model termed “collision coupling” (57). In this model, there is a “transient” encounter of the ligand-bounded receptor with the $G\alpha_s$-cyclase complex during the GTP for GDP exchange after which the receptor dissociates from the complex. As mentioned above, it is reasonable to think that there could be differences between G protein signaling systems. Perhaps, for transducin and $G\alpha_{i/s}$ there is dissociation of the G proteins from each other and from the receptor. However, because of these early studies (and others

(58)), all G proteins were thought to function similarly which simply may not be the case *in vivo*.

In our studies, we find $G\alpha_q$ and $PLC\beta_1$ to be already in a preformed complex in the basal state in living cells. To our knowledge, this is the first time preassociation of a G protein and its effector has been observed in living cells before stimulation and represents the most novel aspect of this work.

**Literature Cited**


1. Berridge, M. J., Lipp, P., and Bootman, M. D. (2000) *Nat Rev Mol Cell Biol* **1**(1), 11-21
2. Rebecchi, M. J., and Pentyala, S. N. (2000) *Physiol Rev* **80**(4), 1291-1335
3. Saunders, C. M., Larman, M. G., Parrington, J., Cox, L. J., Royse, J., Blayney, L. M., Swann, K., and Lai, F. A. (2002) *Development* **129**(15), 3533-3544
4. Zhou, Y., Wing, M. R., Sondek, J., and Harden, T. K. (2005) *Biochem J* **391**(Pt 3), 667-676
5. Hwang, J. I., Oh, Y. S., Shin, K. J., Kim, H., Ryu, S. H., and Suh, P. G. (2005) *Biochem J* **389**(Pt 1), 181-186
6. Kavran, J. M., Klein, D. E., Lee, A., Falasca, M., Isakoff, S. J., Skolnik, E. Y., and Lemmon, M. A. (1998) *J Biol Chem* **273**(46), 30497-30508
7. Yamamoto, T., Takeuchi, H., Kanematsu, T., Allen, V., Yagisawa, H., Kikkawa, U., Watanabe, Y., Nakasima, A., Katan, M., and Hirata, M. (1999) *Eur J Biochem* **265**(1), 481-490
8. Rhee, S. G. (2001) *Annu Rev Biochem* **70**, 281-312
9. Jimenez, J. L., Smith, G. R., Contreras-Moreira, B., Sgouros, J. G., Meunier, F. A., Bates, P. A., and Schiavo, G. (2003) *J Mol Biol* **333**(3), 621-639
10. Guo, Y., Rebecchi, M., and Scarlata, S. (2005) *J Biol Chem* **280**(2), 1438-1447
11. Lopez, I., Mak, E. C., Ding, J., Hamm, H. E., and Lomasney, J. W. (2001) *J Biol Chem* **276**(4), 2758-2765
12. Czech, M. P. (2000) *Cell* **100**(6), 603-606
13. McLaughlin, S., Wang, J., Gambhir, A., and Murray, D. (2002) *Annu Rev Biophys Biomol Struct* **31**, 151-175
14. Tall, E. G., Spector, I., Pentyala, S. N., Bitter, I., and Rebecchi, M. J. (2000) *Curr Biol* **10**(12), 743-746
15. Cullen, P. J., Cozier, G. E., Banting, G., and Mellor, H. (2001) *Curr Biol* **11**(21), R882-893
16. Czech, M. P. (2003) *Annu Rev Physiol* **65**, 791-815

17. Varnai, P., and Balla, T. (1998) *J Cell Biol* **143**(2), 501-510
18. Wettschureck, N., and Offermanns, S. (2005) *Physiol Rev* **85**(4), 1159-1204
19. Oldham, W. M., and H, E. H. (2006) *Q Rev Biophys* **39**(2), 117-166
20. Milligan, G., and Kostenis, E. (2006) *Br J Pharmacol* **147 Suppl 1**, S46-55
21. Wang, T., Dowal, L., El-Maghrabi, M. R., Rebecchi, M., and Scarlata, S. (2000) *J Biol Chem* **275**(11), 7466-7469
22. Park, D., Jhon, D. Y., Lee, C. W., Ryu, S. H., and Rhee, S. G. (1993) *J Biol Chem* **268**(5), 3710-3714
23. Kim, C. G., Park, D., and Rhee, S. G. (1996) *J Biol Chem* **271**(35), 21187-21192
24. Singer, A. U., Waldo, G. L., Harden, T. K., and Sondek, J. (2002) *Nat Struct Biol* **9**(1), 32-36
25. Xu, A., Wang, Y., Xu, L. Y., and Gilmour, R. S. (2001) *J Biol Chem* **276**(18), 14980-14986
26. Cocco, L., Faenza, I., Fiume, R., Maria Billi, A., Gilmour, R. S., and Manzoli, F. A. (2006) *Biochim Biophys Acta* **1761**(5-6), 509-521
27. Gilman, A. G. (1987) *Annu Rev Biochem* **56**, 615-649
28. Biddlecome, G. H., Berstein, G., and Ross, E. M. (1996) *J Biol Chem* **271**(14), 7999-8007
29. Chidiac, P., and Ross, E. M. (1999) *J Biol Chem* **274**(28), 19639-19643
30. Berman, D. M., Kozasa, T., and Gilman, A. G. (1996) *J Biol Chem* **271**(44), 27209-27212
31. Tesmer, J. J., Berman, D. M., Gilman, A. G., and Sprang, S. R. (1997) *Cell* **89**(2), 251-261
32. Popov, S., Yu, K., Kozasa, T., and Wilkie, T. M. (1997) *Proc Natl Acad Sci U S A* **94**(14), 7216-7220
33. Chidiac, P., and Roy, A. A. (2003) *Receptors Channels* **9**(3), 135-147
34. Neubig, R. R., and Siderovski, D. P. (2002) *Nat Rev Drug Discov* **1**(3), 187-197
35. Hollinger, S., and Hepler, J. R. (2002) *Pharmacol Rev* **54**(3), 527-559
36. Hepler, J. R. (2003) *Mol Pharmacol* **64**(3), 547-549
37. Bernstein, L. S., Grillo, A. A., Loranger, S. S., and Linder, M. E. (2000) *J Biol Chem* **275**(24), 18520-18526
38. Hepler, J. R., Berman, D. M., Gilman, A. G., and Kozasa, T. (1997) *Proc Natl Acad Sci U S A* **94**(2), 428-432
39. Roy, A. A., Lemberg, K. E., and Chidiac, P. (2003) *Mol Pharmacol* **64**(3), 587-593
40. Srinivasa, S. P., Bernstein, L. S., Blumer, K. J., and Linder, M. E. (1998) *Proc Natl Acad Sci U S A* **95**(10), 5584-5589
41. Tu, Y., Woodson, J., and Ross, E. M. (2001) *J Biol Chem* **276**(23), 20160-20166
42. Ishii, M., Fujita, S., Yamada, M., Hosaka, Y., and Kurachi, Y. (2005) *Biochem J* **385**(Pt 1), 65-73
43. Ishii, M., Ikushima, M., and Kurachi, Y. (2005) *Biochem Biophys Res Commun* **338**(2), 839-846
44. Singer, S. J., and Nicolson, G. L. (1972) *Science* **175**(23), 720-731
45. Brown, D. A. (2006) *Physiology (Bethesda)* **21**, 430-439
46. Cheng, Z. J., Singh, R. D., Marks, D. L., and Pagano, R. E. (2006) *Mol Membr Biol* **23**(1), 101-110

47. de Weerd, W. F., and Leeb-Lundberg, L. M. (1997) *J Biol Chem* **272**(28), 17858-17866
48. Tsunoda, S., Sierralta, J., Sun, Y., Bodner, R., Suzuki, E., Becker, A., Socolich, M., and Zuker, C. S. (1997) *Nature* **388**(6639), 243-249
49. Dowal, L., Elliott, J., Popov, S., Wilkie, T. M., and Scarlata, S. (2001) *Biochemistry* **40**(2), 414-421
50. Hamm, H. E. (1998) *J Biol Chem* **273**(2), 669-672
51. Janetopoulos, C., Jin, T., and Devreotes, P. (2001) *Science* **291**(5512), 2408-2411
52. Bunemann, M., Frank, M., and Lohse, M. J. (2003) *Proc Natl Acad Sci U S A* **100**(26), 16077-16082
53. Dowal, L., Provitera, P., and Scarlata, S. (2006) *J Biol Chem* **281**(33), 23999-24014
54. Sondek, J., Bohm, A., Lambright, D. G., Hamm, H. E., and Sigler, P. B. (1996) *Nature* **379**(6563), 369-374
55. Lambright, D. G., Sondek, J., Bohm, A., Skiba, N. P., Hamm, H. E., and Sigler, P. B. (1996) *Nature* **379**(6563), 311-319
56. Kozasa, T., and Gilman, A. G. (1995) *J Biol Chem* **270**(4), 1734-1741
57. Levitzki, A. (1988) *Science* **241**(4867), 800-806
58. Levitzki, A., and Klein, S. (2002) *Chembiochem* **3**(9), 815-818

## Chapter 2: Determination of the Contact Energies between a Regulator of G Protein Signaling and G Protein Subunits and Phospholipase $C\beta_1$

This work has been published: Louisa Dowal, John Elliott, Serguei Popov, Thomas M. Wilkie, and Suzanne Scarlata. *Determination of the Contact Energies between a Regulator of G Protein Signaling and G Protein Subunits and Phospholipase $C\beta_1$*. Biochemistry, 2001. **40**: p. 414-421.

Heterotrimeric G proteins are membrane-bound proteins consisting of α, β, and γ subunits (for reviews see (1) and (2). Upon activation, GTP-bound α subunits lose their affinity for Gβγ subunits but increase their affinity for protein effectors (3) and (4). This subsequent interaction alters effector activity and ultimately causes cellular changes. Additionally,Gβγ subunits change the activity of a specific set of effectors (5). There are four families of Gα proteins, and the main effector of the $G\alpha_q$ family is mammalian inositide-specific phospholipase C-β (PLC-β). PLC-β catalyzes the hydrolysis of phosphatidyloinositol 4,5-bisphosphate ($PIP_2$) to produce two second messengers, 1,4,5-inositol trisphosphate ($IP_3$), which causes the release of $Ca^{2+}$ from intracellular stores, and diacylglycerol (DAG), which promotes the activation of protein kinase C (see (6) for recent review).

PLCs have a modular structure (7) consisting of an N-terminal pleckstrin homology domain, which has been shown to confer binding and activation by Gβγ subunits (8) and (9), four elongation factor (EF) hands, a catalytic domain with a long insertion loop, a C2 domain which has been shown to specifically bind $G\alpha_q$ subunits (10), and a 400 residue tail which is needed for activation by $G\alpha_q$ (11), (12), and (13).

Interestingly, residues in this tail have been shown to also accelerate the rate of GTP hydrolysis of $G\alpha_q$ thereby increasing the rate of deactivation of $\alpha_q$ and in turn the rate of deactivation of the PLC-β (14). By deactivating its G protein activator, PLC-βs are able to turn off their own signal.

Adding to the list of players in the inositol-signal transduction is a newly discovered class of proteins called regulators of G protein signaling (RGS) (15). Thus far, the RGS proteins are known to bind to the α subunits of G proteins and increase the rate of GTP hydrolysis by stabilizing the transition state of the complex (4). For example, RGS4, which specifically acts on $G\alpha_i$ and $G\alpha_q$ family members, increases the GTPase activity of $G\alpha_q$ 1000-fold (16). There are many members of the RGS family, and each family member has an ~130 residue homologous core region that is responsible for GAP activity. This core, termed the RGS domain, binds strongly to Gα in the GDP-$AlF_4^-$ bound state (17), and the structure of the RGS4-$G\alpha_{i1}$(GDP)-$AlF_4^-$ suggests that the core stabilizes the GTP to GDP transition state lowering the energetic requirement for hydrolysis (4). This stabilization allows RGSs to turn off the effector signal without diminishing the signal strength.

On each side of the RGS core are flanking regions which presumably dictate the specificity of RGS family members to Gα families or other binding targets. These flanking regions were unresolved in the crystal structure, and the role that they play in RGS function is unclear. The N-terminus of RGS4, which contains several basic and hydrophobic residues, appears to be responsible for targeting to the plasma membrane since removal of the first 33 residues significantly reduces the membrane localization in yeast (18). Another study suggests that the N-terminus targets RGS4 to particular G

protein coupled receptors occupying a position that can prevent coupling between $G\alpha_q$ and $PLC\beta_1$ (19). Although it is clear that RGS4 must be localized near membrane receptors, it is not clear whether it is localized by an intrinsic affinity for membranes or by interactions with receptors, G protein subunits, or effectors. Evidence of membrane localization of RGS4 comes from a recent study showing that phosphatidylinositol 3,4,5-trisphosphate inhibits the GAP activity of RGS4 presumably by directly interacting with the positively charged residues on the surfaces of helices 4 and 5 (20). This inhibition may be overcome by displacement of RGS4 from the membrane by Ca2+/calmodulin, thereby allowing RGS4 to bind and deactivate GR subunits (20).

The idea that RGS4 and other components in the inositol signaling pathway are localized in protein complexes is intriguing, since this would allow for rapid signal flow (21), (22), (23), and (24). There is precedent for these complexes. Association between seven transmembrane receptors and $G\alpha_q$ has been observed in cells (25). Notably, in *Drosophila* a signaling complex involving receptor, PLC-β and protein kinase C and a scaffold protein has been identified (26). In a reconstituted in vitro system, we have found that $G\alpha$(GDP) will bind to the activated PLC-$\beta_2$-$G\beta\gamma$ complex and rapidly turn off the activation without physically disrupting the complex (27). In studies of PLCβ activation, Ross and co-workers have presented kinetic data to argue that $G\alpha_q$ must remain bound to receptor during turnover (14). Taken together, these studies point to a model in which receptor, the G protein heterotrimer, effector, and RGS4 can be colocalized in signaling complexes. However, not all studies support this model. For example, the presence of RGS4 interferes with $G\alpha_q$ activation of $PLC\beta_1$ leading the authors of those studies to speculate that the interaction sites between these proteins are

shared (28). Thus, it is possible that protein complexes will form under some circumstances but not others.

In this study, we begin to define the biophysical conditions under which RGS4, PLC$\beta_1$, and G$\alpha\beta\gamma$ will associate on membrane surfaces using fluorescence methods. As mentioned, we have previously defined the interaction energies between G$\alpha_q$, G$\beta\gamma$ and PLC$\beta$1-3 on membrane surfaces (3). From these studies, we know the local concentrations at which association between the individual species occur. Here, we extend this work to include the conditions for association of RGS4 to components of this pathway. We find that RGS4 not only associates with activated G$\alpha$ subunits, but has secondary interaction with the other components of the signaling system as well. The results of these studies lead to a model in which RGS4 is corralled in the complexes by weaker secondary interactions that allow for rapid transfer of RGS4 contacts to G$\alpha_q$ upon activation.

## Materials and Methods

### *Sample Preparation*

Untagged, recombinant PLC$\beta_1$, G$\alpha_q$, and His6-G$\beta\gamma$ subunits were prepared in Sf9 cells as previously described *(3)*. Preparation of RGS4(1-33) has been described (19). Large, unilamellar vesicles (LUVs), 100nm in diameter, were prepared by extrusion. All lipids were purchased from Avanti Polar Lipids (Alabaster, AL) except for dipalmitoyl PI-3,4,5-trisphosphate, which was synthesized using the method of Reddy et al.(29). The bacterial cell strain pREP4/His6-RGS4 in BL21/DE3 cells was a generous gift from A.G. Gilman and was prepared as described (28) in pure form as determined by western blot

analysis using an RGS4 antibody (Santa Cruz Biochemicals) and MALDIMS analysis. Since it does not affect the GAP activity of the protein, the N-terminal was not removed in these studies. Labeling of the proteins with amine-reactive probes has also been described (3). GAP activity of labeled and unlabeled RGS4 was checked using bacterially expressed recombinant $G\alpha_{i1}$ in a single turnover assay as previously described (17).

*Protein Labeling and Reconstitution*

All probes were purchased from Molecular Probes, Inc. (Eugene, OR). $G\alpha_q$ and $G\beta\gamma$ subunits were covalently labeled with amine reactive probes which do not affect their ability to activate $PLC\beta_1$ or $PLC\beta_2$, respectively. RGS4 and $PLC\beta_1$ were similarly labeled as described (27). The protein:probe labeling ratio was determined by BCA analysis and absorption spectroscopy using the extinction coefficients provided by the probe manufacturer and was ~1:1 (mol/mol) for all preparations. Labeled G-$\alpha_q$ was reconstituted into lipid vesicles by adding the detergent-solubilized protein to a large excess of preformed extruded vesicles.

*Fluorescence Measurements and Data Analysis*

Fluorescence measurements were performed on an ISS spectrofluorometer (Champaign, IL) using a 3 mm cuvette with magnetic stirrer. Adequate stirring was assessed at the beginning of the study by ensuring that upon addition of a dilutant, the emission spectrum was identical after inversion. Also, at the beginning of each study, we verified that the sample was at thermal equilibrium by showing that the initial scan was stable over several scans. Coumarin-labeled proteins were excited at 380 nm and scanned

from 420 to 560 nm. Laurodan probes were excited at 350 nm and scanned from 380 to 560 nm. Coumarin-Dabcyl SE resonance energy transfer was determined by the loss of coumarin fluorescence caused by addition of the nonfluorescent Dabcyl-labeled acceptor protein. Signals were corrected for dilution and compared to loss of fluorescence caused by addition of buffer alone.

To determine the affinities of the protein complexes, energy transfer data were analyzed as binding isotherms assuming that the maximum loss of fluorescence represents the maximum extent of complex formation and that the stoichiometry of this complex is 1:1 (mol/mol). Titration curves were the fit to a bimolecular association constant. Membrane binding was determined using a variety of fluorescence based methods (see ref *28*). To obtain the partition coefficient (*K*p) for membrane, we used the large decrease (~20%) in the intrinsic fluorescence of RGS4 presumably due to quenching of internal Trp/Try residues by the ionic groups on the membrane surface. We note that the *K*p values reported here correspond to apparent partition coefficients since we assume that RGS4 partitions on membranes through nonspecific, electrostatic interactions rather than forming a chemical complex between a particular lipid(s) or nucleotide base(s).

$$K\text{p (i.e., Kapp) } ) ([P]_b/[L])/[P]_f$$

*K*p is defined as the mole fraction of substrate-bound protein, $([P]_b/[L])$, divided by the concentration of free protein $[P]_f$. $[P]_b$ is the concentration of substrate-bound protein and [L] is the concentration of substrate. Each trial as well as the average, was fit to a hyperbola using SigmaPlot (Jandel Inc.).

## Results

### *Binding of RGS4 to Activated and Deactivated $G\alpha_q$ Subunits*

Although it has been well established that RGS4 binds strongly to $G\alpha_q$, we needed to characterize the conditions of this interaction for this study. We thus measured the association energy between RGS4 and $G\alpha_q$ in its activated (i.e., GTPγS-bound) and deactivated (i.e., GDP-bound) forms using fluorescence resonance energy transfer. In this method, $G\alpha_q$ was labeled on a primary amine with a fluorescent probe that is capable of transferring its excited-state energy to an acceptor when the probes are within close proximity. Although many energy transfer probe pairs are known, we used coumarin-SE (abbreviated C-) as the donor because of its high quantum yield and dabsyl-SE (D-) as the acceptor because this probe is not fluorescent and its use eliminates the need for correcting for acceptor contribution to the donor emission spectrum. Experimentally, as the two labeled proteins associate, the emission intensity of the coumarin probe decreases due to transfer to dabcyl. By monitoring the loss in C-$G\alpha_q$ fluorescence as a function of D-RGS4 concentration, an apparent bimolecular dissociation constant can be determined.

Recombinant $G\alpha_q$ subunits were prepared from Sf9 cells, labeled with coumarin, activated with non-hydrodrolyzable GTPγS, and reconstituted on large, unilamellar vesicles of PC:PS:PE (1:1:1) as described (3). We have previously found that labeling C-$G\alpha_q$ at a 1:1 probe:protein does not affect GTPase activity or its ability to activate $PLC\beta_1$. Titrations were then conducted by adding incremental amounts of D-RGS4 in buffer to a solution of membrane-bound C-$G\alpha_q$ (GTPγS) and recording the spectrum. These data were then corrected using data from titrations where buffer was added instead

of D-RGS4. At 10 nM C-G$\alpha_q$ (GTP$\gamma$S) complete binding was observed when a stoichimetric increment of D-RGS4 was added. Reducing the concentration of C-G$\alpha_q$ (GTP$\gamma$S) to1 nM gave identical behavior which indicates that we were operating at concentrations above the dissociation constant and were observing stoichiometric binding rather than true equilibrium binding. These results show that the $K_d$ for this complex is below 1 nM and out of range of accurate determination using this method.

The crystal structure of the RGS4 complex with activated G$\alpha_i$ shows that the major interaction sites are in the G$\alpha$ switch regions (4). Most likely, this is also the case for interaction for G$\alpha_q$ (GTP$\gamma$S). Therefore, deactivation of C-G$\alpha_q$ should weaken its interaction with RGS4, and this idea is supported by fluorescence data (Figure 2.1). Although the association is weakened as compared to C-G$\alpha_q$ (GTP$\gamma$S), it is still close to the detectable limit by fluorescence methods and the apparent dissociation constant is estimated to be 0.2 ± 0.1 nM. To determine whether we were viewing equilibrium binding, we repeated the study at a 10-fold higher C-G$\alpha_q$ (GDP) which shifted the curve appropriately but did not allow better resolution of the apparent $K_d$.

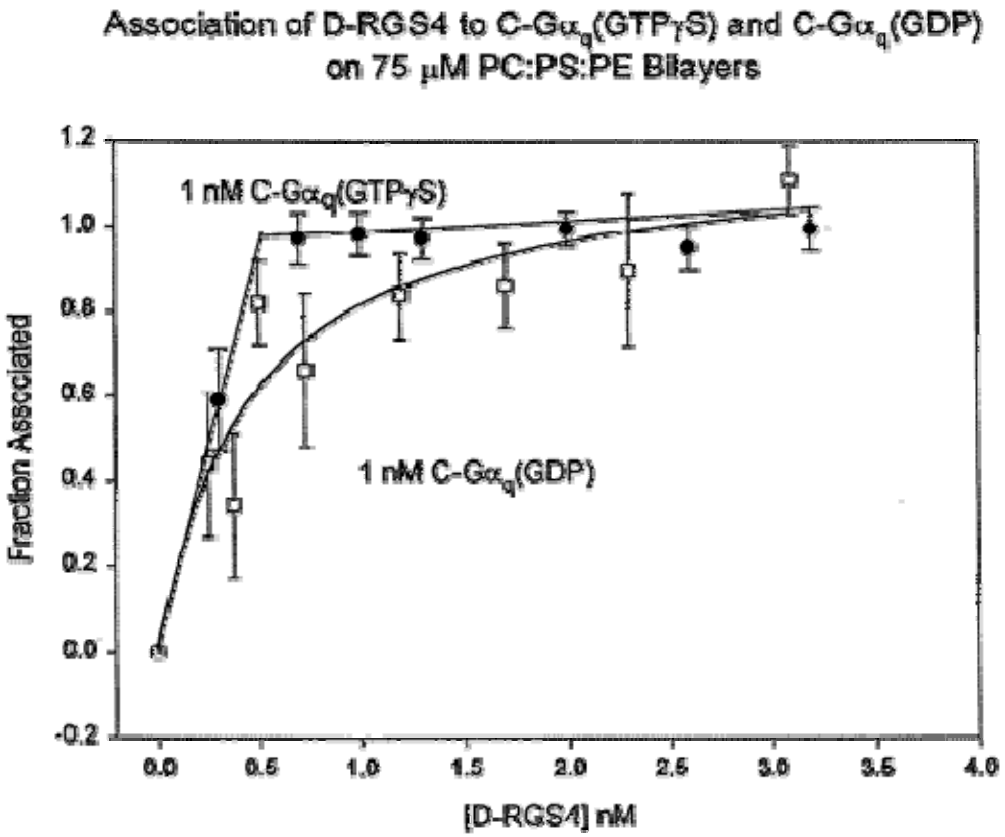


**Figure 2.1**: Fraction of complex formed between RGS4 and activated (●) (n = 11) and deactivated (□) Gq (n = 6) reconstituted on lipid surfaces as measured by fluorescence resonance energy transfer (see method). The fraction formed was determined by the ~15% loss in coumarin (C-) fluorescence as its emission energy is transferred to nonfluorescent dabcyl (D-) probes. The line through the Gq(GTPγS) data shows the curve for protein interactions that are too strong to be accurately quantified by this method. The curve through the Gq(GDP) data is the fitted binding isotherm which gives a Kd = 0.2 ± 0.1 nM.

*Binding of RGS4 to Other Protein Partners*

The idea that RGS4 is part of a signaling complex implies that it has secondary interaction sites for other proteins in the inositol-signaling network. Therefore, we tested the possibility that RGS4 has multiple protein partners by measuring its ability to bind to recombinant C-G$\beta_1\gamma_2$. Binding studies were again done by titrating D-RGS4 into a solution of C-Gβγ reconstituted on lipid membranes and substituting dialysis buffer as a control. The results, shown in Figure 2, indicate a much weaker binding to these G

protein subunits, i.e., a 10-fold higher range of D-RGS4 was needed to achieve binding. The titration curves in Figure 2.2 shows an appropriate shift when the initial C-Gβγ concentration is changed from 10 to 2 nM. If the data in Figure 2 reflect equilibrium binding, then their Kd values should be similar whereas if the data in Figure 2.2 reflect stoichiometric binding, then the apparent K values would identical to the initial concentrations of C-G (i.e., 10 and 2 nM). We find that the dissociation constants are the same within error (5.3 ± 1.7 and 11.5 ± 4.5 nM, for 10 and 2 nM, respectively), indicating that we are viewing equilibrium binding.

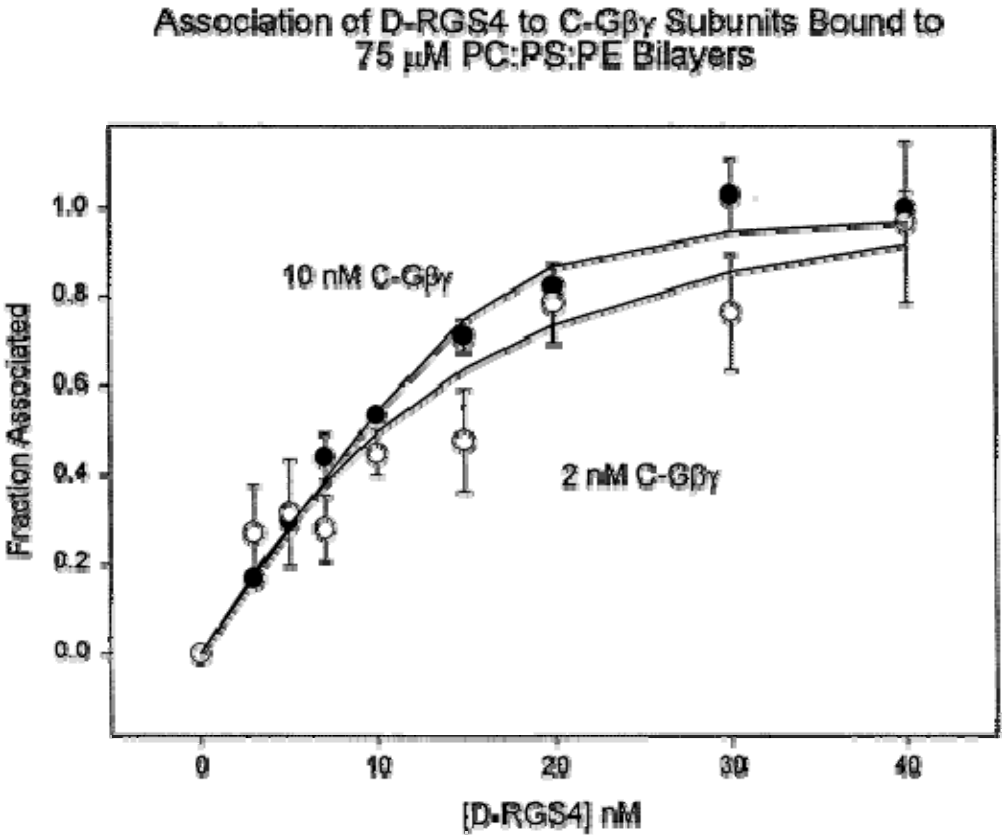


**Figure 2.2:** Plot showing the concentration dependence of the fraction of complex formed, as determined by the ~18% loss in coumarin fluorescence due to resonance energy transfer, between RGS4 and membrane-bound Gβγ subunits at a higher (10 nM, ●) and lower (2 nM, ○) where $n = 3$. The lines are the fitted binding isotherms, that both give similar values for Kd within error (see text).

We then measured the association of RGS4 to membrane-bound PLC$\beta_1$ by fluorescence energy transfer (Figure 2.3) using either buffer of trypsin-treated D-RGS4 as controls. We find that RGS4 binds to PLC$\beta_1$ with an apparent binding constant of 27± 10 nM. Although PLC$\beta_1$ binds very strongly to membranes, it is soluble in aqueous solution. Thus, we were able to compare the effect of lipid on protein association. No changes in the apparent dissociation constant was observed indicating that the site of interaction is not the membrane binding face of PLC$\beta_1$.

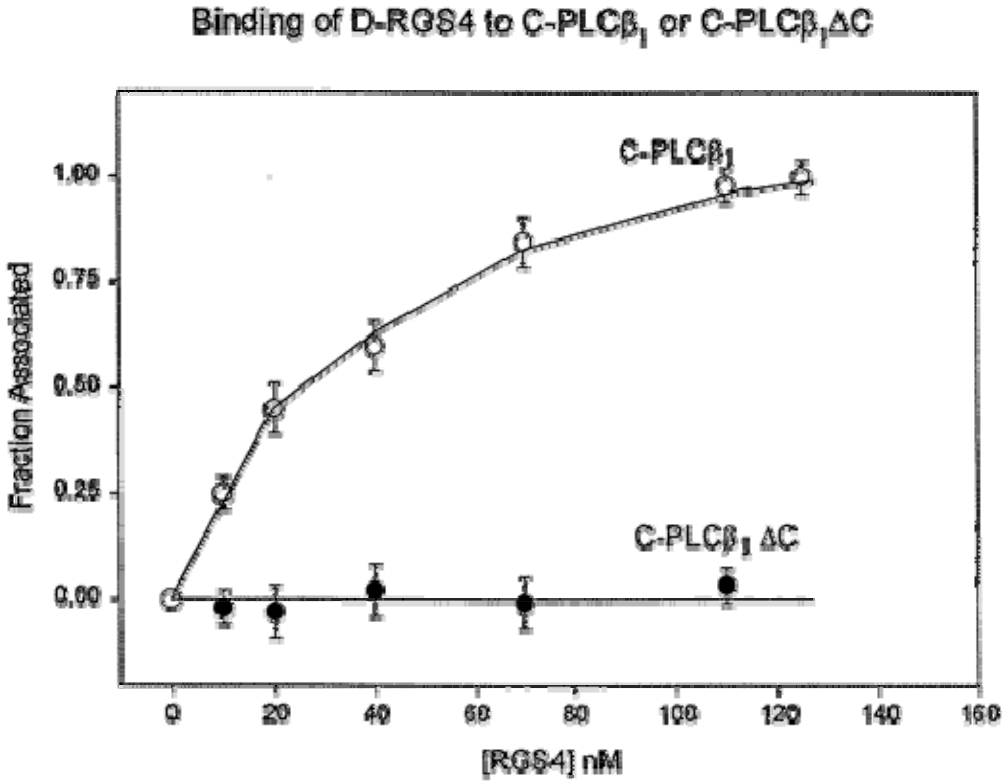


**Figure 2.3**: Plot showing the association, as determined by fluorescence resonance energy transfer that results in a ~16% loss in donor fluorescence, of RGS4 to PLC$\beta_1$ (○) ($n$ = 6) and a C-terminal truncated mutant (●) ($n$ = 3). Identical results were obtained in the presence of 75mM POPC:POPE:POPS (1:1:1) (data not shown).

*Identification of the Interaction Region between RGS4 and PLC$\beta_1$*

$G\alpha_q$ interacts with PLC$\beta_1$ on the regions immediately following the catalytic domain in the linear sequence (3) (10). To determine whether the RGS4 binding site of PLC$\beta_1$ is also localized on the C-terminal region, we measured the binding of RGS4 to a catalytically active, C-terminal deletion mutant of PLC$\beta_1$. No interactions can be seen between these proteins (Figure 2.3). Thus, either RGS4 binds to the C-terminal tail or removal of this tail results in misfolding of the interaction site.

Since receptor specificity of RGS proteins have been linked to its N-terminal domain, we measured the PLC$\beta_1$ binding of a synthetic peptide consisting of residues 1-33 of RGS4 in the absence of lipid membranes. In this series of experiments, the peptide was labeled with coumarin and dabsyl-PLC$\beta_1$ was the titration partner. Control studies using a coumarin-labeled synthetic peptide with a scrambled sequence showed no changes in fluorescence intensity. The results, presented in Figure 4, show that the peptides bind with affinities of 54 ± 13 nM for the 10 nM trials and 75 ± 13 nM for the 80 nM trials. Despite strong sequence homology (30), a peptide consisting of residues 1-33 of RGS16 showed a much weaker interaction with PLC$\beta_1$ (Figure 2.4).

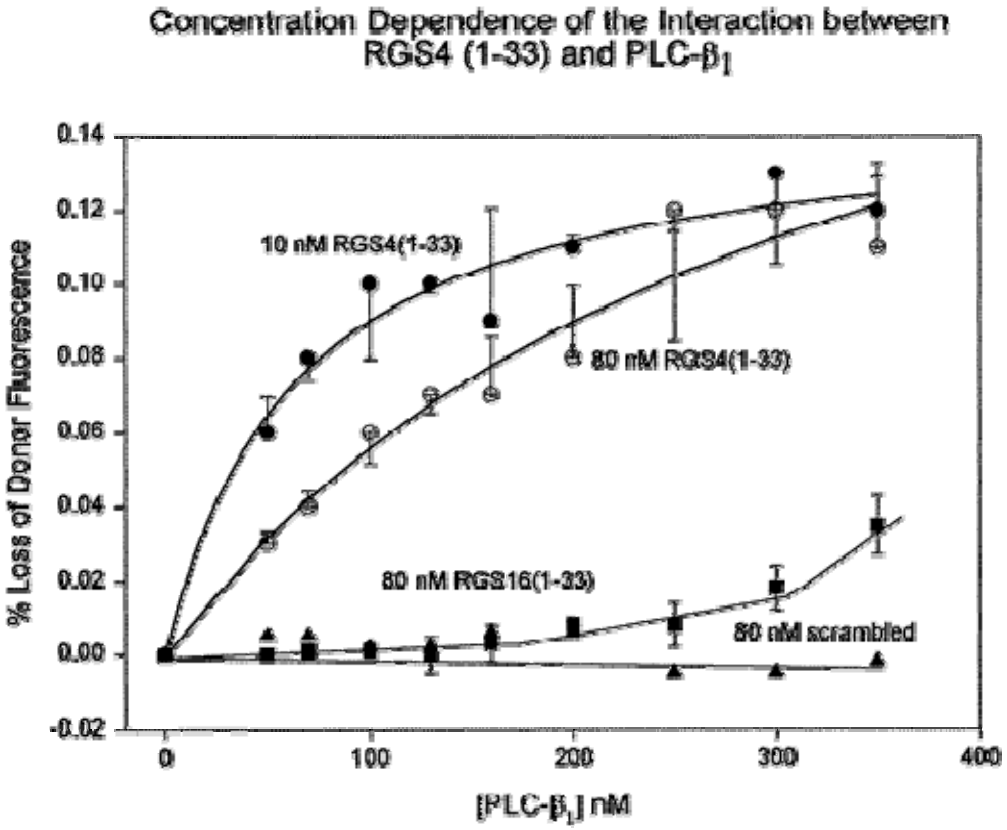


**Figure 2.4**: Concentration dependence of the interaction between the N-terminus of RGS4 and PLC$\beta_1$ as seen in the plot of the loss in donor fluorescence at two different RGS4(1-33) ($n$ = 3) concentrations, 10 nM (·) and 80 nM (○) relative to 80 nM of scrambled peptide (▲). The weak interaction between RGS16(1-33), (■) ($n$ = 3) and PLC$\beta_1$ is also shown.

*Formation of Ternary Complexes*

We explored the possibility that ternary complexes between RGS4, PLC$\beta_1$, and G$\alpha_q$(GTP$\gamma$S) can form. First, we formed complexes between C-RGS4 and G$\alpha_q$(GTP$\gamma$S) on membrane surfaces at concentrations well above the estimated dissociation constant (i.e., 10 nM of each) and titrated in D-PLC$\beta_1$. Although D-PLC$\beta_1$ bound to the complex, the binding was far weaker than the binding of PLC$\beta_1$ to G$\alpha_q$(GTP$\gamma$S) or for RGS4 (see Table 2.1). An example of the titration data, shown in Figure 2.5, shows that saturation is not reached even at high PLC$\beta_1$ concentrations. From these data, we estimate the apparent dissociation to be 300 ± 80 nM.

| **Table 2.1**: Summary of the Apparent $K_d$s of RGS4 to Protein Partners | |
|---|---|
| | RGS4 |
| $G\alpha_q$(GTPγS) | <0.1 nM |
| $G\alpha_q$(GDP) | 0.2 nM |
| Gβγ | 8.4 nM |
| $PLC\beta_1$ | 27 nM |
| $PLC\beta_1$delta*C* | no binding |
| {$PLC\beta_1$-$G\alpha_q$(GTPγS)} | 300 |

The data in Figure 2.5 could correspond to formation of a weak ternary complex as well as to the binary association between D-$PLC\beta_1$ and C-RGS4 in the presence of competing $G\alpha_q$(GTPγS). Thus, we conducted several follow-up studies to determine which is the predominant case. In one series of studies we labeled each protein with Oregon Green and assessed the amount of fluorescence homotransfer that occurs when all three proteins are in the solution (see refs (3) and (31) for background and methodology) at 140-210 nM total protein. The formation of binary complexes results in a reduction in fluorescence anisotropy of 10-15% for this probe. The addition of the third component caused a further (i.e., 7%) reduction in anisotropy, indicating that some of the proteins are aggregating into a ternary complex. In a second series of studies, we added a large excess (400 nM) of unlabeled RGS4 to a 1 nM solution of C-$G\alpha_q$(GTPγS)-D-$PLC\beta_1$. If RGS4 contributed to disparate heterodimes at this RGS4 concentration, we would expect displacement of C-$G\alpha_q$(GTPγS) from D-$PLC\beta_1$ by RGS4 and reversal of the 16% decrease in $G\alpha_q$(GTPγS) fluorescence due to energy transfer. However, no significant changes in fluorescence were observed. In a third series of studies, we measured the ability of unlabeled $PLC\beta_1$ to dissociate C-$G\alpha_q$-D-RGS4 both at 1 nM concentration reconstituted on lipid bilayers. Addition of 100 nM $PLC\beta_1$ increased the donor intensity

by 40% and addition of 250 nM PLC$\beta_1$ increased the intensity 10-fold indicating that PLC$\beta_1$ is inducing some changes in the local environment around the coumarin probe. Since this increase is far greater than the change one would expect by a simple displacement of the energy transfer pair. This result indicates that PLC$\beta_1$ is interacting with the G$\alpha_q$(GTP$\gamma$S)-RGS4 complex. However, the nature and extent of this complex formation is not clear.

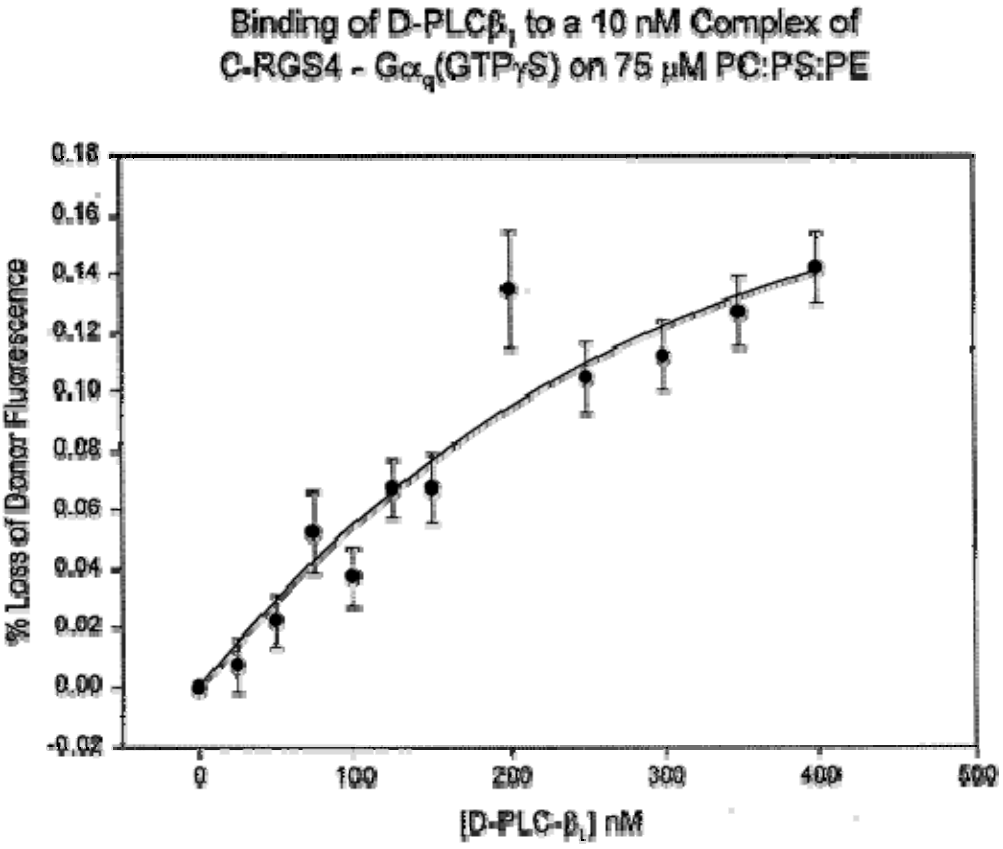


**Figure 2.5:** Binding of D-PLC$\beta_1$ and the C-RGS4-G$\alpha_q$(GTP$\gamma$S) complex ($n$ = 5).

*RGS4 Binds Weakly to Membranes, But Can Be Recruited by PI(3,4,5)$P_3$ and PLC$\beta_1$*

To analyze the protein interactions observed in the above studies, we needed to know whether RGS4 is soluble in the aqueous phase or whether it is membrane bound and laterally associates with PLC$\beta_1$ and G$\alpha_q$ under our conditions (see discussion). We thus measured the membrane partition coefficient of RGS4 alone and in the presence of two membrane-localized partners.

Membrane binding was assessed by several types of fluorescence methods: changes in intrinsic fluorescence as the protein associates to the membrane surface, changes in the fluorescence of coumarin-labeled RGS4, energy transfer between RGS4 Trp donors and membranes doped with a fluorescent probe, and membranes doped with a detergent-like fluorescent probe (Laurdan) that is sensitive to changes in the polarity of the membrane surface. We found that the method that was most sensitive to membrane binding was the ~20% decrease in Trp/Try fluorescence upon membrane binding probably due to quenching of these fluorophores by the ionic headgroups of the lipid. By following the change in intrinsic fluorescence upon membrane binding, we found that binding to large, unilamellar vesicles composed of PC:PS:PE (1:1:1) was weak ($K_p \approx 1$ mM). However, membrane affinity could be increased at least three ways. First, since the binding of RGS4 to membranes has a strong electrical component, (32) we found that the partition coefficient changes to $K_p \approx 300$ μM if we used membranes composed entirely of negatively charged lipids (i.e., POPS). This increase from a weak binding affinity due to negatively charged lipids is supported by sedimentation studies using sucrose-loaded vesicles (A. Arbouzova and S. McLaughlin, unpublished results). Second, the presence of 33% PI(3,4,5)$P_3$ with 67% PC increases the binding affinity to $K_p$ 30 ± 10 μM (Figure

2.6). Third, incorporation of PLC$\beta_1$ increased the affinity to PC:PS:PE (1:1:1) bilayers to $K_p$ = 50 ± 18 μM indicating that RGS4 can also bind to membranes through protein-protein contacts in addition to protein-lipid.

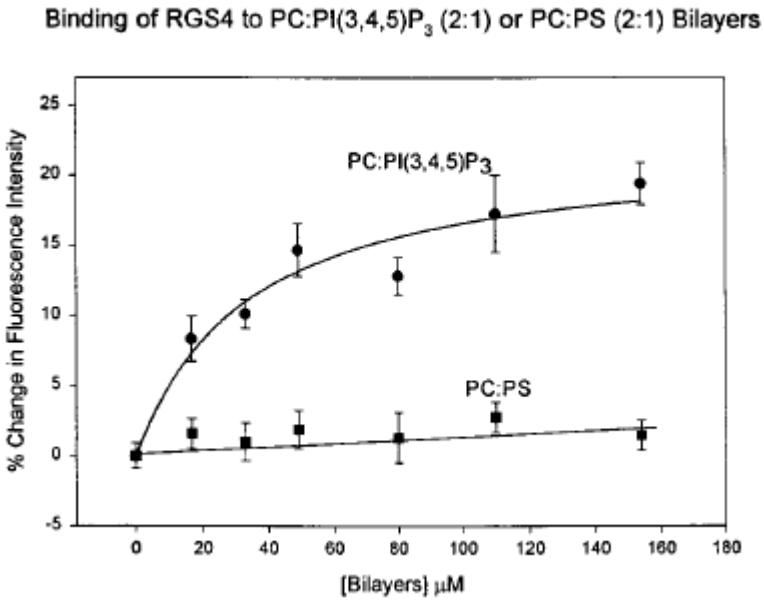


**Figure 2.6:** Comparison of the membrane association, monitored by the _20% decrease in intrinsic fluorescence, of RGS4 to POPC:PI(3,4,5)P3 (2:1) or POPC:POPS (2:1) where *n*=3.

**Discussion**

In this study, we have determined the apparent affinities between RGS4 and G protein subunits and the G protein effector, PLC$\beta_1$. Before analyzing the energies associated with these protein-protein interactions, it is important to know whether RGS4 is concentrated on the membrane surface or freely diffusing in solution. Thus, we measured the affinity of RGS4 to model membranes and found that RGS4 bound only weakly to bilayers containing physiological concentrations of negatively charged lipids (Gennis, et al). Therefore, at the low lipid concentrations used in this study, we will treat

our protein association data assuming that RGS4 is soluble and freely diffusing in solution (see below).

Our membrane-binding results are in accord with Berstein and co-workers (32), who worked at higher (i.e., 1 mM) lipid concentrations to show that RGS4 binds to membranes through an N-terminal amphipathic helix which contributes to its preference for negatively charged lipids. We have found here that the membrane affinity of RGS4 is greatly increased by the presence of $PI(3,4,5)P_3$ to an extent greater than would be expected by charge alone. Specific interactions between RGS4 and $PI(3,4,5)P_3$ have been previously reported (20), and these interactions have the effect of inhibiting the RGS4 GAP activity possibly by occluding RGS4 residues that also interact with Gα subunits. This $PI(3,4,5)P_3$-RGS4 association has been proposed to be part of a feedback mechanism that initially keeps RGS4 sequestered after PI-3-kinase stimulation at the early phase of a G protein signal that produces a high local concentration of $PI(3,4,5)P_3$. As $Ca^{2+}$ levels in the cell increase, RGS4 can be displaced from the membrane by $Ca^{2+}$/calmodulin to deactivate Gα subunits (33).

We also found that RGS4 can be recruited to the membrane by the incorporation of a protein-binding partner due to strong protein interactions (see below). This result implies that if $PIP(3,4,5)P_3$ was also present, then recruitment would be multiplicative unless the two sites on RGS4 were the same. Unfortunately, this idea was not directly testable due to the strong background contribution of $PLC\beta_1$ to the fluorescence assay. Localization of RGS4 by a protein partner has been suggested by studies showing that most of the cytosolic RGS4 can be recruited to the membrane surface by overexpression of a GTPase-deficient $G\alpha_{i2}$ by a region outside the RGS domain (34).

The protein partners of RGS4 studied here are all membrane bound. Since we conducted studies under conditions where soluble RGS4 bound to proteins that were dilute on the membrane surface, we can analyze the dissociation constants assuming a biomolecular association without the need to invoke models that account for membrane association. These are listed in Table 2.1. Note that our estimated picomolar affinity between RGS4 and activated $G\alpha_q$ are in accord with the subnamolar affinity determined for RGS4 and activated $G\alpha_{i1}$ by surface plasma resonance techniques (17). We find that the affinity between RGS4 and activated $G\alpha_q$ was too strong to be quantified by fluorescence energy transfer, but deactivation of $G\alpha_q$ put it in a detectable range. Even so, the association between RGS4 and $G\alpha_q$(GDP) is remarkably strong and this strong residual interaction may keep RGS4 colocalized to the protein complex in the basal state. However, it is expected that other proteins, most notably $G\beta\gamma$ and $G\alpha_q$-specific receptors, would compete with RGS4 for deactivated $G\alpha_q$. A comparison of the crystal structure of the $G\alpha_{i1}$ (GDP-$AF_4^-$)-RGS4 (4) complex with the structure of $G\alpha_{i1}$(GDP)-$G\beta\gamma$ (35) shows that both RGS4 and $G\beta\gamma$ interact with $G\alpha$ switch regions and the complexes formed will be dictated by their relative interaction energies. A direct comparison of the affinities between $G\alpha_q$(GDP)-RGS4 and $G\alpha_q$(GDP)-$\beta\gamma$ derived from fluorescence studies is not possible since the G protein subunits are confined to the membrane surface whereas RGS4 is not. Thus, depending on the available area in which the G protein subunits can laterally associate, their effective concentration is expected to be much higher than the freely diffusing RGS4. From our previous studies that translated the apparent dissociation constant between membrane-bound $G\alpha_q$(GDP) and $G\beta\gamma$ into a $K_d$ that was independent of

lipid (27), we find that, at local lipid concentrations of ~20 μM, Gβγ should compete with RGS4 for deactivated $G\alpha_q$(GDP).

Interestingly, we find that although Gβγ may displace RGS4 from deactivated $G\alpha_q$, it could also serve as a binding partner for RGS4 (Figure 2.2 and Table 2.1). The RGS4 affinity for Gβγ is much weaker than for $G\alpha_q$, but this secondary interaction may serve to keep RGS4 localized in the signaling complex and possibly in an optimal orientation for $G\alpha_q$ rebinding. It may also allow productive palmitoylation on the N-terminus but inhibit palmitoylation at sites in the RGS domain which eliminate its GAP activity (36). It is noteworthy that some RGS families have Gγ-like domains that allow for strong interaction with Gα subunits (see (33)).

We also found that RGS4 will interact with the $G\alpha_q$ protein effector $PLC\beta_1$ which also has GAP activity. This interaction may offer another site which localizes RGS4 in the signaling complex. Unlike RGS4, $PLC\beta_1$ binds strongly to membranes (Reddy *et al*) and will interact laterally with $G\alpha_q$ subunits, but not with Gβγ subunits. Comparing the RGS4-$G\alpha_q$ affinities obtained here to previously determined $PLC\beta_1$-$G\alpha_q$ affinities (3), we find that the primary $PLC\beta_1$ interaction will be expected to be competitive with RGS4 interaction to activated and deactivated $G\alpha_q$ at local lipid concentrations below 100 μM.

Our results suggest that RGS4, $G\alpha_q$(GTPγS), and $PLC\beta_1$ may form weakly associating ternary complexes. We find a 10-fold decrease in the affinity of RGS4 to $PLC\beta_1$ in the presence of $G\alpha_q$(GTPγS). Since the RGS4 interaction with $PLC\beta_1$ appears to be mediated by the C-terminal tail (Figure 2.3), which also partially binds $G\alpha_q$, then the reduction in affinity may be due to occlusion in this region or binding-induced

conformational changes. The suggestion that ternary complexes form at higher concentrations of protein is in accord with previous studies by Helper and co-workers, who worked at lower protein concentrations and found that RGS4 blocks PLC$\beta_1$ activation by G$\alpha_q$(GTP$\gamma$S) (36). It is possible that at high local concentrations of proteins, the close proximity of the two GAPs allows them to rapidly switch off and on G$\alpha$ and greatly increase the rate in which the signal is turned over.

The inherently weak membrane affinity in the absence of PI(3,4,5)$P_3$ and protein partners raises the possibility that RGS4 can be cytosolic and diffuse between different signaling complexes on the plasma membrane depending on the availability of interaction sites, and regulation of RGS4 action may occur by its membrane recruitment. However, the strong interaction of RGS4 with G protein subunits, with G protein effectors, coupled with previous kinetic studies suggesting RGS4 localization with G protein receptors (19) leads to the idea that these proteins may be complexed in a signaling domain through contact of secondary sites. More so, the strength of this association suggests that scaffolding proteins may not be required. Evidence for the localization of RGS4 to a signaling complex comes from studies showing that RGS4 selectively inhibits G$\alpha_q$ responses from particular G-protein receptors indicating that RGS4 is localized to particular receptor types and that localization occurs through the first 33 residues (19). These studies are in accord with our data indicating that, although RGS4 has weak membrane binding ability, it has many partners besides activated G$\alpha$ that can keep it localized to particular areas in cells. In addition, the suggestion that the N-terminus of RGS4 plays a role in PLC$\beta_1$ effector association, along with the suggestion that this

region plays a key role in receptor interaction implies that this region of RGS4 can transfer its protein partner depending on the local conditions.

The results obtained here can be summarized in the cartoon shown in Figure 2.7. In the unstimulated state, $G\alpha_q$(GDP) will be associated with $G\beta\gamma$ at local lipid concentrations of $\leq$20 $\mu$M. Compared to $G\beta\gamma$, $PLC\beta_1$ has a much weaker affinity for $G\alpha_q$(GDP), and the binding of $PLC\beta_1$ to the deactivated heterotrimer and to $G\beta\gamma$ is very weak. Thus, unless the local protein concentrations are high, $PLC\beta_1$ would be expected to either be dissociated from the G protein heterotimer or only loosely associated. Also, RGS4, which can diffuse through the cytoplasm, can associate with membrane-bound $PLC\beta_1$ which in turn facilitates its palmitoylation and keeps it in close proximity to $G\alpha_q$. Upon activation of $G\alpha_q$, $PLC\beta_1$ can displace $G\beta\gamma$ to become activated, but since the effector-bound RGS4 may be situated very close to $G\alpha_q$, it can compete with $PLC\beta_1$ for the full interaction site. It is possible that RGS4 competes with $PLC\beta_1$ for the initial binding to $G\alpha_q$, which would diminish the strength of the signal. Kinetic studies by Ross and co-workers in a reconstituted system show that RGS4 affects the signal duration rather than amplitude (16). The cartoon in Figure 2.7 is a greatly simplified model of the interactions that may occur in a signaling complex, but it may be used as a basis to better define the factors that enhance or antagonize these associations. While it is tempting to define these interactions in terms of composites of free energies as derived from the dissociation constants, the observation that the same interaction sites can be partially occluded from other protein partners means that the energies are not simply additive, and this adds another level of complexity to understanding the interactions in signaling domains.

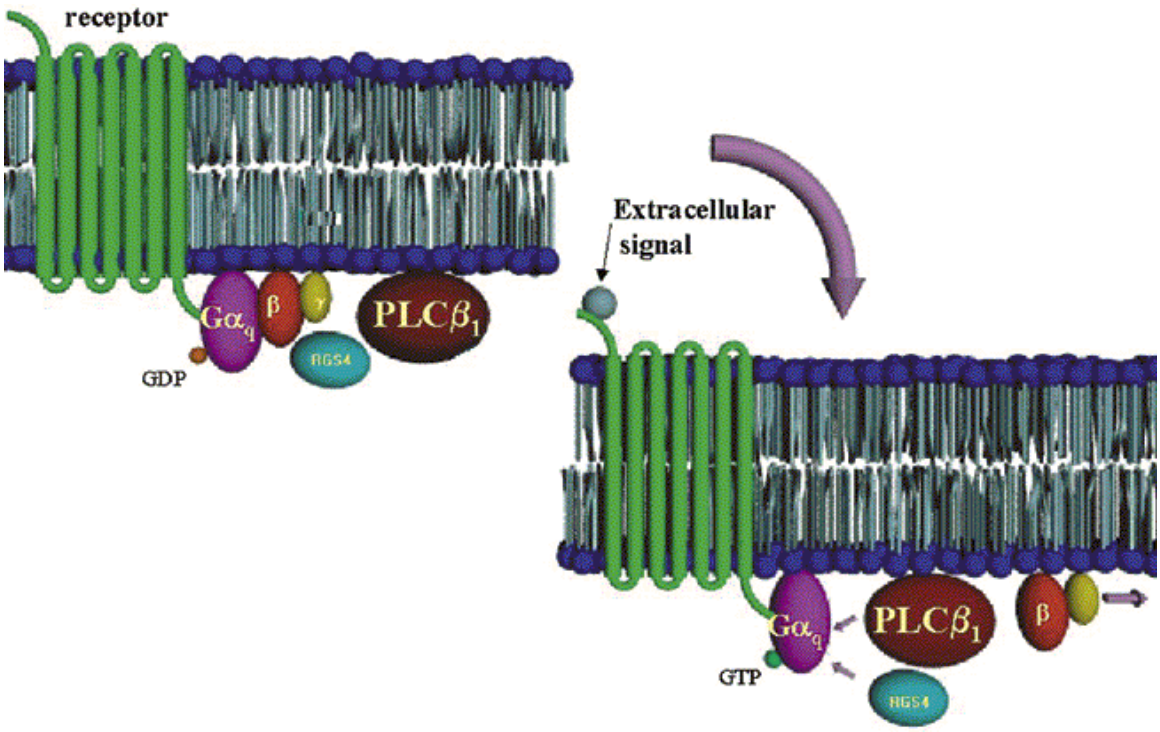


**Figure 2.7:** Model of possible RGS4 interactions with PLC$\beta_1$ and G protein subunits that may accompany stimulation (see text for details).

## Literature Cited


1. Bourne, H. R., Sanders, D. A., and McCormick, F. (1991) *Nature* 349(6305), 117-127
2. Hepler, J. R., and Gilman, A. G. (1992) *Trends Biochem Sci* 17(10), 383-387
3. Runnels, L. W., and Scarlata, S. F. (1999) *Biochemistry* 38(5), 1488-1496
4. Tesmer, J. J., Berman, D. M., Gilman, A. G., and Sprang, S. R. (1997) *Cell* 89(2), 251-261
5. Neer, E. J. (1995) *Cell* 80(2), 249-257
6. Rebecchi, M. J., and Pentyala, S. N. (2000) *Physiol Rev* 80(4), 1291-1335
7. Williams, R. L., and Katan, M. (1996) *Structure* 4(12), 1387-1394
8. Wang, T., Pentyala, S., Rebecchi, M. J., and Scarlata, S. (1999) *Biochemistry* 38(5), 1517-1524
9. Wang, T., Dowal, L., El-Maghrabi, M. R., Rebecchi, M., and Scarlata, S. (2000) *J Biol Chem* 275(11), 7466-7469
10. Wang, T., Pentyala, S., Elliott, J. T., Dowal, L., Gupta, E., Rebecchi, M. J., and Scarlata, S. (1999) *Proc Natl Acad Sci U S A* 96(14), 7843-7846
11. Wu, D., Jiang, H., Katz, A., and Simon, M. I. (1993) *J Biol Chem* 268(5), 3704-3709
12. Park, D., Jhon, D. Y., Lee, C. W., Ryu, S. H., and Rhee, S. G. (1993) *J Biol Chem* 268(5), 3710-3714

13. Lee, S. B., Shin, S. H., Hepler, J. R., Gilman, A. G., and Rhee, S. G. (1993) *J Biol Chem* 268(34), 25952-25957
14. Biddlecome, G. H., Berstein, G., and Ross, E. M. (1996) *J Biol Chem* 271(14), 7999-8007
15. Berman, D. M., and Gilman, A. G. (1998) *J Biol Chem* 273(3), 1269-1272
16. Chidiac, P., and Ross, E. M. (1999) *J Biol Chem* 274(28), 19639-19643
17. Popov, S., Yu, K., Kozasa, T., and Wilkie, T. M. (1997) *Proc Natl Acad Sci U S A* 94(14), 7216-7220
18. Srinivasa, S. P., Bernstein, L. S., Blumer, K. J., and Linder, M. E. (1998) *Proc Natl Acad Sci U S A* 95(10), 5584-5589
19. Zeng, W., Xu, X., Popov, S., Mukhopadhyay, S., Chidiac, P., Swistok, J., Danho, W., Yagaloff, K. A., Fisher, S. L., Ross, E. M., Muallem, S., and Wilkie, T. M. (1998) *J Biol Chem* 273(52), 34687-34690
20. Okamoto, T., Schlegel, A., Scherer, P. E., and Lisanti, M. P. (1998) *J Biol Chem* 273(10), 5419-5422
21. Schlegel, A., Volonte, D., Engelman, J. A., Galbiati, F., Mehta, P., Zhang, X. L., Scherer, P. E., and Lisanti, M. P. (1998) *Cell Signal* 10(7), 457-463
22. Anderson, R. G. (1998) *Annu Rev Biochem* 67, 199-225
23. Xiao, Z., and Devreotes, P. N. (1997) *Mol Biol Cell* 8(5), 855-869
24. de Weerd, W. F., and Leeb-Lundberg, L. M. (1997) *J Biol Chem* 272(28), 17858-17866
25. Tsunoda, S., Sierralta, J., Sun, Y., Bodner, R., Suzuki, E., Becker, A., Socolich, M., and Zuker, C. S. (1997) *Nature* 388(6639), 243-249
26. Runnels, L. W., and Scarlata, S. F. (1998) *Biochemistry* 37(44), 15563-15574
27. Berman, D. M., Kozasa, T., and Gilman, A. G. (1996) *J Biol Chem* 271(44), 27209-27212
28. Runnels, L. W., Jenco, J., Morris, A., and Scarlata, S. (1996) *Biochemistry* 35(51), 16824-16832
29. Reddy, K., Saady, M., and Falck, J. (1995) *J. Org. Chem.* 60, 3385-3390
30. Bernstein, L. S., Grillo, A. A., Loranger, S. S., and Linder, M. E. (2000) *J Biol Chem* 275(24), 18520-18526
31. Gennis, R. B. (1989)
32. Popov, S. G., Krishna, U. M., Falck, J. R., and Wilkie, T. M. (2000) *J Biol Chem* 275(25), 18962-18968
33. Ross, E. M., and Wilkie, T. M. (2000) *Annu Rev Biochem* 69, 795-827
34. Wall, M. A., Coleman, D. E., Lee, E., Iniguez-Lluhi, J. A., Posner, B. A., Gilman, A. G., and Sprang, S. R. (1995) *Cell* 83(6), 1047-1058
35. Tu, Y., Popov, S., Slaughter, C., and Ross, E. M. (1999) *J Biol Chem* 274(53), 38260-38267
36. Hepler, J. R., Berman, D. M., Gilman, A. G., and Kozasa, T. (1997) *Proc Natl Acad Sci U S A* 94(2), 428-432

## Chapter 3: Gα(q) and its Phospholipase Cβ$_1$ Effector are Complexed in Unstimulated Cells

This work has been published: Louisa Dowal, Paxton Provitera, and Suzanne Scarlata. *Gα(q) and its Phospholipase Cβ$_1$ Effector are Complexed in Unstimulated Cells*. Journal of Biological Chemistry, 2006. **281**(33):23999-4014.

The Gα$_q$ family of G proteins transduces signals connected to agents such as angiotensin II, catecholamines, endothelin 1, and prostaglandinF2α. In its activated GTP-bound state,Gα$_q$ will stimulate the catalytic activity of its main effector phospholipase C_ (PLCβ). PLCβ enzymes catalyze the hydrolysis of the signaling lipid, phosphatidylinositol 4,5-bisphosphate, to generate two second messengers that result in an increase in intracellular $Ca^{2+}$ and a host of proliferative and mitogenic changes in the cell (for review see (1) and (2)). There are four forms of PLCβ (PLCβ$_{1-4}$) that differ in their tissue distribution and their regulation by G protein subunits. Here we will focus on PLCβ$_1$, which is strongly activated by Gα$_q$ subunits. PLCβ$_1$ is widely distributed and is most highly expressed in neuronal tissue where it may participate in rapid intracellular $Ca^{2+}$ signaling (2).

Activation of PLCβ$_1$ by Gα$_q$(GTP) is thought to occur through direct contact between the enzyme and the activated G protein subunit. This idea stems from the close correlation between the lateral association of PLCβ$_{1-3}$ and Gβγ subunits and the concentration dependence of activation (3). However, this mechanism may differ from Gα subunits that undergo significant conformational changes upon activation unlike Gβγ

subunits (4).

The rate of activation of PLC$\beta_1$ by G$\alpha_q$(GTP) will depend on the rate of association and the rate of the conformational changes that lead to effector activation. If the two proteins are complexed prior to G$\alpha_q$ activation, the signal will no longer depend on the diffusion rates of the two proteins, and the on rate of PLC$\beta_1$ activation would be greatly accelerated. There is now accumulating evidence that higher order complexes of signaling proteins exist in cells. Ross and co-workers (5) found that the rate of G$\alpha_q$-PLC$\beta_1$ signaling was so rapid that dissociation of G$\alpha_q$ from the receptor was not probable, and indeed, association between seven transmembrane receptors and G$\alpha_q$ has been observed in cells (6). In *Drosophila,* a signaling complex involving receptor, a PLC$\beta$ homolog, a protein kinase C homolog, and a scaffold protein has been identified (7). More evidence for signaling complexes comes from RGS4-dependent $Ca^{2+}$ oscillations in cells using a PLC-$\beta$ agonist (8), suggesting that the G protein-coupled receptor, the G protein heterotrimer, and PLC could be localized in a signaling complex. Although these studies are suggestive, to date the physical association of a G protein subunit and its corresponding effector have not yet been reported in living cells.

Although preformed G protein-effector complexes would not only give rise to rapid signals as mentioned above, the localization of the signal would no longer depend on the localization of the two proteins but rather on the diffusion of the products generated. Most importantly, these signals would only be generated by a specific receptor type. For PLC$\beta_1$-G$\alpha_q$, the second messengers generated are expected to have very rapid diffusion as compared with the proteins, thus further enhancing signal speed.

The ability of proteins to form complexes depends on their local concentration as well as their affinities. We have previously used fluorescence methods to quantify the affinities of PLCβ enzymes to Gαq, Gβγ, and other components in this pathway on model membranes using purified proteins ((9) and (10)). As expected, the binding of $PLC\beta_1$ to $G\alpha_q(GTP\gamma S)$ is extremely strong as compared with binding to deactivated $G\alpha_q$. Although this reduction in affinity is significant, it is important to note that if the local cellular concentrations of $PLC\beta_1$ and $G\alpha_q$ are above this dissociation constant, then they would remain together in the activated as well as the deactivated states.

In this study, we have determined the ability of $PLC\beta_1$ and $G\alpha_q$ to form complexes in the basal and stimulated states *in vitro* and in two cell lines using fluorescence resonance energy transfer (FRET) between fluorescent-tagged proteins. FRET measurements are based on the probability of transfer of excited energy from a donor fluorophore to an acceptor. This probability depends on the electronic properties of the donor and acceptor as well as their intermolecular distance (11) and (12). Because the amount of FRET depends on the 6th power of this distance, it is a sensitive measure of protein-protein associations. For the eCFP-eYFP donor-acceptor FRET pair, the distance at which 50% of the donor fluorescence is lost to transfer is 30 Å, making this pair useful to monitor protein association (13). By using this method, we find that $PLC\beta_1$ and $G\alpha_q$ are complexed even when $G\alpha_q$ is in the deactivated state, although the nature of the association differs. In cells, we find that these proteins are strongly complexed in the unstimulated state despite their low affinity. These pre-formed $PLC\beta_1$-$G\alpha_q(GTP\gamma S)$ complexes allow for rapid signaling through changes in protein orientation during G protein turnover and delocalization of the signal through diffusion of the second

messengers produced by activation. Based on the cellular concentration of the proteins and their affinities, our results suggest that co-localization must occur through unidentified factors.

## Materials and Methods

*Reagents*

eCFP-$G\alpha_q$ was derived from $G\alpha_q$-GFP as previously described (14) and was a generous gift from Dr. Catherine Berlot (Geisinger Clinic, Danville, PA) as were the constituatively active eCFP-$G\alpha_q$ (R183C) (eCFP-$G\alpha_q$RC) (15), and eCFP-$G\beta_1$ (see)(16). eYFP-PLC$\beta_1$ was a generous gift from Loren Runnels (Dept. of Cell Biology, Rutgers University). This construct shows wild type basal activity and activation by $G\alpha_q$.

*In vitro FRET studies*

In vitro affinities between PLCβ1 and Gαq(GTPγS) or Gαq(GDP) were determined as previously described (10). Briefly, the proteins were expressed in Sf9 cells through a baculovirus system and purified. GDP-bound Gαq was then labeled with an amine reactive probe, coumarin SE (Molecular Probes, Inc.) and reconstituted on large unilamellar vesicles composed of POPC:POPS:POPE (1:1:1) and the center of spectra mass and intensity was monitored as purified, unlabeled PLCβ1 was incrementally added. Gαq was activated using the procedure of (17). This procedure results in at least 80% nucleotide exchange.

*Trypsin digestion*

Samples of either PLCβ1 alone or in a 1:1 mixture with Gαq(GTPγS) or Gαq(GDP) were preincubated on ice before the addition of trypsin. Proteolysis was allowed to proceed at 37$^{o}$C for either 5 or 20 minutes before addition of 10% SDS. Samples were then boiled for 3 minutes and subjected to SDS PAGE electrophoresis. Bands were visualized using silver stain.

*Cell Culture and Transfection*

Rat pheochromocytoma cells (PC12), derived from the adrenal gland (ATCC, #CRL-1721), were cultured in Dulbecco's modified Eagle's medium (DMEM) supplemented with 10% equine serum, 5% fetal bovine serum, and 100mM sodium pyruvate and were incubated at 37$^{o}$ C with 5% $CO_2$. Nerve growth factor (NGF, Sigma, St. Louis, MO) was added to a final concentration of 100ng/ml to induce differentiation. Prior to transfection, cells were grown in T-25 flasks to 80-90% confluency.

Plasmids were introduced into cells by electroporation using a protocol adapted from Maniatis (18). Briefly, the DMEM was aspirated, and the PC12 cells were harvested by adding 5mL of fresh media and pipetting multiple times over the bottom of the flask. Cells were spun down for 5 minutes at 1500 x g and resuspended in 5mL of phosphate buffered saline (PBS). One mL of cells was removed, counted, and the cell suspension was diluted to 5 x $10^6$ cells/ml. Cells (500μL) were pipeted into 0.4cm BioRad cuvettes and incubated on ice for 10 minutes. Then, 10-30 μg of plasmid DNA was added to each cuvette and gently mixed. The electroporator (BioRad Gene Pulser Xcell) was set to 0.25 kV with a capacitance of 500 μF. Cuvettes were placed in the

shocking chamber and pulsed once. After the pulse, the cells were allowed to rest for 1-2 minutes and 1mL of DMEM was then added to each cuvette. Cells were placed in 15mL conical tubes containing 3 mL of DMEM. Tubes were spun down at 1500 x g for five minutes and cells were brought up in 1.5 mL DMEM and plated onto Lab Tek chambers coated with 50μg/mL fibronectin (Sigma). Three to four hours post-transfection, the wells were washed with 1mL PBS and 1.5mL DMEM containing 100ng/mL NGF was added. After three days of incubation with NGF, transfected cells were differentiated and used for imaging.

HEK cells were cultured in DMEM plus 10% FBS and 1% PenStrep at 37ºC with 5% $CO_2$. Plasmids were introduced to HEK cells as described except they were not preincubated on ice before the pulse, and the electroporator was set to 0.2kV with a 960μF capacitance.

*Calcium Release*

PC12 cells, in T-25 flasks, were washed two times with PBS. Cells were collected in Hank's Buffered Salt Solution (HBSS, 15mM Hepes (pH 7.67), 118mM NaCl, 5mM KCl, 1mM $CaCl_2$, 1mM $MgCl_2$, 5mM glucose, and 1mg/ml BSA) and spun down at 1500 x g. Cells were counted and adjusted to a concentration of $1 \times 10^7$ cells/ml. Fura-2 AM (5 mM) (Sigma) was added to the cells, and cells were incubated in the dark at 37° C for 40 minutes with rotation. After labeling, cells were spun down at 1500 x g and resuspended in HBSS. To make measurements, cells were diluted to $1.0 \times 10^6$

cells/ml in HBSS. One mL cell suspensions were put into a cuvette with a stir bar and placed in the fluorometer. The samples were excited at 340 and 380nm and the emission was measured at 510nm, and the ratios of the two excitations were recorded over time.

To measure calcium release upon stimulation, cells were stimulated with 1μM acetylcholine or carbocol, and the ratio was measured again. To break open the cells, 10% Triton X-100 was added followed by calcium chelation with 2 mM EDTA to obtain the maximal and minimal amounts. To calculate internal calcium concentration:

$$[Ca^{2+}]_i \text{ free(nM)} = [(R-R_{min})/(R_{max}-R)] \times [F_{max380}/F_{min380}] \times 225$$

where R is the measured ratio (fluorescence emitted at 340 and 380nm), $R_{min}$ and $R_{max}$ are the ratios with EDTA and detergent, $F_{min}$ is the fluorescence in the presence of EDTA (i.e. minimum calcium) and $F_{max}$ the fluorescence in the presence of detergent (i.e. maximum calcium). The $K_d$ of Fura-2 AM is ~ 225nM (19).

*Cell Fractionation and Western Blot Analysis*

PC12 cells were transfected with protein expression vectors as described above. Five identical transfections were combined into a T-25 flask and differentiated for three days with NGF. Then, PC12 cells were harvested from T25 flasks and washed two times with PBS. After the second wash, the cells were brought up in PBS containing 1mM PMSF and 10μg/ml aprotinin, placed on ice, and homogenized. Nuclei were removed by a low speed centrifugation at 750 x g for five minutes at $4^o$ C. The supernatant was removed and spun at 28,000 rpm for 35 minutes at 4 C. The supernatant or cytosolic fraction was removed and the resulting pellet or membrane fraction was brought up in PBS containing 1mM PMSF and 10μg/ml aprotinin. The protein concentration for the

cytosolic and membrane fractions was assayed and 4-15μg was loaded into each well of a SDS-PAGE gel. Proteins were then transferred to nitrocellulose; the membrane was blocked overnight, and then probed for $G\alpha_q$ and $PLC\beta_1$ using a 1:200 dilution for primary antibody (Santa Cruz) and 1:2000 dilution for secondary (Sigma). Western blots were developed using alkaline phosphatase reaction, and the amount of over-expressed protein per μg of protein loaded was calculated using a standard curve generated from purified $G\alpha_q$ and $PLC\beta_1$.

*Immunofluorescence*

For secondary immunofluorescence for endogenous expression of $G\alpha_q$ and $PLC\beta_1$, PC12 cells were plated and differentiated as described above. The cells were washed twice with PBS and fixed with 1.5 ml of 3% paraformaldehyde at room temperature for 10 minutes. The fixing solution was removed, and the cells were washed three times for 10 minutes each with MSM-PIPES Buffer (Modified Shierdls Media; 18mM $MgSO_4$, 5mM $CaCl_2$, 40mM KCl, 24mM NaCl, 5mM PIPE (pH = 6.8), 0.5% Triton X-100, 0.5% Nonidet P-40). After washing, the cells were blocked in PBS containing 5% goat serum, 1% BSA and 50mM glycine for 15 minutes. Cells were incubated with the primary antibody (1:200 dilution) in PBS containing 0.5% BSA at 37°C for 1 hour, and then washed 3 times with PBS for 10 minutes each. Cells were incubated with FITC-conjugated secondary antibody (1:2000 dilution) in PBS containing 0.5% BSA at 37°C for 1 hour, and then washed 3 times with PBS for 10 minutes each. PBS was then added to wells and the cells were imaged.

*Preparation of membrane fractions*

HEK-293 cells (12.5 x $10^6$ per 150-mm dish) were transfected using DEAE-dextran (20) or using 62.5 μl of Lipofectamine 2000 Reagent (Invitrogen) according to the manufacturer's instructions. 48 hours after transfection, membranes were prepared as described (21). The amounts of plasmids used in the transfections are given in the legend to Fig. 7.

*Instrumentation*

Confocal images were taken at the University Microscopy Center (UMIC) on a BioRad apparatus. Pixel analysis of confocal images was done using Image J (NIH). All other images, time-lapses, and z-stacks were taken on a Zeiss Axiovert 200M with an AxioCam MRm camera using Axiovision software. Fluorescence spectra were taken on a photon-counting spectrofluorometer, ISS-PC (ISS, Urbana, IL).

*Single cell FRET measurements*

FRET measurements were determined using the procedure of Devreotes (21). Bleed-through values were obtained by transfecting PC12 cells with 10μg of free eCFP or free eYFP plasmid vectors and imaging under the appropriate filter sets (Chroma, Inc.). Cells expressing only CFP or YFP were then imaged under the CFP (Chroma #31044v2) or YFP (Chroma #41029) and FRET (Chroma #31052) filter sets to determine the FRET/CFP or FRET/YFP ratio. Averaging over 12 cells, on our system, the bleed-through values for CFP and YFP are 39% and 28% respectively using the background-

corrected intensities calculated using ImageJ software from N.I.H. To generate a net FRET image by accounting for bleed-through emission,

$$nF = I_{FRET} - I_{YFP} \times a - I_{CFP} \times b$$

where a and b equal the percentage of bleed-through of YFP and CFP under the FRET filter set. However, to compare FRET values among cells with varying protein expression levels, the net FRET (*nF*) value can be normalized ($N_{FRET}$). From the entire intensity value of the image, one can calculate $N_{FRET}$. Normalized FRET ($N_{FRET}$) is given as (22):

$$N_{FRET} = \frac{I_{FRET} - I_{YFP} \times a - I_{CFP} \times b}{\sqrt{I_{YFP} \times I_{CFP}}}$$

where *a* and *b* equal the percentage of bleed-through of CFP and YFP under the FRET. $N_{FRET}$ was determined as described (22).

*Image analysis*

Images were processed using ImageJ (NIH). Before any analysis, images were corrected for background as follows. First, the background was calculated from a 50x50 pixel box at the top left corner of the raw image and this intensity was subtracted from the entire image. Then, uneven illumination was removed from the image using three iterations of the Background Correction Plugin. This image was binary thresholded and then inverted to make the cell white (255) and the background black (0). Next, the image was divided by 255 to make the pixel values for white 1. Finally, the background subtracted image was multiplied by the thresholded image. These manipulations remove the background by making the background 0. Using the method of Xia (22), *nF* images

were created by multiplying the background corrected donor image by the donor correction factor, the background corrected acceptor image by the acceptor correction factor, and then subtracting each of these from the background corrected FRET image. $N_{FRET}$ images were created by multiplying the background corrected donor and acceptor images and then taking the square root creating a resultant image. The *nF* image was then divided by the resultant image. A global, normalized FRET value was calculated by averaging each individual pixel's normalized FRET value. This program also calculates the corresponding normalized FRET ranges (0-10%, 10-20%, etc.) for the image.

To analyze the distribution of endogenous and overexpressed proteins within a z-stack, the images were run through a program which lists the pixel intensity value at a user specified x,y coordinate for a 3 x 3 pixel area (9 pixels through the cell) for all images within the stack. Intensity values for each pixel per slice were then averaged and plotted.

*FRET measurements of membrane preparations*

FRET measurements of membranes that were co-transfected with eCFP and eYFP tags were determined by the increase in eYFP fluorescence in the absence and presence of eCFP using the exciting wavelength of the donor. The FRET value is thus a ratio of the emission maxima of the two peaks centered 490 and 527 nM at the exciting wavelength of the donor (440 nm) (see (23)).

Membranes, prepared as described above, were thawed and diluted with PBS buffer so that the absorption at 433 nm for CFP samples or at 514 nm YFP samples was below 0.1 O.D. unit. Fluorescence measurements were made at room temperature. A

475 nm cut-on filter was placed before the emission monochromater. After taking the verifying emission spectra of the samples, the intensity of each sample was monitored at 1s intervals for 3 minutes while stirring. We note that the intensities were stable over time period and identical values were obtained taking the intensities of the samples under nitrogen.

Since these FRET measurements are done on a fluorometer where the emission is better isolated as compared to a microscope, the percent FRET values were calculated either by comparing the acceptor emission when only acceptor or donor is excited, i.e. using eCFP and eYFP excitation (i.e. $\lambda$ = 440nm and 475 nm) and monitoring the emission at 525 nm to obtain R, where R = I(490) / I(475)). FRET was then determined by comparing the R values for eCFP / eYFP transfected samples to samples individually transfected with one of the fluorophores. Thus,

$$\%FRET = 100 * [(R(s) - R(YFP)] / [R(CFP-R(YFP)]$$

where R(s) is the intensity ratio of the sample. Real time changes in FRET were also monitored by the change in the intensity ratio of the donor and acceptor (490 nm/ 527 nm) at the donor is excited (440 nm).

**Results**

*In Vitro Binding of purified PLCβ1 to Gαq in the activated and deactivated states*

We have previously determined the affinity of PLCβ1 to activated Gαq laterally associating on model membrane surfaces (9) using fluorescence methods. Here, we have repeated this measurement and determined the decrease in affinity between the proteins when Gαq is in the deactivated state. These measurements were carried out by covalently

attaching the fluorescent probe coumarin to Gαq, reconstituting it on large, unilamellar vesicles, and monitoring the change in coumarin fluorescence intensity as PLCβ1 is added. We note that these studies were done at lipid concentrations exceeding the membrane binding constant of the proteins and so only lateral association between the membrane-bound proteins are viewed (24), (25). The binding curves were fit assuming a bimolecular association although we cannot discount the possibility that different conformational states of Gαq contribute to the curve. The data in Figure 3.1a show that PLCβ1 binds ~300 fold (Kapp = 640+68 nM versus 2.8+0.7 nM) more weakly to deactivated as opposed to activated Gαq(GTPγS). Thus, for complexes to form in the basal state, the proteins would have to be colocalized at high concentrations (i.e. above 500 nM). Gα subunits undergo significant conformational changes upon nucleotide exchange and it is likely that the protein-protein interface between PLCβ1 and Gαq differs in the activated and deactivated states. To determine whether this is the case, we formed complexes between PLCβ1 and Gαq(GDP), PLCβ1 and Gαq(GTPγS) on membranes and subjected the complexes to protein digestion using trypsin (Figure 3.1b). Interestingly, we find that association of PLCβ1 to deactivated Gαq results in more protection to digestion as compared to isolated PLCβ1 or PLCβ1 bound to Gαq(GTPgS). Taken together, these studies quantify the binding between PLCβ1 and Gαq(GDP) and suggest that the proteins associate with an interface that differs between from activated $G\alpha_q$.

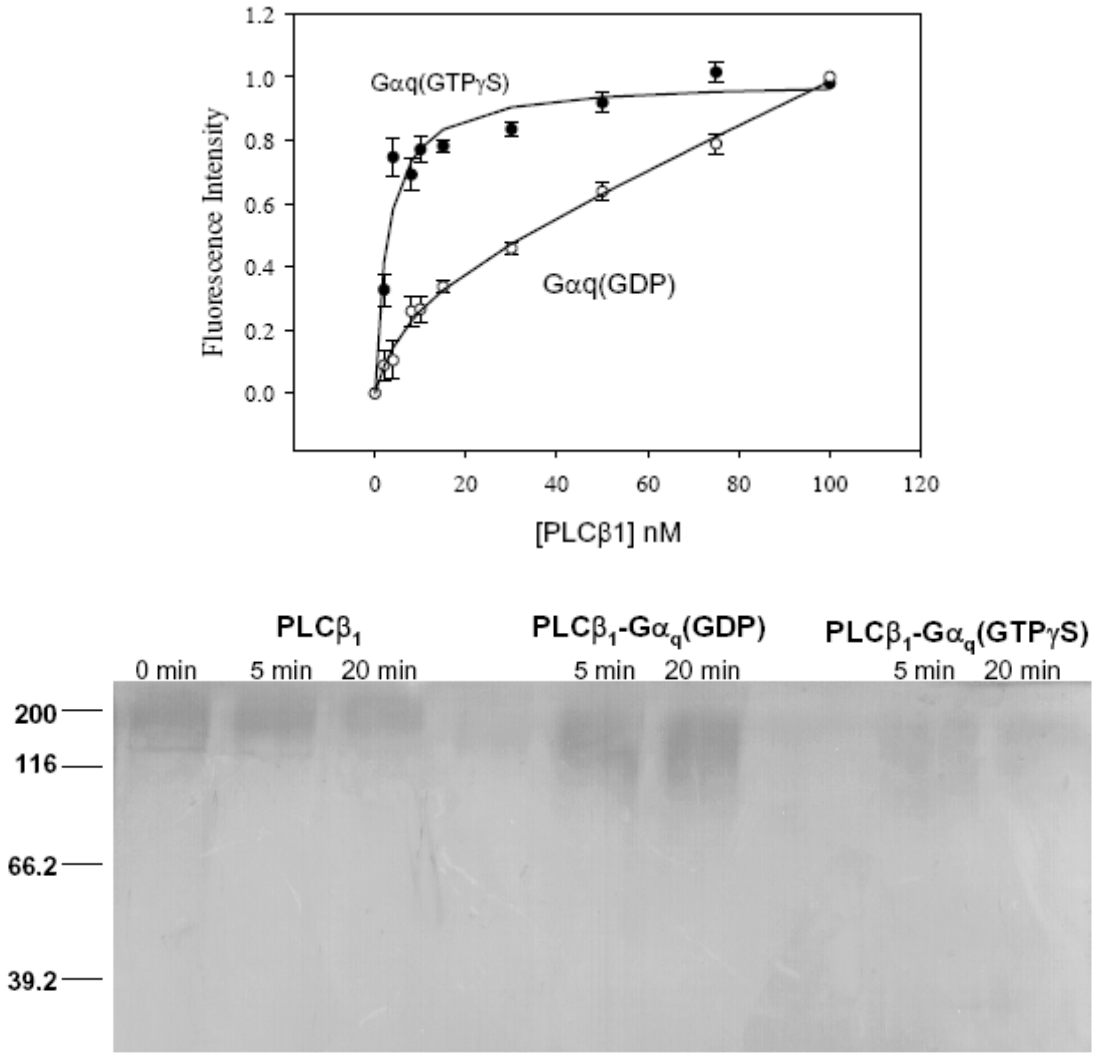


**Figure 3.1**: **(A)** Binding of purified PLCβ1 to either 2 nM CM-Gαq(GDP) or CM-Gαq(GTPγS) reconstituted on 300 uM large, unilamellar vesicles composed of POPC:POPS: POPE (1:1:1) where *n=3*. Binding was followed by the shift in the emission energy of the coumarin probe upon binding. Control studies substituted buffer for enzyme. The binding curves were fit to a bimolecular association constant using SigmaPlot and standard error is shown. **(B)** SDS-PAGE electrophoresis gel showing the extent of trypsin digestion at either 5 or 20 minute incubation of PLCβ1 when bound to Gαq(GDP) or Gαq(GTPγS).

*Quantifying the endogenous and overexpressed $G\alpha_a$ and $PLC\beta_1$ in cells*

In this study, we have overexpressed fluorescent-tagged $G\alpha_q$ and $PLC\beta_1$ in cells and monitored their complex formation by fluorescence spectroscopy. To determine whether the higher concentration of the overexpressed proteins promotes complex formation, we quantified the amount of overexpressed eCFP-$G\alpha_q$ and eYFP-$PLC\beta_1$ in differentiated PC12 cells and compared these to endogenous levels found in cells transfected with empty vector (see methods) by western blot analysis. This was accomplished by placing four different amounts of purified $G\alpha_q$ or $PLC\beta_1$ (see (7)) to generate a calibration curve. The growth and morphology of the transfected cells were identical to untransfected suggesting that at our levels of expression, neither protein is disruptive to cell function. Differentiated PC12 cells (see methods) were harvested, ruptured and the membrane and cytosolic fractions were isolated. We find that eCFP-$G\alpha_q$ levels in the membrane fractions were $0.33 \pm .06$ μg/mg total protein compared to $0.17 \pm .02$ μg/mg protein of endogenous protein. Thus, overexpressed protein is approximately two fold higher than endogenous under our transfection conditions.

Similarly, for eYFP-$PLC\beta_1$, the ratio of transfected to endogenous is roughly 3 fold (0.006 versus 0.002 μg/mg protein). Similarly, the cellular activity is 10% higher in the transfected cells consistent with the higher level of $PLC\beta_1$ and noting that other, more active PLC enzymes (e.g. PLCδ) are expressed in PC12 cells (see (26)) suggesting that the transfected eYFP-$PLC\beta_1$ is functional This study shows that the overexpressed amounts of eCFP-$G\alpha_q$ and eYFP-$PLC\beta_1$ are proportional and not high enough to elicit abnormal cellular responses.

*Distribution of eCFP-G$\alpha_q$ and eYFP-PLC$\beta_1$ in differentiated PC12 cells*

We characterized the cellular distribution of eCFP-G$\alpha_q$ and eYFP-PLC$\beta_1$ in transfected PC12 cells by confocal microscopy. Initial studies were done using GFP-G$\alpha_q$. We found that in over 20 cells viewed, GFP-G$\alpha_q$ was entirely localized on the plasma membrane with only trace amounts in the cytosol. None could be found in the nucleus. An example of a differentiated PC12 cell expressing GFP-G$\alpha_q$ is shown in Figure 1a which shows a top and side view of a cell. In Fig. 3.2b, we present the intensity distribution through a single point of the cell (red point in the enlarged top image of 3.2 a). This analysis shows that all of the GFP-G$\alpha_q$ intensity is found on the top and bottom surfaces of the cell, which is consistent with plasma membrane localization. In this cell, most of the fluorescence intensity is concentrated on the cell bottom and a smaller amount is on the apical side suggesting a larger number of signaling networks are localized on the basolateral side of the cell.

We assessed the amount of GFP-G$\alpha_q$ in the cytoplasm by pooling the intensities from 5.0 – 14.6μ, which should correspond to the cytosol, and dividing by the pooled intensities from a top-to-bottom distance of 0 – 4.8 μ, which should correspond to the plasma membrane. This calculation gives an intensity ratio of the cytosolic/plasma membrane of 0.06.

**Figure 3.2:** (**A**) Localization of GFP-Gαq in a PC12 cell. The Gαq image shows a cell of ~10 x 20 μ and is a reconstruction from 82 slices. A rotated side view is presented at the bottom of the figure. In the inset we show a red dot corresponding to a point in the x-y plane (9 pixels) where we collected the intensity through the z axis of the cell (red line). (**B**) Histograph of the intensity distribution of eGFP-Gαq along the red line running through the cell.

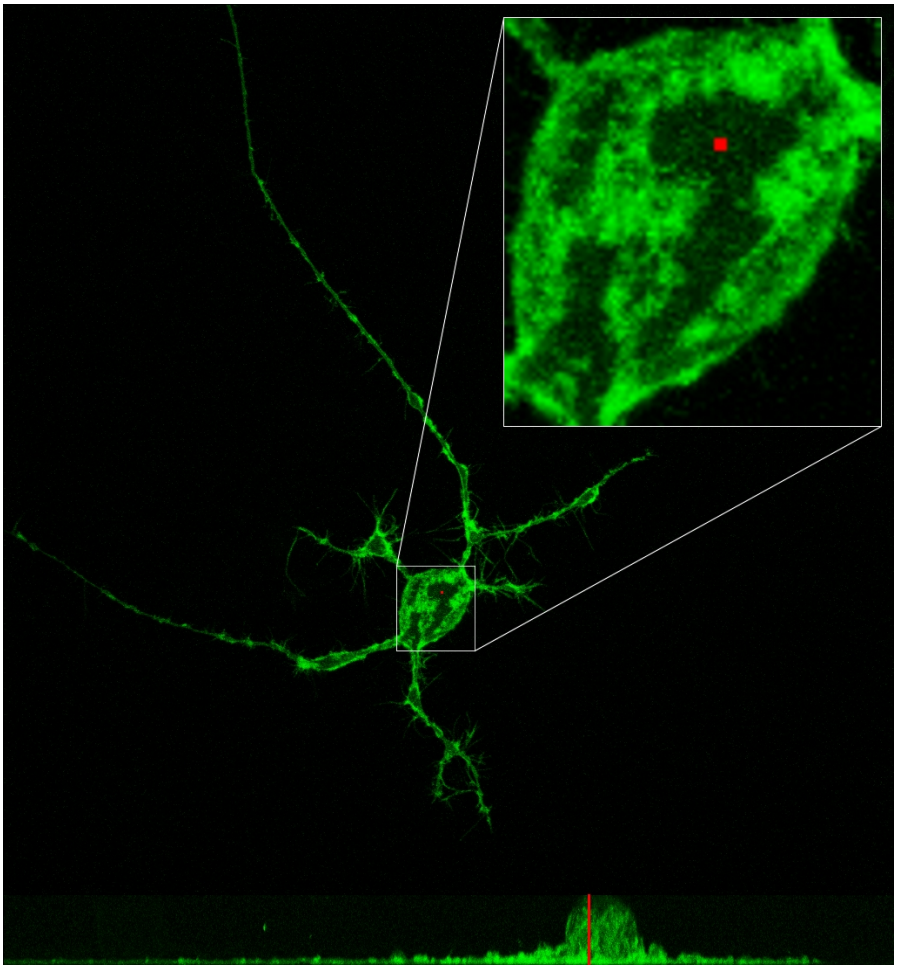

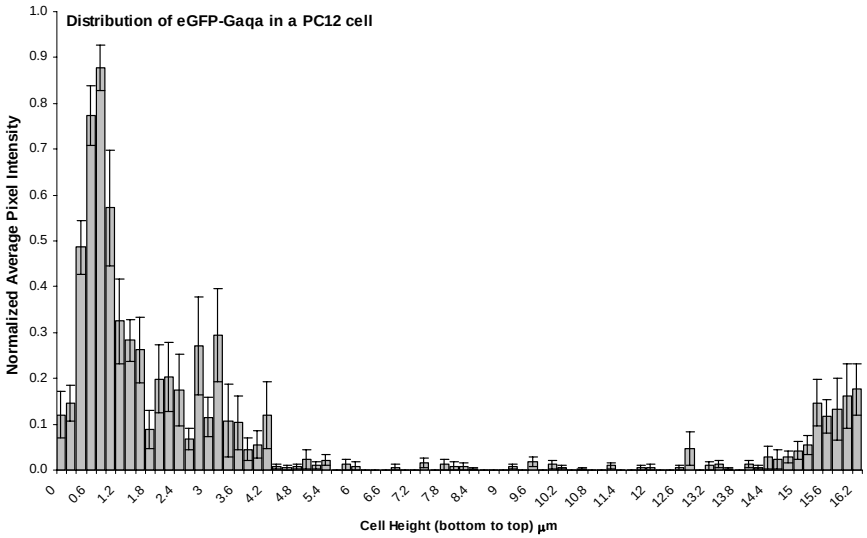
Distribution of eGFP-Gaqa in a PC12 cell
Normalized Average Pixel Intensity
1.0
0.9
0.8
0.7
0.6
0.5
0.4
0.3
0.2
0.1
0.0
0
0.6
1.2
1.8
2.4
3
3.6
4.2
4.8
5.4
6
6.6
7.2
7.8
8.4
9
9.6
10.2
10.8
11.4
12
12.6
13.2
13.8
14.4
15
15.6
16.2
Cell Height (bottom to top) μm

**Figure 3.3:** (**A**) Localization of YFP-PLCβ1 microscopy in a PC12 cell distinct from the one shown in Fig. 3.2. The eYFP-PLCβ1 image a cell of ~12 x 16 μ and is a reconstruction from 45 slices. A rotated side view is presented at the bottom of the figure. In the insets we show a red dot corresponding to a point in the x-y plane (9 pixels) where we collected the intensity through the z axis of the cell (red line). (**B**) Histograph of the intensity distribution of YFP-PLCβ1 along the red line running through the cell.

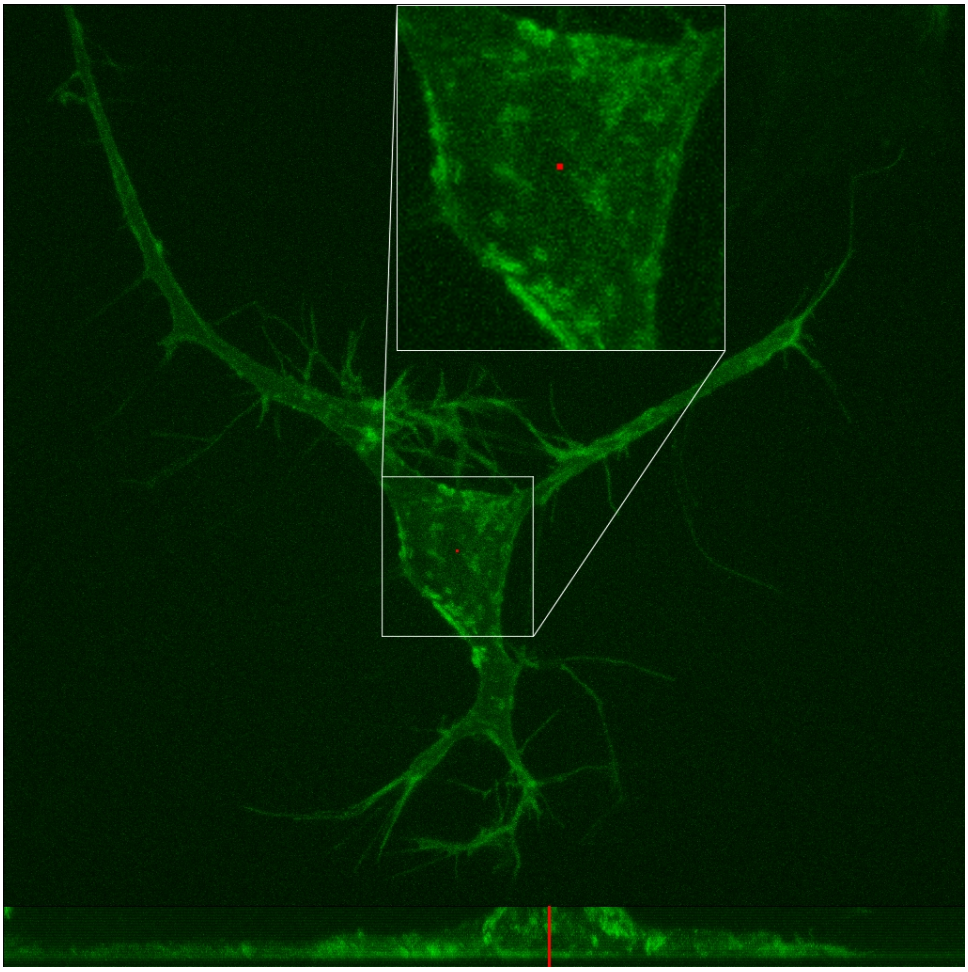

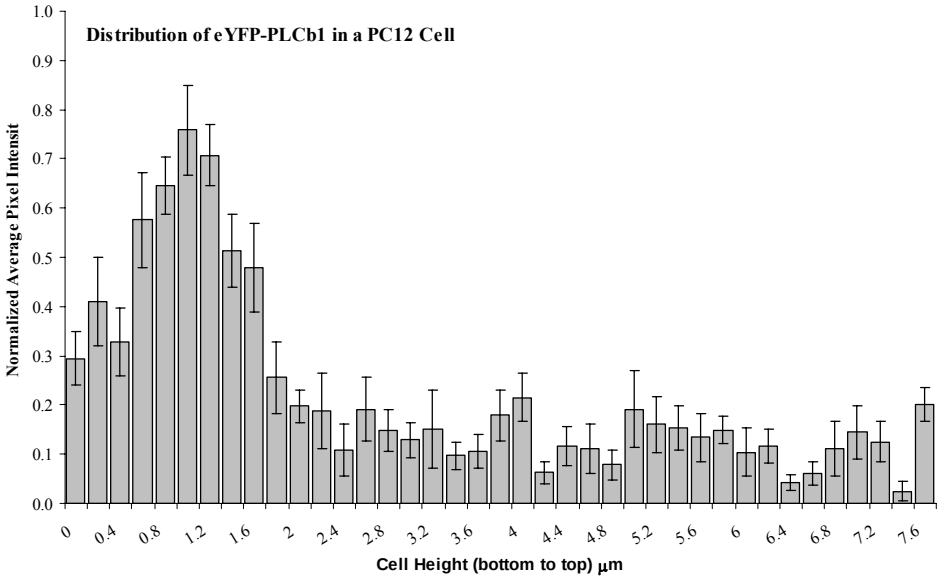
Distribution of eYFP-PLCb1 in a PC12 Cell
Normalized Average Pixel Intensit
1.0
0.9
0.8
0.7
0.6
0.5
0.4
0.3
0.2
0.1
0.0
0
0.4
0.8
1.2
1.6
2
2.4
2.8
3.2
3.6
4
4.4
4.8
5.2
5.6
6
6.4
6.8
7.2
7.6
Cell Height (bottom to top) μm

The localization of eYFP-PLC$\beta_1$ was also viewed. Unlike GFP-G$\alpha_q$, a larger percent of the protein was seen in the cytosol (Figure 3.3 A and B). To insure that the cytosolic population of eYFP-PLC$\beta_1$ was not caused by over-expression, we collected z-stack images of endogenous PLC$\beta_1$i n fixed PC12 cells stained with a PLC$\beta_1$ monoclonal antibody (Fig. 3.4a). The distribution of endogenous PLC$\beta_1$ matched that of over-expressed eYFP-PLC$\beta_1$.

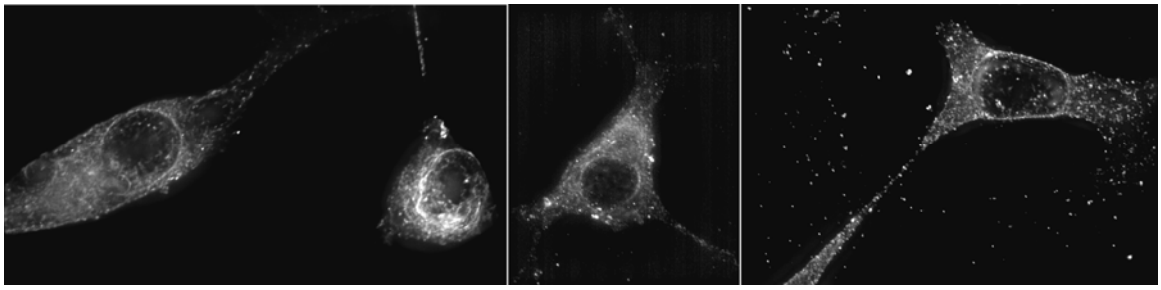

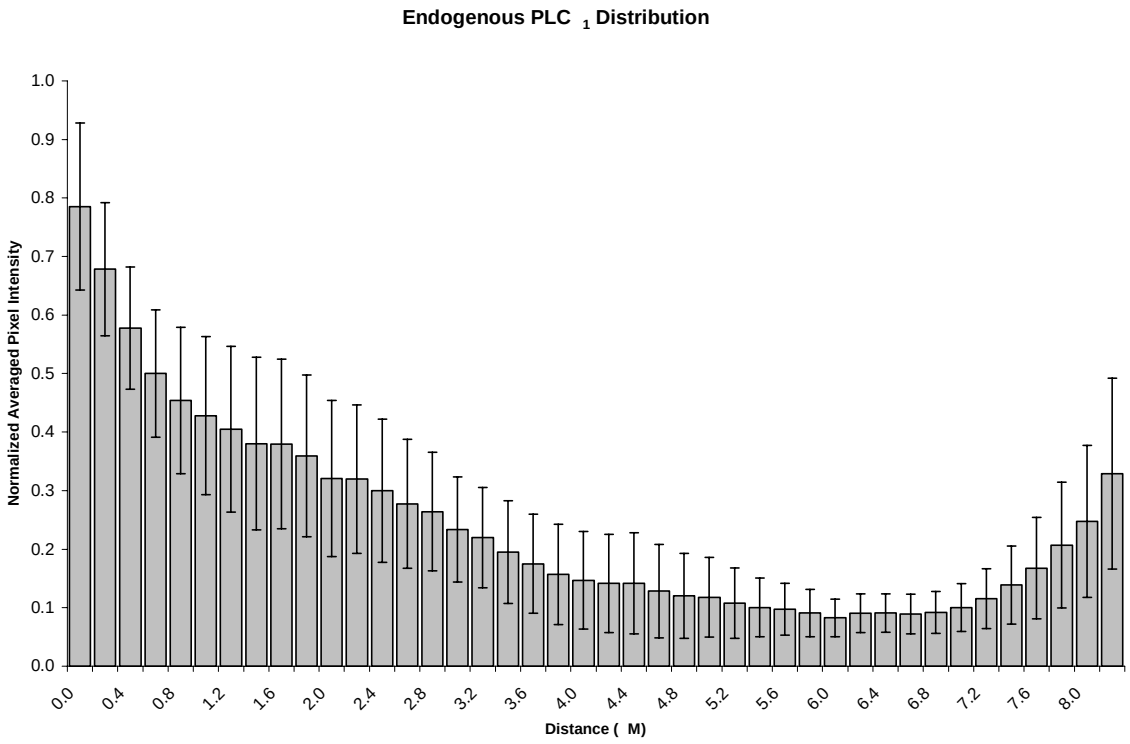


**Figure 3.4:** (**A**) - Immunofluorescence of endogenous expression of PLCβ1 in differentiated PC12 cells. Each image shown is a reconstruction from 41 slices. (**B**) Distribution analysis in cell sections averaged over 6 cells.

We verified that PC12 cells contain a significant population of cytosolic PLC$\beta_1$ by western blot analysis of the cytosolic and membrane fractions of non-transfected and transfected cells. Comparing the pooled ratios of the histograph intensities from the cytosolic (2.4 – 6.0 μ) divided by plasma membrane populations (0 – 2.2 μ), we obtain a value of 0.48. This value is far higher than the ratio obtained for GFP-G$\alpha_q$ of 0.06. Similar results were obtained over a wide range of cells allowing us to conclude that differentiated PC12 cells have two populations of PLC$\beta_1$ in the resting state; one localized on the plasma membrane and another in the cytosol. In contrast, G$\alpha_q$ is almost entirely localized on the plasma membrane.

*PLC$\beta_1$ is associated with G$\alpha_q$ in quiescent cells*

We then determined the amount of eCFP-G$\alpha_q$ complexed with eYFP-PLC$\beta_1$ in PC12 cells by FRET studies using fluorescence microscopy. These studies were carried out by co-transfecting eYFP-PLC$\beta_1$ and eCFP-G$\alpha_q$ into differentiated PC12 cells and collecting z-stack images every 0.2 μ in three channels, (CFP, YFP, and FRET). To quantify the amount of eYFP-PLC$\beta_1$ / eCFP-G$\alpha_q$ FRET over time, we collected images focusing on the bottom of the cell every 5 s for a total of 100 s and calculated the amount of FRET for each time point. A normalized FRET image was then generated (*see methods*). In all cells, we find the highest FRET on the plasma membrane (e.g. Fig. 3.5a-d) correlating well with the plasma membrane localization of G$\alpha_q$. Calculating the cellular distribution and magnitude of the intensity of the FRET signal between eYFP-PLC$\beta_1$ and eCFP-G$\alpha_q$ shows the FRET to be constant over time suggesting a stable

association in the basal state (see Fig. 3.5a-d). These results suggest eYFP-PLC$\beta_1$ and eCFP-G$\alpha_q$ are colocalized in cells even in the quiescent state.

**Figure 3.5a-d: Examples of normalized FRET images of four PC12 cells expressing eCFP-G$\alpha_q$ and eYFP-PLC$\beta_1$ after NGF treatment (see "Materials and Methods").** For each example, the 1st image corresponds to the basal FRET, and the 2nd image is 30 s after stimulation with 1 μM acetylcholine. These images were taken focusing on or close to the bottom of the cells, and the normalized FRET was analyzed using the method of Xia. Also shown are surface plots depicting the distribution of the FRET signal over time for each cell, where the *y* axis is the percent FRET, the *x* axis is the percent pixels in each FRET range, and the *z* axis is time. One can see the percentage of pixels within each FRET range does significantly change upon stimulation, indicating that there is not a redistribution of the signal.

**Figure 3.5a**

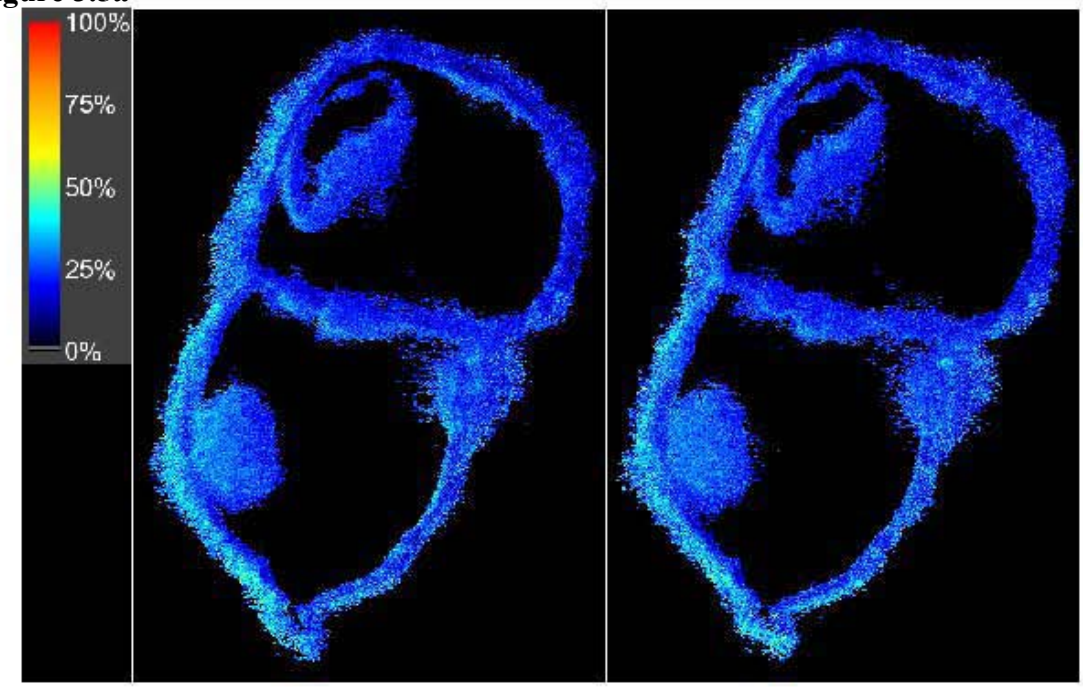
100%
75%
50%
25%
0%

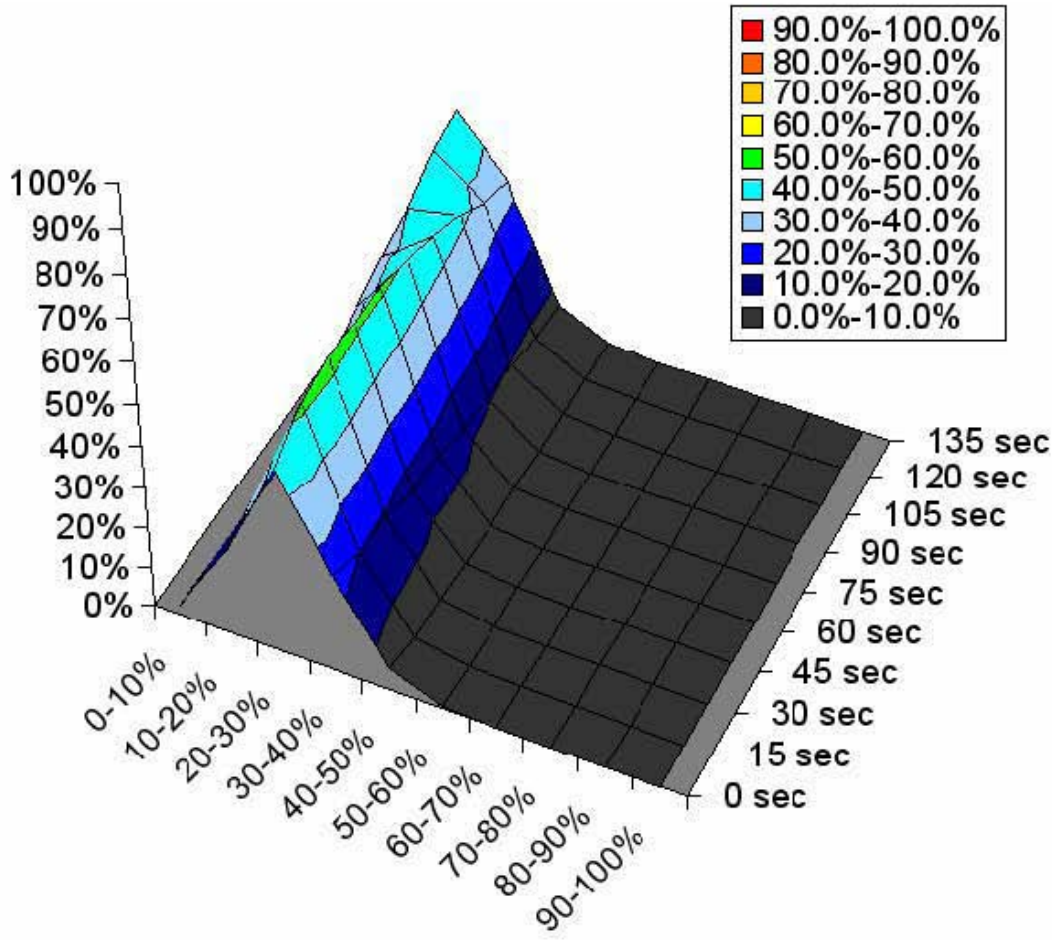
90.0%-100.0%
80.0%-90.0%
70.0%-80.0%
60.0%-70.0%
50.0%-60.0%
40.0%-50.0%
30.0%-40.0%
20.0%-30.0%
10.0%-20.0%
0.0%-10.0%
100%
90%
80%
70%
60%
50%
40%
30%
20%
10%
0%
0-10%
10-20%
20-30%
30-40%
40-50%
50-60%
60-70%
70-80%
80-90%
90-100%
135 sec
120 sec
105 sec
90 sec
75 sec
60 sec
45 sec
30 sec
15 sec
0 sec

**Figure 3.5b**

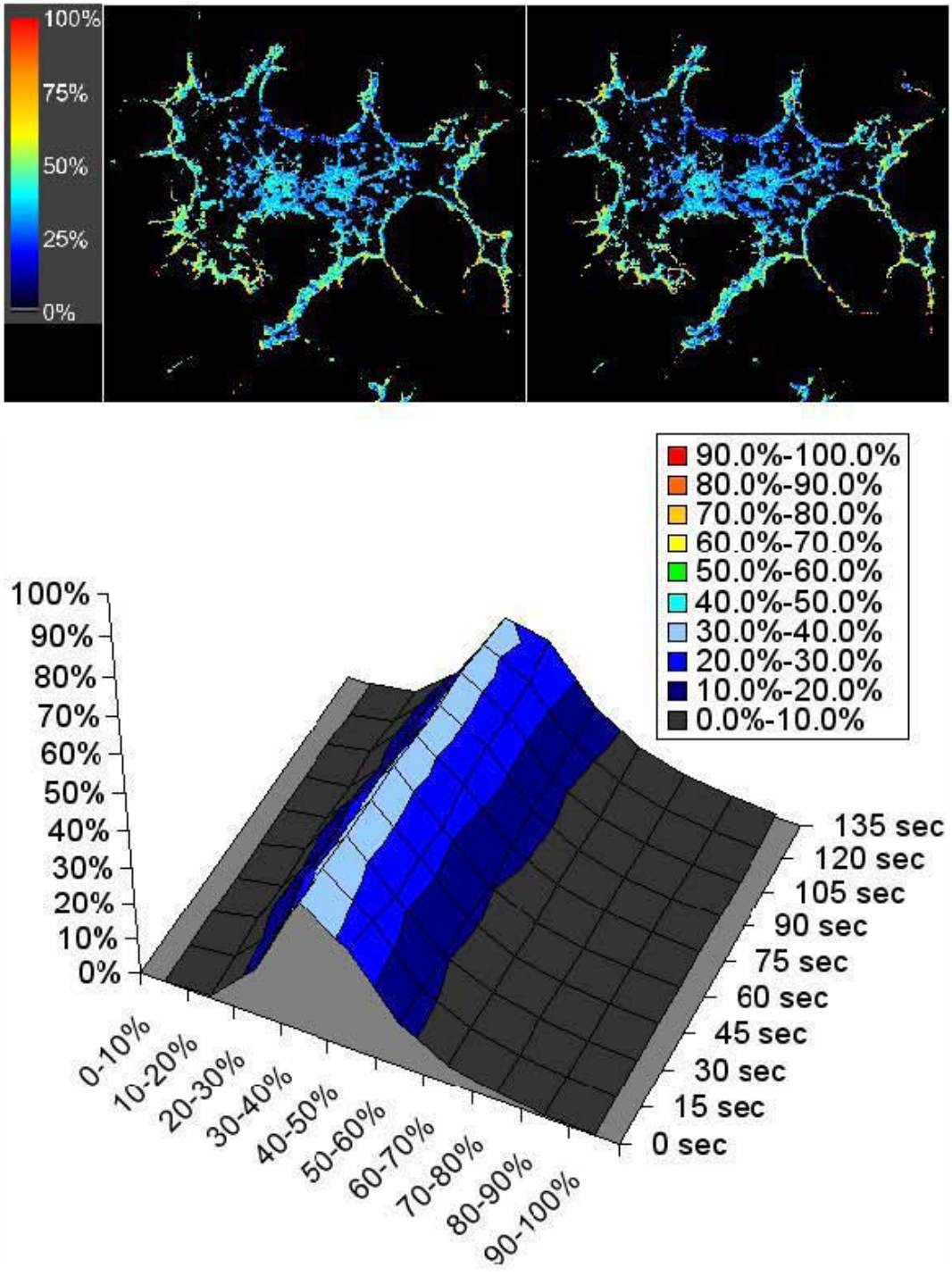
100%
75%
50%
25%
0%
90.0%-100.0%
80.0%-90.0%
70.0%-80.0%
60.0%-70.0%
50.0%-60.0%
40.0%-50.0%
30.0%-40.0%
20.0%-30.0%
10.0%-20.0%
0.0%-10.0%
100%
90%
80%
70%
60%
50%
40%
30%
20%
10%
0%
135 sec
120 sec
105 sec
90 sec
75 sec
60 sec
45 sec
30 sec
15 sec
0 sec
0-10%
10-20%
20-30%
30-40%
40-50%
50-60%
60-70%
70-80%
80-90%
90-100%

**Figure 3.5c**

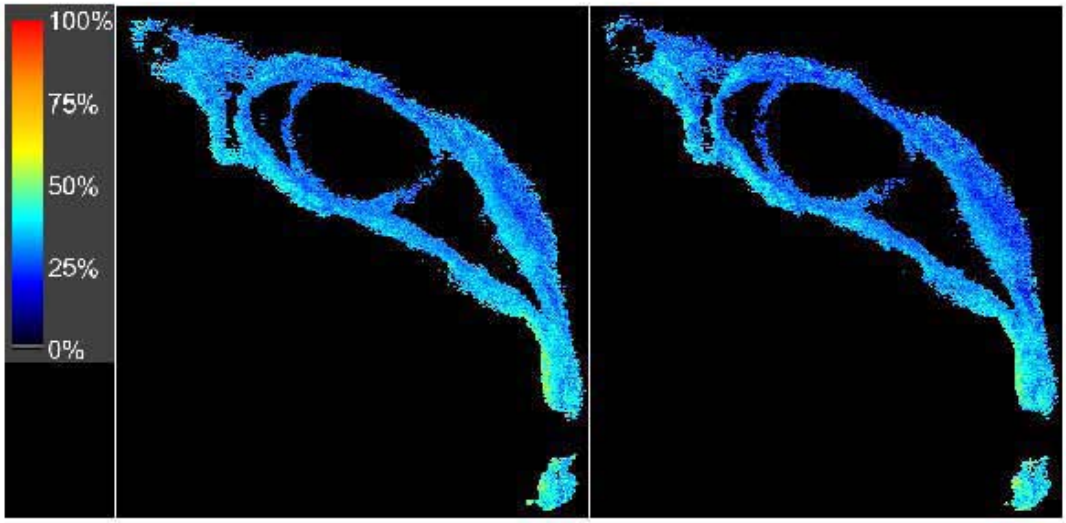
100%
75%
50%
25%
0%

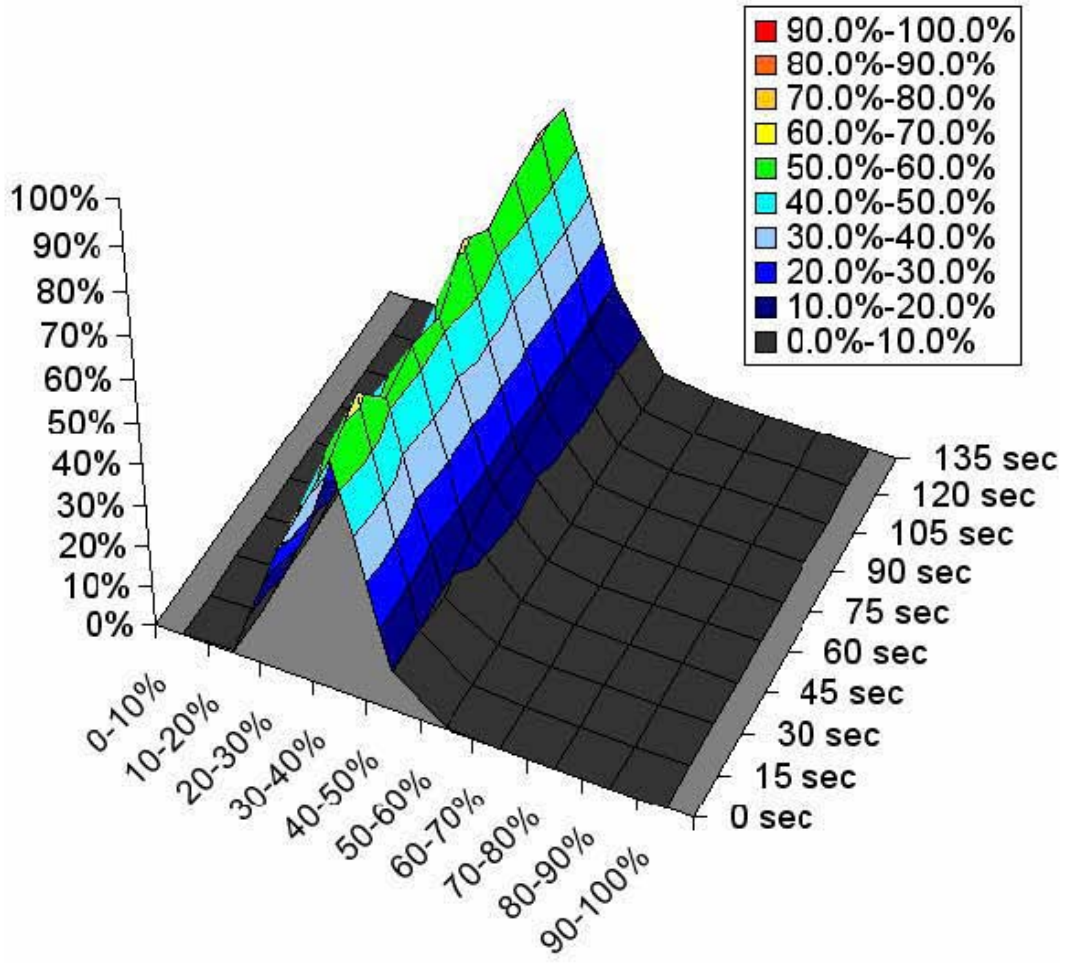
90.0%-100.0%
80.0%-90.0%
70.0%-80.0%
60.0%-70.0%
50.0%-60.0%
40.0%-50.0%
30.0%-40.0%
20.0%-30.0%
10.0%-20.0%
0.0%-10.0%
100%
90%
80%
70%
60%
50%
40%
30%
20%
10%
0%
135 sec
120 sec
105 sec
90 sec
75 sec
60 sec
45 sec
30 sec
15 sec
0 sec
0-10%
10-20%
20-30%
30-40%
40-50%
50-60%
60-70%
70-80%
80-90%
90-100%

**Figure 3.5d**

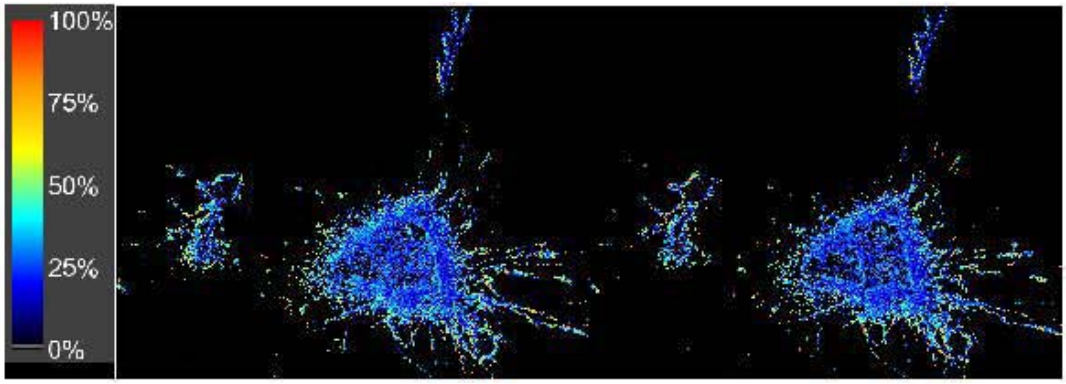
100%
75%
50%
25%
0%

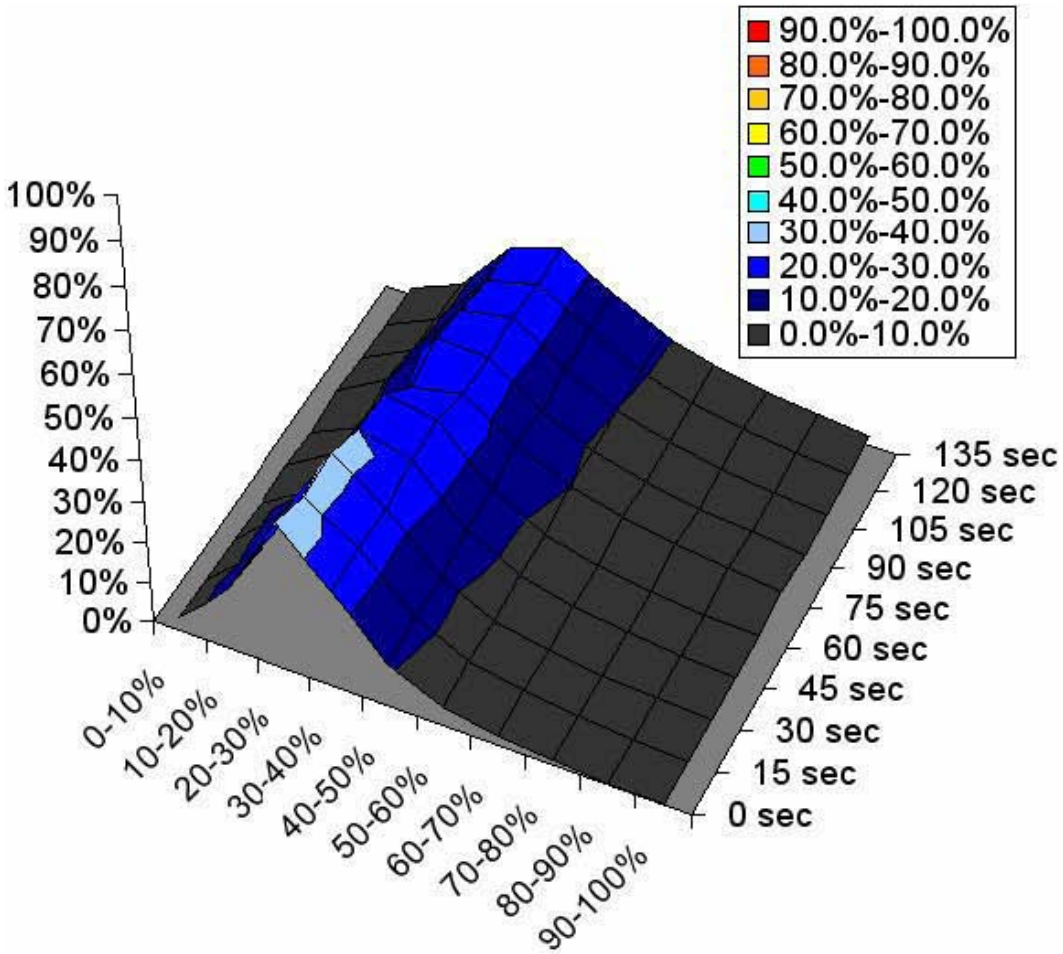
90.0%-100.0%
80.0%-90.0%
70.0%-80.0%
60.0%-70.0%
50.0%-60.0%
40.0%-50.0%
30.0%-40.0%
20.0%-30.0%
10.0%-20.0%
0.0%-10.0%
100%
90%
80%
70%
60%
50%
40%
30%
20%
10%
0%
0-10%
10-20%
20-30%
30-40%
40-50%
50-60%
60-70%
70-80%
80-90%
90-100%
135 sec
120 sec
105 sec
90 sec
75 sec
60 sec
45 sec
30 sec
15 sec
0 sec

To determine the specificity of the FRET signal, we measured the extent of FRET between two groups of non-interacting proteins. In the first, we co-expressed eCFP-$G\alpha_q$ and eYFP-$PLC\delta_1$ which should not interact (see (26)). For these cells, the range of FRET was 8-18% with a mean value of 14% (n=5). In a second series of controls, we coexpressed free CFP and free YFP at levels higher than the eCFP-$G\alpha_q$ / eYFP-$PLC\beta_1$ pair. We obtain a FRET of 18 $\pm$ 2% (n=8). These data give a non-specific level of FRET that most likely reflects the limitations of the optics used in our studies, and, in particular, our inability to completely eliminate bleed-through fluorescence. These controls give us a lower limit on the extent of FRET from specific interactions. As described below, for the eCFP-$G\alpha_q$ / eYFP-$PLC\beta_1$ pair, the much higher extent of FRET as compared to these controls suggests specificity.

All cells expressing eCFP-$G\alpha_q$ / eYFP-$PLC\beta_1$ displayed a significant level of FRET in the unstimulated state, we note that the amount of FRET has a cell to cell variation which follows a gaussian distribution ranging from 19-63% with the mean close to 40% (data not shown). We found that this variation is loosely correlated to the expression level of the proteins. In cells expressing high levels of protein, larger FRET values are obtained whereas cells expressing very low amounts of protein show low FRET values. The transfection efficiency for eCFP-$G\alpha_q$ and eYFP-$PLC\beta_1$ was 60-80% for both proteins, and we note that FRET had a very small dynamic range for protein expression in that changing the expression level of one of the protein partners reduced the FRET to non-specific values (i.e. below 20% FRET).

To determine whether a basal population of eCFP-$G\alpha_q$ / eYFP-$PLC\beta_1$ complexes could be seen in other types of cells, we carried out the same study using HEK293 cells.

Similar to that seen in PC12 cells, these cells showed a cytosolic population of eYFP-PLC$\beta_1$ and a plasma membrane population that is complexed with eCFP-G$\alpha_q$ in the unstimulated state. Thus, this same cellular localization is seen in other cell lines.

The measurements described above were performed on single cells. Even though many cells were viewed, there is a possibility that eYFP-PLC$\beta_1$ and eCFP-G$\alpha_q$ FRET in the basal state only occurs in limited cases. To determine the amount of FRET in a large number of cells, we co-transfected cells with eYFP-PLC$\beta_1$ and eCFP-G$\alpha_q$ and measured the degree of FRET for $10^6$ cells in a spectrofluorometer. We found that the range of FRET for this large population of cells was identical to single cell measurements as described below (Fig. 6) showing that a significant fraction of eYFP-PLC$\beta_1$ and eCFP-G$\alpha_q$ are complexed in the basal state (see below).

*The eYFP-PLC$\beta_1$ and eCFP-G$\alpha_q$ FRET pair remains complexed and bound to the plasma membrane with stimulation*

Stimulation of G proteins should promote their association to effectors. With this in mind, we measured changes in FRET with stimulation by either the addition of 1 μM carbachol or 1 μM acetylcholine. The results for four cells are shown in Fig. 3.5a-d. In all cells viewed and analyzed (n>12), we find that the amount of FRET does not significantly change upon the addition of a G$\alpha_q$ agonist. Moreover, stable colocalization of eYFP-PLC$\beta_1$ / eCFP-G$\alpha_q$ was also observed for eYFP-PLC$\beta_1$ / eCFP-G$\alpha_q$ complexes in HEK293 cells suggesting that this behavior may be general.

To confirm the single cell studies above, we measured relative changes in FRET between eYFP-PLC$\beta_1$ / eCFP-G$\alpha_q$ expressed in ~$10^6$ PC12 cells in a fluorometer as

described above. Similar to the single cell studies, these results (Fig. 4a) also show that the number of eYFP-PLC$\beta_1$ / eCFP-G$\alpha_q$ complexes does not significantly change with cell stimulation.

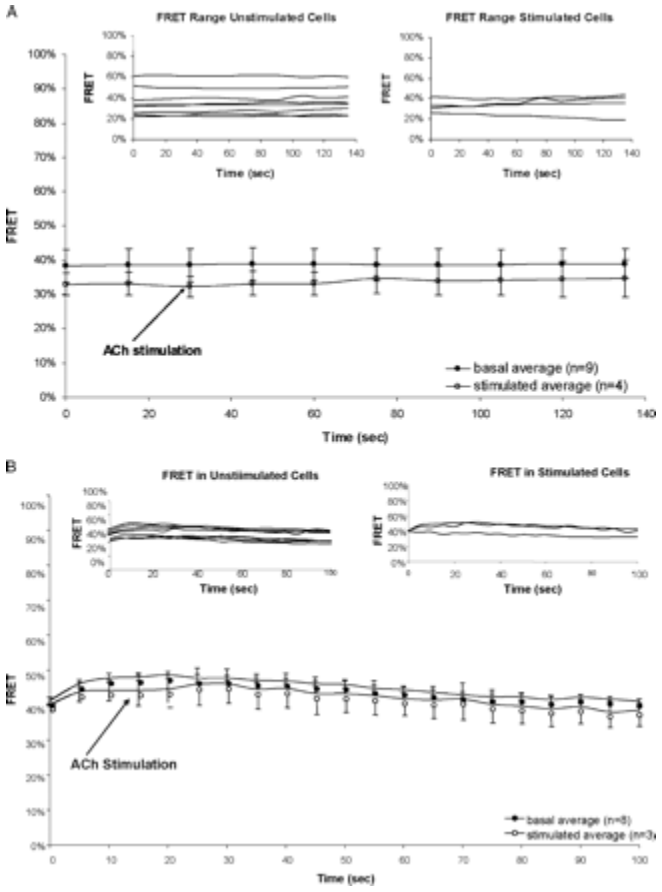


**Figure 3.6: (A)** Analysis of time lapse FRET images of PC12 cells expressing eCFP-G$\alpha_q$ and eYFP-PLC$\beta_1$. The variation of the percentage of FRET for stimulated and unstimulated cells is shown in the *insets* where stimulation was carried out by the addition of 1 μM acetylcholine (*ACh*) after obtaining a flat base line for 30 s. *Error bars* indicate S.E. for each time point. **(B)** Identical study as in *A,* except that cells expressed the constitutively active eCFP-G$\alpha_q$-RC, rather than wild type.

To verify that the lack of an increase in FRET with stimulation is not due to a lack of eCFP-G$\alpha_q$ activation, we measured the amount of FRET between eCFP-G$\alpha_q$-RC and eYFP-PLC$\beta_1$. This point mutant produces a constitutively active G$\alpha_q$ which is expected to be strongly associated with PLC$\beta_1$ in the unstimulated state (see (27)), and we expect

this association to change little with the addition of agonist. However, we find the association of eCFP-$G\alpha_q$RC to eYFP-PLC$\beta_1$ is similar to wild type (Fig.3.6b) suggesting that basal level complexation of the two proteins is not related to the stimulated state.

To insure that the eCFP-$G\alpha_q$ / eYFP-PLC$\beta_1$ expressed in cells are part of a signaling complexes coupled to a $G\alpha_q$ receptor, specifically, the m1 and m5 mucarinic receptors in PC12 cells (28)), and have the ability to increase intracellular calcium upon stimulation, we measured the amount of $Ca^{2+}$ released upon the addition of 1μM acetylcholine in $10^6$ PC12 cells. The results, presented in Fig. 3.7, show that in the basal state, all four cell groups have similar levels of internal $Ca^{2+}$ as expected from its tight cellular regulation. Upon the addition of agonist, a similar robust increase in intracellular $Ca^{2+}$ from non-transfected and singly transfected cells is observed. However, the doubly transfected cells gave a significantly higher amount of released $Ca^{2+}$. Considering that the $G\alpha_q$ – coupled m1 and m5 receptors constitute only 5% of the muscarininc receptors in these cells (28), this increase suggests that a large and significant population of the transfected proteins are functional and coupled to muscarinic receptors.

While eYFP-PLC$\beta_1$ / eCFP-$G\alpha_q$ complexes may not dissociate upon stimulation, it is possible that their localization in the cell changes during activation. We tested this idea using the commercially available plasma membrane markers YFP-MEM and CFP-MEM. These markers were highly expressed in the cells at 100% transfection efficiency and a high enough level of marker DNA was used to give a significant and reliable

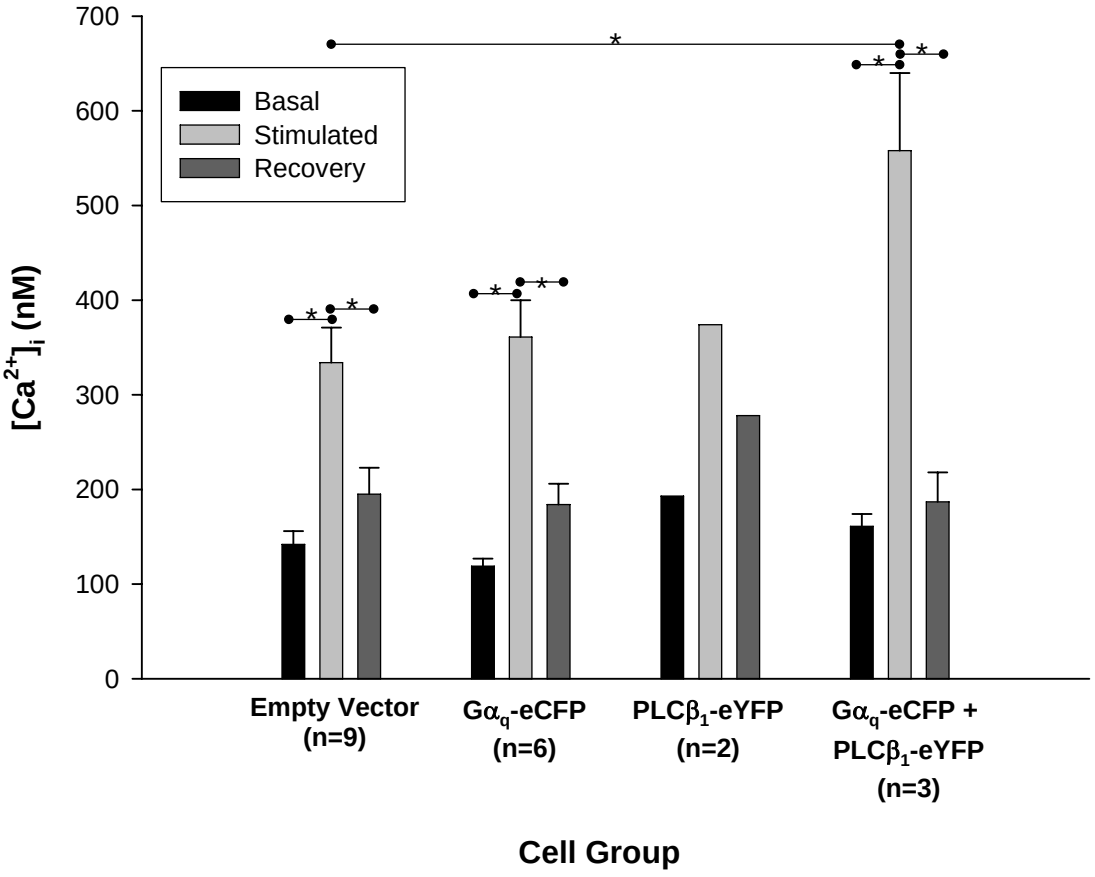


**Figure 3.7:** Internal $Ca^{2+}$ levels of PC12 cells in the basal, stimulated, and recovery states (200 s after stimulation) for four groups of transfected cells labeled with Fura-2AM as follows: empty vector, $G\alpha_q$-eCFP, $PLC\beta_1$-eYFP, and co-transfected $G\alpha_q$-eCFP and $PLC\beta_1$-eYFP. *Asterisks* indicate significant difference ($p < 0.05$) between groups or between different states within each individual group. The only significant difference between groups resulted from comparing the stimulated state of empty vector and the co-transfected cells. *Error bars* indicate S.E.

amount of FRET with eCFP-$G\alpha_q$ or eYFP-$PLC\beta_1$ (i.e. 46% and 41%, respectively). Terminally differentiated PC12 cells were either co-transfected with CFP-MEM and eYFP-$PLC\beta_1$, or YFP-MEM and eCFP-$G\alpha_q$, and changes in FRET with stimulation were measured for $10^6$ cells in a fluorometer (see above) using the procedure described by

Lohse (29). After measuring a stable basal level of eYFP/eCFP emission for 5 minutes, the cells were stimulated and both the CFP and YFP emission intensity was monitored over thirty minutes. Both time and stimulation did not affect the intensity of the CFP and YFP emissions. These results (Fig. 3.8a) indicate that the proteins do not move off the membrane upon stimulation with acetylcholine or carbachol.

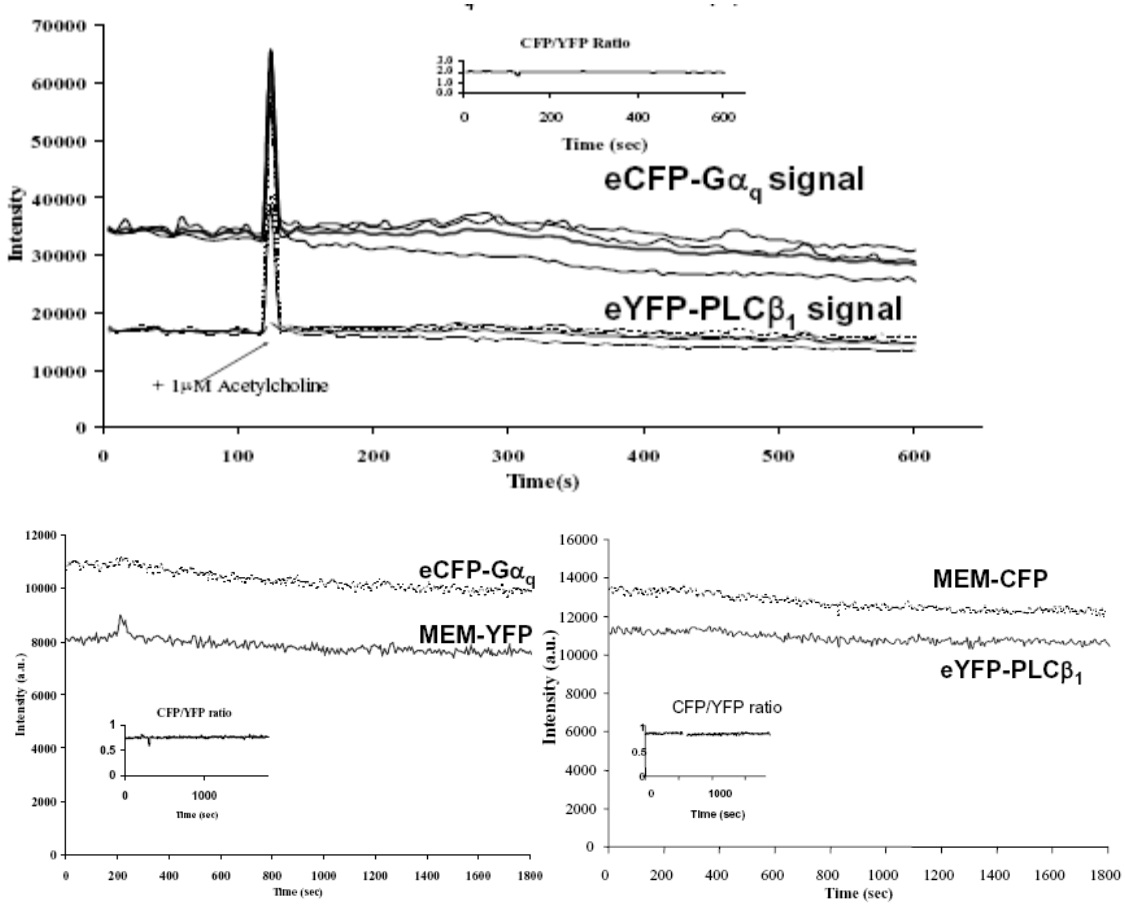


**FIGURE 3.8:** (**A)** Emission signal and ratio from cells co-transfected with eCFP-G$\alpha_q$ and eYFP-PLC$\beta_1$. The spike in the emission signal indicates when the stimulus was added. **(B)** Emission signal and ratio from cells co-transfected with eCFP-G$\alpha_q$ and MEM-YFP. **(C)** Emission signal and ratio from cells co-transfected with eYFP-PLC$\beta_1$ and MEM-CFP. Cells in *A* were stimulated at the 120-s time point, and cells in **B** and **C** were stimulated at the 300-s time point.

A stable localization of the proteins during stimulation was also assessed by taking 2.4 μ slices through a cell starting at the bottom, and measuring regions of interest that encompassed most of the plasma membrane and calculating its intensity through the cell stack before and after stimulation. This analysis, compiled for 8 cells, also showed stable localization before and after stimulation (Fig. 3.9).

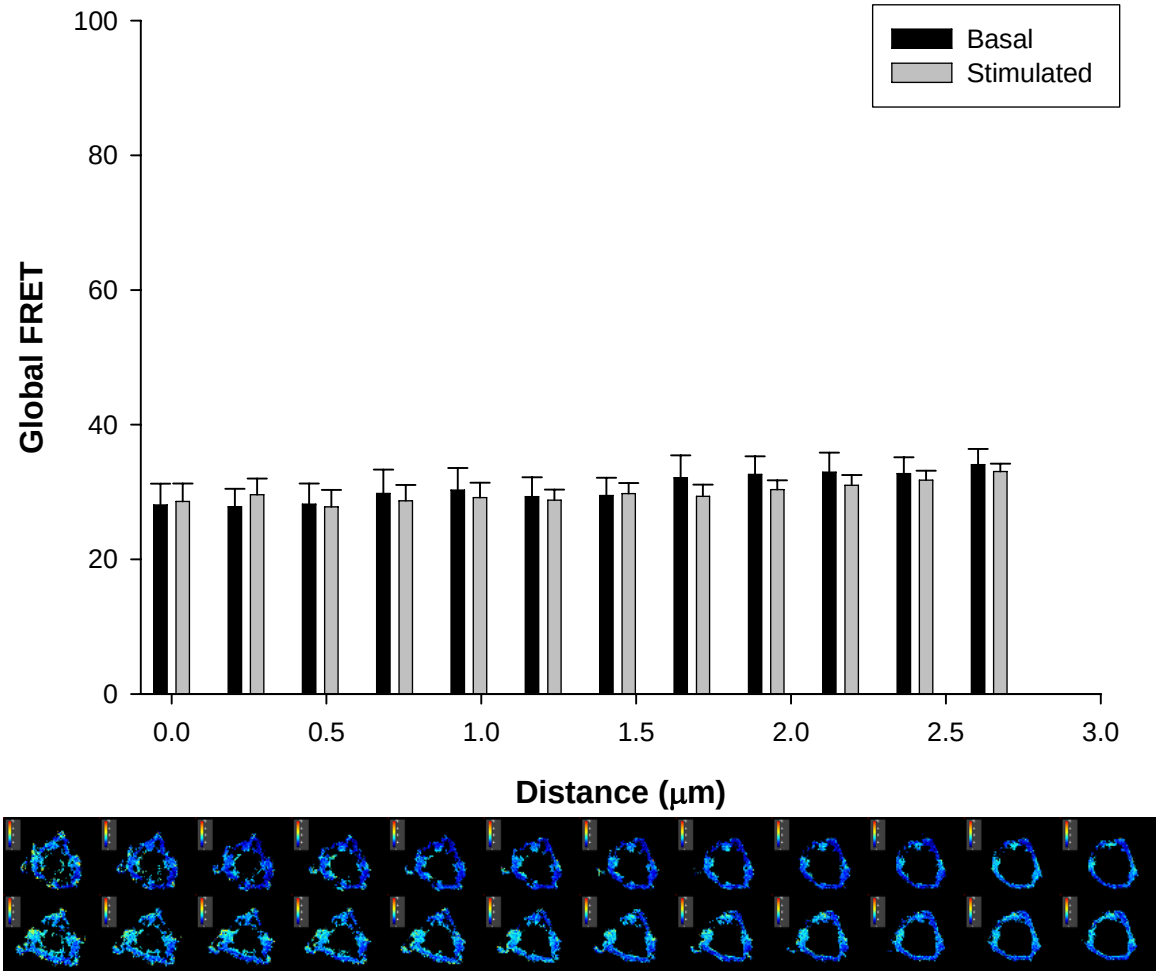


**FIGURE 3.9: (A)** Behavior of the normalized FRET for unstimulated and stimulated (*i. e.* 1 μM acetylcholine 30s) cells starting at the bottom of the cell (slice 1) and moving up in the *z* plane at 0.24-μm intervals. The data shown are a composite of nine cells. where the *error bars* indicate S.E. *B,* montage of z-stack images showing the FRET through a PC12 cell in the unstimulated and stimulated states where each frame corresponds to 0.24 μ. **(B)** *top* and *bottom panels* were stimulated at the 300-s time point.

*Studies of YFP-PLC$\beta_1$ - eCFP-G$\alpha_q$ complexes in membrane preparations*

The FRET results of live cell studies performed above clearly showed eYFP-PLC$\beta_1$ / eCFP-G$\alpha_q$ complexes in the quiescent state. The presence of these complexes suggests that some cellular factors, such as protein scaffolds, may stabilize eCFP-G$\alpha_q$ / eYFP-PLC$\beta_1$ in the basal state. We extended the cellular studies using membrane preparations of cells expressing these proteins and related partners to better understand whether eYFP-PLC$\beta_1$ / eCFP-G$\alpha_q$ complexes are stabilized by cytoskeletal or cytosolic proteins. We expressed pairs of G$\alpha_q$RC, G$\alpha_q$, PLC$\beta_1$, G$\beta_1\gamma_7$ and G$\alpha_s$ with either CFP- or YFP-tags in HEK293 cells by transient transfection and prepared membrane fractions (see methods). We then determined the extent of eCFP/eYFP FRET in each membrane preparation by the ratio of donor and acceptor emission maximum intensities at 490nm/527nm using an exciting wavelength of 440 nm as described above(21).

In an initial series of studies, the degree of FRET was measured as a function of the amount of cDNA used in the transfection. Similar to whole cell studies, our results show a systematic increase in the amount of FRET between eCFP-G$\alpha_q$ and eYFP-PLC$\beta_1$ from 18 to 100% with increasing cDNA used for transfection. Treating the samples showing 100% FRET with SDS reduced the level of FRET to ~20%. Taken together, these results show that in the absence of cytoskeletal and cytosolic components, eCFP-G$\alpha_q$ and eYFP-PLC$\beta_1$ form stable and titratable complexes on membrane surfaces, and that these complexes can be seen in the basal state even under low levels of transfection.

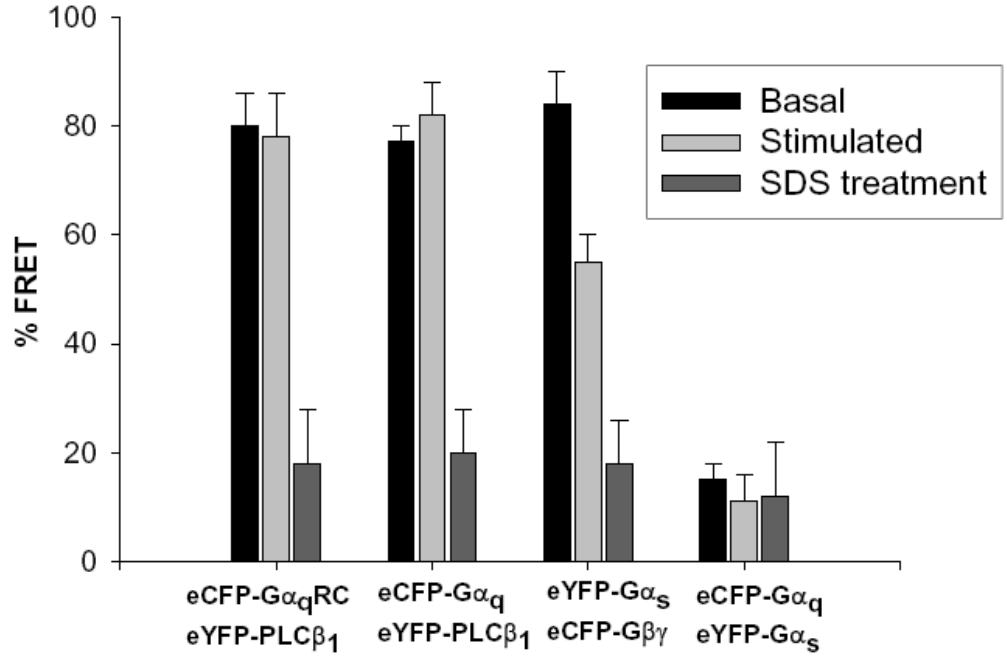


**FIGURE 3.10:** Percent FRET of membranes prepared from HEK293 cells (see "Materials and Methods") expressing the constructs as noted where stimulation was carried out by the addition of 200 μM carbachol for membranes expressing eCFP-$G\alpha_q$ and 100 μM isoproterenol for membranes expressing eYFP-$G\alpha_s$ in the presence of 100 μM GTPγS.

In Fig. 3.10 we show a comparison of different protein pairs in the basal and stimulated states at moderate levels of transfection. High levels of FRET are seen with the eCFP-$G\alpha_q$RC / eYFP-PLC$\beta_1$ probe pair, but comparably high levels are also seen for eCFP-$G\alpha_q$ / eYFP-PLC$\beta_1$ pair. Stimulation of membranes containing the eCFP-$G\alpha_q$ / eYFP-PLC$\beta_1$ pair does not cause a significant increase in the level of FRET in accord with the results seen in living cells. This lack of change occurred for 18/21 samples regardless of the initial FRET value which ranged from 68-92% for identical transfection conditions.

Although eCFP-$G\alpha_q$ to eYFP-$PLC\beta_1$ complexes showed a strong and stable FRET through stimulation, the amount of FRET for other complexes changed. We found a high percentage of FRET between eYFP-$G\alpha_s$ and eCFP-$G\beta_1\gamma_7$. These proteins should form strong complexes in the basal state that weaken upon stimulation (i.e. isoproterenal and GTPγS) (7, 44) and the data in Fig. 3.10 support this idea. The lowest FRET values are obtained for eYFP-$G\alpha_s$ and eCFP-$G\alpha_q$ in both the basal and stimulated states suggesting that the majority of these proteins are not interacting.

*FRAP Studies of Complex Diffusion*

If eYFP-$PLC\beta_1$ / eCFP-$G\alpha_q$ complexes were also stably associated with other proteins in higher order complexes, their cellular diffusion would be limited. To determine whether this is the case, we used fluorescence recovery after photobleaching (FRAP) to measure the diffusion rates of eCFP-$G\alpha_q$ and eYFP-$PLC\beta_1$. This was accomplished by laser pulsing a 2 $\mu^2$ spot on the bottom of the cell to bleach the fluorophores, and taking images every 0.5 - 2 seconds, depending on the sample. Images were analyzed by determining the change in intensity with time of the region that was bleached versus a region of the cell far from the bleach. For simplicity, we fit the data to 1-3 exponential decay curves to determine the number of decay mechanisms and their corresponding time constants. Free eYFP diffusing in the cell body fit best to a single exponential with a time constant of $0.5 \pm 0.05$ s (n=5) correlating well with previous work (30). For simplicity, we will give comparative values of these rates in PC12 cells: 76.2% of eYFP-$PLC\beta_1$ is mobile and diffuses with a single exponential rate that is 40 fold slower than free YFP (n=7). 63.5% of eCFP-$G\alpha_q$ is mobile and shows 2 diffusion

rates which are 10 and 40 fold slower than free YFP (n=5). These results show that the proteins have restricted diffusion, both proteins have a significant immobile population, and a slower, similar diffusion that is on the order of those reported for membrane-bound cellular proteins (30).

**Discussion**

Signal transduction through heterotrimeric G proteins in part involves transient association of activated Gα subunits to specific effector(s) that in turn results in a series of coordinated events in the cell. In this study, we find a significant population of $G\alpha_q$ subunits and its main effector, $PLC\beta_1$, are pre-associated in the basal state in two cell lines, PC12 and HEK293. This pre-association will shorten the time scale of the signal and also will direct the signal along a specific pathway.

We measured the association of $G\alpha_q$ and $PLC\beta_1$ by overexpressing fluorescent-tagged proteins. First, we determined whether overexpression of the protein would promote complex formation by comparing the level of expressed protein to endogenous levels. We find that our level of expression is only 2-3 fold higher than that of the endogenous protein which, as detailed below, is not expected to significantly promote complex formation. Western blot analysis of the protein levels found in a known number of cells allows us to roughly estimate the endogenous cellular concentrations. We find that these approximate concentrations are low in the cell (e.g. 20 fM for $G\alpha_q$ and 3 fM for $PLC\beta_1$). To determine whether overexpression would affect the degree of association, we note that we have previously characterized the affinity between these proteins in purified form on model systems. We find that if the proteins are not confined to the membrane

surface, the affinity of PLC$\beta_1$ is ~10 nM for activated G$\alpha_q$ and 10 μM for GDP-bound G$\alpha_q$. Considering that the dimerization constant of GFP is ~100 μM (31) attachment of eYFP and eCFP to the proteins is not expected to contribute to their association. In contrast, confinement of the proteins to a membrane surface would significantly reduce these values as much as 100 fold (see (32)). Given these orders of magnitude differences in affinities, increasing the levels of the proteins 2-3 fold is not expected to alter the results obtained here.

Not only are the cellular concentrations of G$\alpha_q$ and PLC$\beta_1$ estimated to be much lower than their $K_d$ values, but we also find their cellular localization does not completely overlap. While G$\alpha_q$ appears to be almost entirely localized to the plasma membrane, we find a significant amount of PLC$\beta_1$ localized in cytosol as well as the plasma membrane in both of the cell lines studied here, i.e. differentiated PC12 cells and HEK293 cells. This distribution is supported by immunofluorescence of the endogenous enzyme using monoclonal antibodies and by cell fractionation. We note that cytsolic PLC$\beta_1$ has also been observed by cell fractionation in COS cells (e.g. (33)). Interestingly, previous localization studies of the closely related eGFP-PLC$\beta_2$ have been carried out by overexpression of the protein in HEK293 cells (34). These authors find that eGFP-PLC$\beta_2$, which binds G$\alpha_q$(GTP) ~20 fold more weakly than PLC$\beta_1$, is cytosolic until cell stimulation where it then moves to the plasma membrane presumably due to the release of activated G protein subunits.

To understand the basis of the cytosolic and plasma membrane populations of PLC$\beta_1$, we note that its cellular localization should be a function of its intrinsic membrane binding constant and the presence of protein partners. We have characterized

the membrane binding properties of purified PLC$\beta_1$ to lipid bilayers of varying composition (24). These studies showed that PLC$\beta_1$ binds strongly and fairly non-specifically to membranes with a membrane partition coefficient of ~50 μM. Based on these membrane affinities, we expect almost all PLC$\beta_1$ to be bound to cellular membranes. Localization of PLC$\beta_1$ due to membrane interactions rather than specific interactions with G$\alpha_q$ would be expected to give rise to both cytosolic and plasma membrane populations. This idea also correlates well with the low cellular concentrations of the two proteins.

Gα − effector activation has been thought to occur by the large increase in effector affinity that occurs upon GDP/GTP exchange. Our studies using FRET strongly suggest that Gαq and PLC$\beta_1$ are pre-associated even in the basal state. This observation is seen for the proteins expressed in PC12 cells as well as HEK293 cells and is supported by co-immunoprecipation studies. While FRET is only related to the distance between two probes and cannot assess whether two proteins are in close proximity or interacting, we note that the distance at which 50% of excited light from the donor is lost to transfer (Ro) is on the order of the size of the proteins used here (i.e. 30 Angstroms (13) and the FRET dependence goes as the sixth power of the distance (i.e. E=1/ [1+(R/R0)6]) assuming free rotation of the probes. If we crudely estimate the approximate dimensions of Gαq and PLC$\beta_1$ based on the crystal structures of G$\alpha_{i1}$ and the catalytic domain of PLC$\delta_1$ (4), (35) then proteins of areas 150x50 and 50 x 50 Angstroms will be laterally associating on the membrane surface (as shown in Figure 5, FRET is confined to the plasma membrane). While we do not yet know the orientation of the two proteins when they are complexed, we do know the placement of the fluorescent tags (i.e. on the N-terminus of PLCβ1 and

towards the middle $G\alpha_q$ (14)). The observation of an average FRET of ~0.5 in the unstimulated state suggests that the probe separation must be over ~35 Angstroms supporting the idea that the proteins are physically adjacent.

While the high degree of FRET between eCFP-$G\alpha_q$/eYFP-$PLC\beta_1$ in the basal state may be due to intrinsic factors that co-localize the proteins, it is more likely that scaffold proteins exist. We attempted to address this question by measuring FRET between eCFP-$G\alpha_q$ / eYFP-$PLC\beta_1$ in membrane preparations, but FRET results similar to the whole cells were obtained. Thus, either factors that promote self-assembly are retained in these preparations, or the proteins have the ability to self-scaffold. This idea stems from previous studies showing that several of these proteins have strong binding sites for their functional partners and secondary weaker sites for other related proteins in their signaling domain (10).

The function of the cytosolic population of $PLC\beta_1$ is unclear. It is possible that this population serves as an exchange factor for the plasma membrane population that is complexed with $G\alpha_q$ allowing for rapid delocalization of the signal. It is possible that the turnover rate of $PLC\beta_1$ in this cell line is high and the cytosolic population represents nascent protein. Alternately, the cytosolic population of $PLC\beta_1$ may serve as a reservoir in the case of rapid and high levels of $G\alpha_q$ related agonists which may release previously unavailable $G\alpha_q$. However, our studies showing that this cytosolic population of $PLC\beta_1$ is stable upon stimulation argue against this idea. Yet another possibility is that $PLC\beta_1$ regulates the phosphoinositol levels of internal membranes. Studies are underway to discriminate between these possibilities.

Both single cell and cell suspension studies show a high degree of eCFP-$G\alpha_q$ / eYFP-$PLC\beta_1$ FRET which is far higher than the value obtained for control samples viewing non-interacting proteins. This high degree is surprising since not all cellular $PLC\beta_1$ is localized on the plasma membrane and since the cellular concentration of $G\alpha_q$ is approximately 3 fold higher than $PLC\beta_1$. Thus, the overall FRET value of ~40% may correlate with complete association of the plasma membrane population of eYFP-$PLC\beta_1$, and may additionally correlate to higher order donor/acceptor complexes. The strong driving force for complex formation is unclear, since the two proteins exist at fairly low cellular concentrations, and since the affinity between unactivated versus activated $G\alpha_q$ and $PLC\beta_1$ is considerably weaker even when the two are confined to the membrane surfaces. Thus, there must be other factors, such as multiple interactions with other localized partners, which allow the local concentrations of the two proteins to be above their apparent dissociation constant and cause the proteins to remain bound.

Stable $G\alpha_q$ - $PLC\beta_1$ complexes are also supported by FRAP studies in which we bleached spots on the plasma membrane. Analysis of these results showed that both proteins have a large immobile population (i.e. ~24% for eYFP-$PLC\beta_1$ and 36% for eCFP-$G\alpha_q$) and that the rate of eYFP-$PLC\beta_1$ recovery matches one of the two fitted rates of eCFP-$G\alpha_q$ recovery. While there are multiple interpretations of these results, the simplest one that is supported by our FRET studies, is that there are stable $G\alpha_q$ / $PLC\beta_1$ complexes that are immobile, and also stable but slowly diffusing complexes. The faster rate observed for $G\alpha_q$ may correspond to protein that is not complexed with $PLC\beta_1$. The presence of a large percentage of slowly diffusing and immobile populations suggests that $G\alpha_q$ and $PLC\beta_1$ signals in part may not be spatially delocalized by protein diffusion,

but rather by the rapid diffusion of the Ins(1,4,5)$P_3$ and diacylglycerol second messengers generated upon activation of phospholipase C.

Suprisingly, we do not see significant changes in the amount of eYFP-PLC$\beta_1$-eCFP-G$\alpha_q$ FRET in living cells upon stimulation. As mentioned above, this observation implies that activated G$\alpha_q$ does not recruit a significant population of cytosolic PLC$\beta_1$ to the plasma membrane even though the concentration of G$\alpha_q$ exceeds PLC$\beta_1$. A lack of recruitment was confirmed by distribution analysis. Thus, either plasma membrane G$\alpha_q$ or cytosolic PLC$\beta_1$ are inaccessible to their partner, or the local concentrations of these proteins are not high enough to drive the association of cytosolic PLC$\beta_1$ to the plasma membrane to complex with G$\alpha_q$ (see(25)). One factor that may contribute to the lack of further recruitment of PLC$\beta_1$ to the plasma membrane is occlusion of activated G$\alpha_q$ by other proteins in the signaling complex. Alternately, recruitment can be diminished by the ability of PLC$\beta_1$ to stimulate the GTPase activity of G$\alpha_q$ subunits (i.e. its GAP activity) (36); The duration of G$\alpha_q$ signaling is greatly shortened allowing for a strong, short-lived signal. Enhancement of the GTPase activity of G$\alpha_q$ by PLC$\beta_1$ may eliminate the significant difference in affinity of PLC$\beta_1$for activated and non-activated G$\alpha_q$ and maintain the cytosolic level of PLC$\beta_1$.

If G$\alpha_q$ and PLC$\beta_1$ are preassociated in the basal state, then enzyme activation must occur through changes in G$\alpha_q$ - PLC$\beta_1$ molecular interactions presumably induced by the G$\alpha_q$ conformational changes that occur during GDP/GTP exchange. In Figure 3.11, we present a model of this activation process. This model is supported by our results showing that proteolysis of PLC$\beta_1$ differs when it is complexed to activated versus deactivated G$\alpha_q$. It is noteworthy that activation of PLC$\beta_2$ by G$\beta\gamma$ subunits appears to

involve small, low energy conformational changes that can be reversed by subtle changes in the protein-protein interface (3), (37). Thus, it is likely that activation by $G\alpha_q$ involves similar movements produced by effective interaction between only the GTPbound and not the GDP-bound Gα subunit.

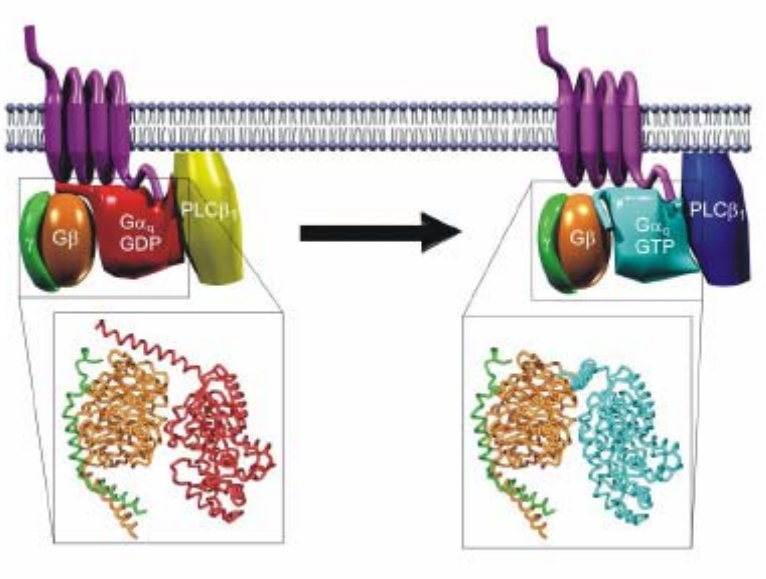


**FIGURE 3.11:** Model of activation of pre-associated $PLC\beta_1$-$G\alpha_q$(GDP) in which the change in interaction between Gα and Gβγ subunits because of agonist binding to a G protein-coupled receptor causes a change in the protein interface between Gα and its PLCβ effector.

It is notable that FRET has been used to study the interactions between G protein subunits during activation. Some studies suggest heterotrimer dissociation (23) whereas others suggest changes in orientation between stably associated Gα-Gβγ (29). It is unclear whether these conflicting reports are due to experimental differences including

differences in the level of protein expression. However, our results showing a stable $G\alpha_q$ and $PLC\beta_1$ population in the unstimulated state favor these latter studies and suggest a model of receptor-G protein-effector complexes that may self-scaffold due to multiple interactions. Previous measurements of RGS4 interactions with both $G\beta\gamma$ and $PLC\beta_1$ as well as $G\alpha_q$ support this idea (10) while further studies suggest a very specific nature of these multiple interactions (25). It would be interesting to see whether these $PLC\beta_1$-$G\alpha_q$ complexes are in turn associated with other proteins in particular signaling pathways to give rise to the rapid and specific signals needed in neural signaling.

**Literature Cited**


1. Rhee, S. G. (2001) *Annu Rev Biochem* **70**, 281-312
2. Rebecchi, M. J., and Pentyala, S. N. (2000) *Physiol Rev* **80**(4), 1291-1335
3. Runnels, L. W., and Scarlata, S. F. (1998) *Biochemistry* **37**(44), 15563-15574
4. Wall, M. A., Coleman, D. E., Lee, E., Iniguez-Lluhi, J. A., Posner, B. A., Gilman, A. G., and Sprang, S. R. (1995) *Cell* **83**(6), 1047-1058
5. Biddlecome, G. H., Berstein, G., and Ross, E. M. (1996) *J Biol Chem* **271**(14), 7999-8007
6. de Weerd, W. F., and Leeb-Lundberg, L. M. (1997) *J Biol Chem* **272**(28), 17858-17866
7. Tsunoda, S., Sierralta, J., Sun, Y., Bodner, R., Suzuki, E., Becker, A., Socolich, M., and Zuker, C. S. (1997) *Nature* **388**(6639), 243-249
8. Zeng, W., Xu, X., Popov, S., Mukhopadhyay, S., Chidiac, P., Swistok, J., Danho, W., Yagaloff, K. A., Fisher, S. L., Ross, E. M., Muallem, S., and Wilkie, T. M. (1998) *J Biol Chem* **273**(52), 34687-34690
9. Runnels, L. W., and Scarlata, S. F. (1999) *Biochemistry* **38**(5), 1488-1496
10. Dowal, L., Elliott, J., Popov, S., Wilkie, T. M., and Scarlata, S. (2001) *Biochemistry* **40**(2), 414-421
11. van der Meer, W., Coker, G., and Chen, S. S.-Y. (1994) *Resonance Energy Transfer, Theory and Data*, VCH Publishers, Inc., New York
12. Lakowicz, J. (1999), 368-390
13. Patterson, G. H., Piston, D. W., and Barisas, B. G. (2000) *Anal Biochem* **284**(2), 438-440
14. Hughes, T. E., Zhang, H., Logothetis, D. E., and Berlot, C. H. (2001) *J Biol Chem* **276**(6), 4227-4235
15. Conklin, B. R., Chabre, O., Wong, Y. H., Federman, A. D., and Bourne, H. R. (1992) *J Biol Chem* **267**(1), 31-34
16. Lo, W., Rodgers, W., and Hughes, T. (1998) *Biotechniques* **25**(1), 94-96, 98
17. Chidiac, P., Markin, V. S., and Ross, E. M. (1999) *Biochem Pharmacol* **58**(1), 39-48
18. Sambrook, J., Fritsch, E. F., and Maniatis, T. (1989) Molecular Cloning: A Laboratory Manual. In: Irwin, N. (ed). Cold Spring Harbor Press, Inc., Plainview, NY
19. Grynkiewicz, G., Poenie, M., and Tsien, R. Y. (1985) *J Biol Chem* **260**(6), 3440-3450
20. Ausubel, F. M., Brent, R. E., Kingston, R. E., Moore, D. D., Smith, J. A., Seidman, J. G., and Struhl, K. (1987). In. *Current Protocols in Molecular Biology*, John Wiley & Sons, Inc., New York
21. Medina, R., Grishina, G., Meloni, E. G., Muth, T. R., and Berlot, C. H. (1996) *J. Biol. Chem.* **271**, 24720-24727
22. Xia, Z., and Yuechueng, L. (2001) *Biophys.J.* **81**, 2395-2402
23. Janetopoulos, C., Jin, T., and Devreotes, P. (2001) *Science* **291**, 2408-2411
24. Runnels, L. W., Jenco, J., Morris, A., and Scarlata, S. (1996) *Biochemistry* **35**(51), 16824-16832
25. Philip, F., and Scarlata, S. (2004) *Biochemistry* **43**(37), 11691-11700

26. Rebecchi, M., and Pentylana, S. (2000) *Physiological Reviews* **80**, 1291-1335
27. Conklin, B. R., Chabre, O., Wong, Y. H., Federman, A. D., and Bourne, H. R. (1992) *J. Biol. Chem.* **267**, 31-34
28. Berkeley, J. L., and Levey, A. I. (2000) *J.Neurochem.* **75**, 487-493
29. Buneman, M., Frank, M., and Lohse, M. (2003) *Proc Natl Acad Sci U S A* **100**, 16077-16082
30. Partikian, A., Olveczky, B., Swaminathan, R., and Verkman, A. S. (1998) *J.Cell Biol.* **140**, 821-829
31. Philips, G. N. J. (1997) *Curr.Opin.Struc.Biol.* **7**, 821-827
32. Runnels, L. W., and Scarlata, S. (1999) *Biochemistry* **38**, 1488-1496
33. Kim, C. G., Park, D., and Rhee, S. G. (1996) *J Biol Chem* **271**(35), 21187-21192
34. Illenberger, D., Walliser, C., Strobel, J., Gutman, O., Niv, H., Gaidzik, V., Kloog, Y., Gierschik, P., and Henis, Y. (2003) *J.Biol.Chem.* **278**, 8645-8652
35. Essen, L. O., Perisic, O., Cheung, R., Katan, M., and Williams, R. L. (1996) *Nature* **380**(6575), 595-602
36. Berstein, G., Blank, J. L., Jhon, D.-Y., Exton, J. H., Rhee, S. G., and Ross, E. M. (1992) *Cell* **70**, 411-418
37. Scarlata, S. (2005) *Biophys J* **88**(4), 2867-2874

## General Conclusions

Study of the interactions between members of the $G\alpha_q$ inositol signaling pathway has led us to a model where members of this pathway have the ability to self scaffold. In the first series of studies, we looked at the binding affinities between purified proteins on membrane surfaces. We found that secondary interactions between RGS4 and $G\alpha_q$ and $G\beta\gamma$ could keep it close to the membrane surface which would be important for RGS4 function as it has very weak membrane affinity. RGS4 had a high (less than 1nM) affinity for activated $G\alpha_q$ and also a strong affinity for deactivated $G\alpha_q$. A strong residual interaction between RGS4 and deactivated $G\alpha_q$ would help keep RGS4 localized to the plasma membrane. In addition, we also found that RGS4 had a strong binding affinity for $G\beta\gamma$. Although this binding was 10-fold weaker than that for deactivated $G\alpha_q$, again, a residual interaction would aid in keeping RGS4 localized to the signaling complex. Presumably, RGS4 would compete with receptor and $G\beta\gamma$ for binding to deactivated $G\alpha_q$ in the basal state, and secondary interactions with $G\beta\gamma$ may keep it localized and in the proper orientation for binding to $G\alpha_q$ upon reactivation.

Another major finding of this study was that RGS4 had binding affinity for the $G\alpha_q$ effector, $PLC\beta_1$. This interaction seemed to be mediated by the C-terminal tail of $PLC\beta_1$ as RGS4 did not bind to a truncation mutant. Again, $PLC\beta_1$ may provide an additional site for localization of RGS4 to the signaling complex. This led us to our initial model wherein, in the basal state, $G\alpha_q$ and $G\beta\gamma$ are bound and associated with their

receptor. Although PLC$\beta_1$ has affinity for deactivated G$\alpha_q$, this affinity is not as strong as that of G$\beta\gamma$. Secondary interactions would additionally keep RGS4 localized to the signaling complex. Upon activation, PLC$\beta_1$ would displace G$\beta\gamma$ from activated G$\alpha_q$, and PLC$\beta_1$ and RGS4 could compete for binding to G$\alpha_q$ which would modulate the strength of the signal.

After this initial series of studies, we set out to test this model in living cells. We were interested in whether we could observe protein complexes in living cells. To our surprise, we found that G$\alpha_q$ and PLC$\beta_1$ were in preformed complexes in the basal state. Upon stimulation, this association remained unchanged. Thus, the major finding of these studies indicated that activation of PLC$\beta_1$ took place via intramolecular changes rather than through diffusion and association of G$\alpha_q$.

In addition, we looked at the distribution of G$\alpha_q$ and PLC$\beta_1$ in differentiated PC12 cells. As expected, we found both to be localized to the plasma membrane; however, there was a large, significant cytosolic population of PLC$\beta_1$. This cytosolic population was not the result of over-expression as we observed the same distribution for endogenous PLC$\beta_1$. This led us to speculate that perhaps the cytosolic population of PLC$\beta_1$ acted as a pool or PLC$\beta_1$ reservoir and could be recruited to the plasma membrane upon stimulation. This does not seem to be the case however, as we did not observe movement of PLC$\beta_1$ from the cytosol to the plasma membrane, leaving the function of this cytosolic population unknown.

Physiologically, it is known that a very rapid rise in calcium is required for such processes as neuronal plasticity and cardiovascular function. Preformed complexes would allow for very rapid signaling through GPCRs. Additionally, it would direct

signaling along a certain pathway through that of PLC$\beta_1$ as G$\alpha_q$ would not have to diffuse through the plasma membrane in search of its effector. By relieving this burden, signaling limitations would be placed on the resulting second messengers, $IP_3$ and DAG, which, because they are small, should diffuse very rapidly to bring about a rapid rise in intracellular calcium and the concomitant activation of PKC.

The field of $IP_3$ study began over 50 years ago (for a perspective see (1)). Although the suggestion of preformed complexes between G$\alpha_q$ and PLC$\beta_1$ is provocative, there are still many unanswered questions and future directions for the study of the interactions between these self-scaffolding proteins. First, what is the orientation of the G$\alpha_q$-PLC$\beta_1$ complex on the membrane surface? Second, how does the orientation of the two proteins to one another change upon G$\alpha_q$ activation? Presumably, PLC$\beta_1$ activation is brought about due to a more effective interaction with G$\alpha_q$ when it is in the GTP versus GDP bound form. Modeling studies to predict the most likely interaction sites would be a good start to begin investigating these questions, especially in light of the recently solved crystal structure of PLC$\beta_2$ in complex with Rac1 (2). In addition, where do preformed G$\alpha_q$-PLC$\beta_1$ complexes leave G$\beta\gamma$ and other members of the signaling pathway? To address this question, studies using the *in vivo* FRET technique described in Chapter 3 to look at the interaction between labeled G$\alpha_q$ and G$\beta\gamma$ and labeled G$\alpha_q$ and labeled RGS4 in the presence and absence of unlabeled PLC$\beta_1$ might begin to provide an answer.

Our data do not indicate the cytosolic population of PLC$\beta_1$ functions as a reservoir for the plasma membrane, and although we have not observed its translocation to the nucleus from the cyotplasm, it may do so. A function of cytosolic PLC$\beta_1$ may be

to control $PI(4,5)P_2$ levels of internal membranes and aid in cytoskeletal rearrangement processes that dictate cell shape (3). However, how this cytosolic population would be regulated is unclear as G proteins are localized to the plasma membrane. Currently, we are attempting to address whether there are additional mechanisms for $PLC\beta_1$ regulation (see Appendix A). It has been shown for nuclear $PLC\beta_1$ and other PLCβ isoforms that it can be phosphorylated by PKC and PKA, and in general, this phosphorylation attenuates their activity (4). To this end, we have made point mutations of $PLC\beta_1$ at serine 887, which is the residue phosphorylated by PKC in the nucleus, down regulating $PLC\beta_1$ activity (5). Initial results indicate that the point mutant mimicking the phosphorylated state (serine to aspartic acid substitution) is more cytosolic than the wild-type enzyme. Whether or not this is due to loss of interaction with protein binding partners at the plasma membrane is still unclear. However, phosphorylation may be a viable mechanism for regulation of the cytosolic $PLC\beta_1$ population.

Although it has not been mentioned previously, we also observed a nuclear population of $PLC\beta_1$ in undifferentiated PC12 cells. Localization to this cellular compartment would be lost upon application of nerve growth factor and cell differentiation. It is thought that the role of nuclear $PLC\beta_1$ is to aid in the progression of the cell cycle which would drive cell proliferation and/or differentiation (6). Currently there is debate over how much $PLC\beta_1$ is in the nucleus and differences in the percentages of the 1a and 1b splice variants in the cytosol and nucleus is most likely due to differences in cell lines used for study.

There is data to indicate that $PLC\beta_1$ may be localized to nuclear speckles. Nuclear speckles are subnuclear structures and within them are mRNA splicing factors,

protein kinases and phosphatases and other elements of $PI(4,5)P_2$ metabolism have been found there as well (7). Preliminary data, in our laboratory, indicate that $PLC\beta_1$ is localized to subnuclear structures in HEK293 cells. Studies are currently underway to investigate potential binding partners for $PLC\beta_1$ in these subnuclear structures, and co-localization studies of fixed and stained cells indicate that it may be associated with RNA binding proteins.

It is interesting to think about the exact composition of signaling complexes. Certainly, activators and effectors cannot be in a single large complex with receptor, and they must have some freedom of movement. Although our data indicate that $G\alpha_q$, $G\beta\gamma$, $PLC\beta_1$ and RGS4 could all be in a signaling complex, we do not know which interactions are more favorable over others or the role of the receptor. In addition, $G\beta\gamma$ has its own effectors (i.e. most notably $PLC\beta_2$ and ion channels) and does not simply function to regulate or sequester $G\alpha_q$ in the absence of receptor stimulation (8), and we do not know how close these effectors are or would have to be to the receptor-signaling complex. Most likely, primary interactions are dictated by what state the cell is in – basal or stimulated. For example, in the basal state, $G\alpha_q$ would have the strongest interaction with receptor and $G\beta\gamma$, and from the crystal structure of the $G\alpha_q$-$G\beta\gamma$ complex, $G\beta\gamma$ interacts with the switch II of $G\alpha_q$, and upon GTP for GDP exchange switch II is freed (9) allowing for interaction of all three switch regions with RGS4 (10). Interestingly, a recent study suggests that, upon stimulation, $G\alpha_i$ and $G\beta\gamma$ subunits do not dissociate upon activation leading the authors to speculate that the subunits undergo rearrangement rather than dissociation (11).

Although it is known that $G\alpha_q$ interacts with the C-terminus of $PLC\beta_1$, we do not yet know the orientation of these two proteins to one another in the signaling complex or how RGS4 fits into the signaling complex as it too interacts with the C-terminus of $PLC\beta_1$. Perhaps its strong, secondary interactions with $G\beta\gamma$ are more important in keeping it localized to the signaling complex and/or the GPCR itself (for recent RGS review see (12)). Also, there is data in the literature to suggest that GPCRs can form dimers or higher order oligomers. Although GPCR dimerization appears to function in proper delivery of receptors to the plasma membrane, dimers or oligomers at the cell surface would provide a large binding face for assembly and docking of many different signaling proteins (13).

Finally, our data does not address the role of lipid rafts or caveolae in organizing these signaling complexes. These lipid domains could serve to concentrate signaling proteins bringing about amplification of the signal. However, our FRAP data does provide additional evidence that $PLC\beta_1$ and $G\alpha_q$ are indeed part of higher order signaling complexes. Diffusion rates of G proteins on the plasma membrane are similar to those found for receptors (Philip *et al*, submitted for publication), and the presence of a large immobile fraction for both proteins supports the concept of a self-scaffolding model rather than one of "collision coupling" (14).

The three observed populations of $PLC\beta_1$ in PC12 cells, plasma membrane, cytosolic and nuclear, raise many questions about the function of the enzyme in these different compartments and points to the versatility of $PLC\beta_1$ in the regulation of a diverse set of cell functions. The emerging picture or model of GPCR signaling is becoming increasingly complex (for an interesting review see (15)). Most likely, the

organization of signaling domains is not homogenous throughout the plasma membrane, and it is more probable that discrete domains with their own, separate functions exist. This would lead to a mechanism for the action of a cell to be the result of the integration of a vast array of inputs.

**Literature Cited**


1. Irvine, R. F. (2003) *Nat Rev Mol Cell Biol* **4**(7), 586-590
2. Jezyk, M. R., Snyder, J. T., Gershberg, S., Worthylake, D. K., Harden, T. K., and Sondek, J. (2006) *Nat Struct Mol Biol*
3. Popova, J. S., and Rasenick, M. M. (2000) *J Neurosci* **20**(8), 2774-2782
4. Rebecchi, M. J., and Pentyala, S. N. (2000) *Physiol Rev* **80**(4), 1291-1335
5. Xu, A., Wang, Y., Xu, L. Y., and Gilmour, R. S. (2001) *J Biol Chem* **276**(18), 14980-14986
6. Faenza, I., Matteucci, A., Manzoli, L., Billi, A. M., Aluigi, M., Peruzzi, D., Vitale, M., Castorina, S., Suh, P. G., and Cocco, L. (2000) *J Biol Chem* **275**(39), 30520-30524
7. Martelli, A. M., Fiume, R., Faenza, I., Tabellini, G., Evangelista, C., Bortul, R., Follo, M. Y., Fala, F., and Cocco, L. (2005) *Histol Histopathol* **20**(4), 1251-1260
8. Oldham, W. M., and H, E. H. (2006) *Q Rev Biophys* **39**(2), 117-166
9. Tesmer, V. M., Kawano, T., Shankaranarayanan, A., Kozasa, T., and Tesmer, J. J. (2005) *Science* **310**(5754), 1686-1690
10. Tesmer, J. J., Berman, D. M., Gilman, A. G., and Sprang, S. R. (1997) *Cell* **89**(2), 251-261
11. Bunemann, M., Frank, M., and Lohse, M. J. (2003) *Proc Natl Acad Sci U S A* **100**(26), 16077-16082
12. Abramow-Newerly, M., Roy, A. A., Nunn, C., and Chidiac, P. (2006) *Cell Signal* **18**(5), 579-591
13. Milligan, G. (2006) *Biochim Biophys Acta*
14. Nobles, M., Benians, A., and Tinker, A. (2005) *Proc Natl Acad Sci U S A* **102**(51), 18706-18711
15. Werry, T. D., Wilkinson, G. F., and Willars, G. B. (2003) *Biochem J* **374**(Pt 2), 281-296

## Appendix A: Significance of PKC Phosphorylation of PLC$\beta_1$ Residue 887 in PLC$\beta_1$ Localization and its Interaction with G$\alpha_q$

Protein Kinase C (PKC) is a family of serine/threonine phosphotransferases which are activated by second messengers (for review see (1)). To date, in mammals, eleven PKC isotypes have been described and are divided into three subgroups conventional, novel and atypical that differ in their requirements for activation. Conventional PKCs ($\alpha$, $\beta$I, $\beta$II, and $\gamma$) require calcium and phospholipids for activation (phosphatidylserine, diacyglycerol and phorbal esters). Novel PKCs ($\delta$, $\varepsilon$, $\eta$, $\theta$, $\mu$/PKD) are calcium independent but do require phosphatidylserine and diacylglycerol for activation as well. And, lastly, atypical PKCs ($\zeta$, $\iota/\lambda$) are dependent on phosphatidylserine, inositol lipids or phosphatidic acid.

PKC structure consists of constant regions broken up by variable regions. The N-terminal portion of the protein contains a regulatory domain with cysteine rich repeats. Within this regulatory domain there are two conserved regions, C1 which is responsible for binding to DAG, and C2 which confers calcium sensitivity and is found only in the conventional PKCs. Joined to the regulatory domain by a hinge region is a catalytic domain, that also contains two conserved regions, C3 which has an ATP binding site and C4 which is responsible for substrate binding (2).

Conventionally, it is thought that PKC is inactive and resident in the cytoplasm until it translocates to the plasma membrane in response to various cell stimuli. There are a multitude of cellular processes that are regulated by PKC including proliferation, cell

cycle progression, differentiation, tumorogenesis, apoptosis, cytoskeletal remodeling, ion channels, and secretion (3).

It is well-known and documented that the phospholipase Cβ (PLCβ) family is regulated by G Proteins (for recent reviews see (4) and (5)). However, there is additional evidence that this family is regulated by phosphorylation of specific residues by protein kinase C (PKC), and PLCβs are substrates for PKC (6). For example, in cells treated with the PKC activator, 12-O-tetradecanoylphorbol-13 acetate (TPA), only the phosphorylation state of PLCβ changed while that of PLCγ and PLCδ remained the same (7). In addition, this group found that incubation of PKC with PLCβ purified from bovine brain resulted in incorporation of phosphate at serine 887. However, phosphorylation of the enzyme at this site did not affect its catalytic activity leading them to speculate that, instead of altering its activity, phosphorylation may alter the interaction of PLCβ with G protein subunits.

Phosphorylation may provide an additional layer of regulation of the enzyme beyond that of G proteins and is an intriguing idea as it would uncouple PLCβ activity from a G Protein Coupled Receptor (GPCR) pathway. Because the DAG product of PLCβ activates PKC this would provide a negative feedback signal, shortening the magnitude and duration of the signal. Accumulating evidence suggests that higher order signaling complexes exist between receptors, G Proteins, and their effector enzymes, and other accessory proteins. If the nature of these interactions is due to weak, secondary interactions between these proteins, then modifications, such as phosphorylation may play a role in regulating these interactions and may alter the proper orientation these proteins require for efficient activation and rapid signaling.

Evidence for regulation of PLC$\beta_1$ by PKC comes from studies done on nuclear PLC$\beta_1$. There is a separate, nuclear inositol signaling pathway that is distinct from that which occurs at the plasma membrane (for review see (8)). For example, activation of the MAP kinase pathway in mouse fibroblasts by insulin or IGF-1 results in translocation of MAP kinase to the nucleus where it phophorylates PLC$\beta_1$ on serine 982 resulting in increased nuclear PLC activity. Increased PLC$\beta_1$ activity increases the hydrolysis of phosphatidylinositol(4,5)-bisphate (PI(4,5)$P_2$) into inositol triphposphate ($IP_3$) and diacylglycerol (DAG). Accumulation of DAG attracts PKC$\alpha$ to the nucleus where it phosphorylates PLC$\beta_1$ on serine 887 and inactivates it (9).

Results of studies on the regulation of nuclear PLC$\beta$ differ from those of PLC$\beta_1$ at the plasma membrane. In these studies, attenuation of nuclear PLC$\beta_1$ activity in Swiss 3T3 cells by PKC$\alpha$ activation has clearly been demonstrated (10), and regulation of nuclear PLC$\beta$ by PKC$\alpha$ makes sense as, to date, G Proteins have yet to be found in nucleus. Whether plasma membrane PLC$\beta_1$ is similarly negatively regulated by PKC$\alpha$ remains to be seen.

In their Swiss 3T3 cell studies, Xu *et al* presents four lines of evidence for negative regulation of nuclear PLC$\beta_1$ by PKC$\alpha$. First, direct interaction between PLC$\beta_1$ and PKC$\alpha$ during an IGF-1 stimulation time course was demonstrated. In cells overexpressing PLC$\beta_1$, immunoprecipitation with a PLC$\beta_1$ monoclonal antibody of nuclear proteins resulted in an increase in the amount of PCK$\alpha$ pulled down over the time course. This association reached a maximum at 30 minutes. Second, accumulation of PKC$\alpha$ in the nucleus, during IGF-1 stimulation, resulted in a decrease of nuclear PLC$\beta_1$

activity. Third, inhibition of PKCα during IGF-1 stimulation resulted in an increase in $PLC\beta_1$ activity. And, fourth, $PLC\beta_1$ harvested from nuclei can be directly phosphorylated by purified, recombinant PKCα *in vitro*.

There are studies, using different PLCβ isoforms, which point to the possibility that plasma membrane $PLC\beta_1$ could be regulated by PKC as well. Some evidence stems from studies in which the role phosphorylation of $PLC\beta_3$ in terminating the response to platelet activating factor (PAF) (11) was investigated. PAF plays an important role in inflammation and signals through GPCRs which activate the PLC pathway. In these studies, RBL-2H3 cells were stimulated with PAF at different concentrations and over time. Immunoprecipitation of $PLC\beta_3$ using a $PLC\beta_3$ specific antibody from the cell lysate demonstrated increased phosphorylation of $PLC\beta_3$ which was dose- and time-dependent. When this group used an inhibitor of PKC, PAF induced phosphorylation of $PLC\beta_3$ was greatly reduced.

Studies by Sanborn and colleagues ((12) and (13)) revealed additional evidence for PKC phosphorylation modulating $PLC\beta_3$ activity. This group identified $PLC\beta_3$ residue serine 1105 as the phosphorylation site for PKC and PKA. In these studies, in four different cell lines overexpressing $PLC\beta_3$, phosphoinositide turnover stimulated via $G\alpha_q$ and $G\alpha_i$ coupled receptors was found to be inhibited upon activation of PKC with PMA. Mutation of serine 1105 to alanine relieved this inhibition on $G\alpha_q$ stimulation of $PLC\beta_3$ activity. Interestingly, phosphorylation of serine 1105 did not have any effect on $G\beta\gamma$ activation of $PLC\beta_3$ (12).

Turkey PLCβ (PLCβT) bears the greatest sequence homology to PLCβ$_2$ (69% identical). In studies using a turkey erythrocyte model, phosphorylation of PLCβT by PKC reduced its catalytic activity (14). In this study, the authors found using a reconstituted membrane system that the catalytic activity of PLCβT decreased proportionally as a result of increased phosphorylation by PKC. In addition, in this system, PKC phosphorylation inhibited stimulation of PLCβT both in the presence and absence of $AlF_4^-$ activated Gα$_q$. This result lead the authors to conclude that since there was no effect on the stimulation of PLCβT, then phosphorylation must result in an overall decrease in catalytic activity of the enzyme and not by altering the regulation of the enzyme by Gα$_q$. In assays using Gβγ, a reduction in phosphorylated PLCβT activity was not observed.

Since there was strong evidence in the literature that PLCβ is phosphorylated by PKC, we decided to investigate the role of phosphorylation on the localization and regulation of plasma membrane PLCβ$_1$. In particular, we were interested in serine 887 as phosphorylation of this residue by PKC attenuates the activity of nuclear PLCβ$_1$. We sought to determine if it plays a physiologically significant role at the plasma membrane as well. We reasoned that phosphorylation of this residue may also regulate PLCβ$_1$ at the plasma membrane since, upon activation, production of DAG and a rise in intracellular calcium via $IP_3$ production attracts PKC to the plasma membrane where, presumably it would have access to PLCβ$_1$. To this end, we made two point mutants: eYFP-PLCβ$_1$S887A and eYFP-PLCβ$_1$S887D. The serine to alanine mutant should not be able to be phosphorylated by PKC, and the serine to aspartic acid mutant should mimic the phosphorylated state.

In our previous work ((15) and (16)), we demonstrated that higher order signaling complexes exist between members of the $G\alpha_q$ signaling pathway, and these complexes may have the ability to self-scaffold. If phosphorylation of $PLC\beta_1$ disrupted its interaction or changed its interaction with $G\alpha_q$, we might see differences in localization of the protein. In addition, we have demonstrated that $G\alpha_q$ and $PLC\beta_1$ are preassembled in a complex in the basal state. Phosphorylation of $PLC\beta_1$ may alter its association with $G\alpha_q$ perhaps by changing its orientation to the G Protein.

Using methods we have employed previously, we looked at the localization of these point mutants in PC12 cells, quantified the interaction between these mutants and $G\alpha_q$ in the basal state using an *in vivo* Fluorescence Resonance Energy Transfer FRET technique, and looked at the mobility of these point mutants in comparison to wild-type $PLC\beta_1$ using Fluorescence Recovery After Photobleaching (FRAP).

Preliminary results indicate that, in comparison to wild-type eYFP-$PLC\beta_1$, the point mutants have a greater expression in the cytosol. Whether this redistribution of the protein to the cytosol is physiologically relevant or related to the mutation of residue 887 is still unclear. Studies of the interaction between the point mutants and $G\alpha_q$ using *in vivo* FRET demonstrate a stable association between the proteins in the basal state which is similar to wild-type.

## Materials and Methods

### *Reagents*

eCFP-$G\alpha_q$ was derived from $G\alpha_q$-GFP as previously described (17) and was a generous gift from Dr. Catherine Berlot (Geisinger Clinic, Danville, PA). eYFP-$PLC\beta_1$

was a generous gift from Loren Runnels (Dept. of Cell Biology, Rutgers University). This construct shows wild type basal activity and activation by $G\alpha_q$.

*Point Mutant Construction*

eYFP-PLC$\beta_1$S887A and eYFP-PLC$\beta_1$-S887D point mutants were generated from the wild-type eYFP-PLC$\beta_1$ plasmid. To mutate serine 887 to alanine, the forward primer was CAGCCTGCTCCAGGGGCTGTGAAGGCACCC and the reverse primer was GGGTGCCTTCACAGCCCCTGGAGCAGGCTG. To mutate serine 887 to aspartate, the forward primer was CAGCCTGCTCCAGGGGATGTGAAGGCACCC, and the reverse primer was GGGTGCCTTCACATCCCCTGGAGCAGGCTG.

*Instrumentation*

Images, time-lapses, and z-stacks were taken on a Zeiss Axiovert 200M with an AxioCam MRm camera using Axiovision software. Pixel analysis of confocal images and image analysis of FRET data was done using Image J (NIH). Fluorescence spectra were taken on a photon-counting spectrofluorometer, ISS-PC (ISS, Urbana, IL).

*Cell Culture and Transfection*

Rat pheochromocytoma cells (PC12), derived from the adrenal gland (ATCC, #CRL-1721), were cultured in Dulbecco's modified Eagle's medium (DMEM) supplemented with 10% equine serum, 5% fetal bovine serum, and 100mM sodium pyruvate and were incubated at 37$^o$ C with 5% $CO_2$. Nerve growth factor (NGF, Sigma,

St. Louis, MO) was added to a final concentration of 100ng/ml to induce differentiation. Prior to transfection, cells were grown in T-25 flasks to 80-90% confluency.

Plasmids were introduced into cells by electroporation using a protocol adapted from Maniatis (18). Briefly, the DMEM was aspirated, and the PC12 cells were harvested by adding 5mL of fresh media and pipetting multiple times over the bottom of the flask. Cells were spun down for 5 minutes at 1500 x g and resuspended in 5mL of phosphate buffered saline (PBS). One mL of cells was removed, counted, and the cell suspension was diluted to 5 x $10^6$ cells/ml. Cells (500μL) were pipeted into 0.4cm BioRad cuvettes and incubated on ice for 10 minutes. Then, 10-30 μg of plasmid DNA was added to each cuvette and gently mixed. The electroporator (BioRad Gene Pulser Xcell) was set to 0.25 kV with a capacitance of 500 μF. Cuvettes were placed in the shocking chamber and pulsed once. After the pulse, the cells were allowed to rest for 1-2 minutes and 1mL of DMEM was then added to each cuvette. Cells were placed in 15mL conical tubes containing 3 mL of DMEM. Tubes were spun down at 1500 x g for five minutes and cells were brought up in 1.5 mL DMEM and plated onto Lab Tek chambers coated with 50μg/mL fibronectin (Sigma). Three to four hours post-transfection, the wells were washed with 1mL PBS and 1.5mL DMEM containing 100ng/mL NGF was added. After three days of incubation with NGF, transfected cells were differentiated and used for imaging.

HEK293 cells were cultured in DMEM plus 10% FBS and 1% PenStrep at 37ºC with 5% $CO_2$. Plasmids were introduced to HEK293 cells by calcium phosphate precipitation. 16-20 hours post-transfection, the media was changed, and two days later, the cells were ready for imaging.

*Activity Measurements*

PC12 cells were transfected with protein expression vectors eYFP-PLC$\beta_1$, eYFP-PLC$\beta_1$S887A, eYFP-PLC$\beta_1$S887D and empty vector. Five identical transfections were combined into a T-25 flask. Then, PC12 cells were harvested from T25 flasks and washed two times with PBS. After the second wash, the cells were brought up in PBS containing 1mM PMSF and 10μg/ml aprotinin, placed on ice, and homogenized. Nuclei were removed by a low speed centrifugation at 750 x g for five minutes at 4$^o$ C. The supernatant was removed and spun at 28,000 rpm for 35 minutes at 4 C. The supernatant or cytosolic fraction was removed and the resulting pellet or membrane fraction was brought up in PBS containing 1mM PMSF and 10μg/ml aprotinin. The protein concentration for the cytosolic and membrane fractions was assayed, and 5μg of material was used in each assay tube (19). The linear range of activity was determined for the samples, and one minute incubation at 37°C was chosen as the reaction time.

*Single cell FRET measurements*

FRET measurements were determined using the procedure of Devreotes. Bleed-through values were obtained by transfecting PC12 cells with 10μg of free eCFP or free eYFP plasmid vectors and imaging under the appropriate filter sets (Chroma, Inc.). Cells expressing only CFP or YFP were then imaged under the CFP (Chroma #31044v2) or YFP (Chroma #41029) and FRET (Chroma #31052) filter sets to determine the FRET/CFP or FRET/YFP ratio. Averaging over 12 cells, on our system, the bleed-through values for CFP and YFP are 39% and 28% respectively using the background-

corrected intensities calculated using ImageJ software from N.I.H. To generate a net FRET image by accounting for bleed-through emission,

$$nF = I_{FRET} - I_{YFP} \times a - I_{CFP} \times b$$

where a and b equal the percentage of bleed-through of YFP and CFP under the FRET filter set. However, to compare FRET values among cells with varying protein expression levels, the net FRET (*nF*) value can be normalized ($N_{FRET}$). From the entire intensity value of the image, one can calculate $N_{FRET}$. Normalized FRET ($N_{FRET}$) is given as (20):

$$N_{FRET} = \frac{I_{FRET} - I_{YFP} \times a - I_{CFP} \times b}{\sqrt{I_{YFP} \times I_{CFP}}}$$

where *a* and *b* equal the percentage of bleed-through of CFP and YFP under the FRET. $N_{FRET}$ was determined as described (20).

*Image analysis.*

Images were processed using ImageJ (NIH). Before any analysis, images were corrected for background as follows. First, the background was calculated from a 50x50 pixel box at the top left corner of the raw image and this intensity was subtracted from the entire image. Then, uneven illumination was removed from the image using three iterations of the Background Correction Plugin. This image was binary thresholded and then inverted to make the cell white (255) and the background black (0). Next, the image was divided by 255 to make the pixel values for white 1. Finally, the background subtracted image was multiplied by the thresholded image. These manipulations remove the background by making the background 0. Using the method of Xia (20), *nF* images were created by multiplying the background corrected donor image by the donor

correction factor, the background corrected acceptor image by the acceptor correction factor, and then subtracting each of these from the background corrected FRET image. $N_{FRET}$ images were created by multiplying the background corrected donor and acceptor images and then taking the square root creating a resultant image. The *nF* image was then divided by the resultant image. A global, normalized FRET value was calculated by averaging each individual pixel's normalized FRET value. This program also calculates the corresponding normalized FRET ranges (0-10%, 10-20%, etc.) for the image.

To analyze the distribution of endogenous and overexpressed proteins within a z-stack, the images were run through a program which lists the pixel intensity value at a user specified x,y coordinate for a 3 x 3 pixel area (9 pixels through the cell) for all images within the stack. Intensity values for each pixel per slice were then averaged and plotted.

*FRAP Studies*

Fluorescence recovery after photobleaching (FRAP) measurements were carried out using an $N_2$ laser (Spectra Physics) of 100-milliwatt power to photobleach a circular region of 2 μ diameter on specific regions of the cells. The intensity of the photobleached portion was allowed to recover over time, and the recoveries were fit to a single exponential curve.

## Results

*Distribution of eYFP-PLC$\beta_1$S887A and eYFP-PLC$\beta_1$S887D in differentiated PC12 cells*

In differentiated PC12 cells, over-expressed eYFP-PLC$\beta_1$ has mainly a plasma membrane distribution. However, there is a significant cytosolic population, and a cytosolic population is observed for endogenous protein as well (16). We conducted a similar series of studies for the point mutants in differentiated PC12 cells. To characterize the localization of the point mutants, we collected z-stacks using confocal microscopy and looked at the intensity of the fluorescence in a region of interest from the bottom to the top of the z-stack. If there was a complete plasma membrane distribution of the proteins, we would observe most of the intensity at the bottom and top of the cell corresponding to the plasma membrane. And, although we do observe the over-expressed point mutants in the plasma membrane, there is a greater localization of it in the cytosol compared to wild-type (see figure A.1 and A.2). In comparison to eYFP-PLC$\beta_1$S887A, eYFP-PLC$\beta_1$S878D has a much greater distribution to the cytosol. Whether this observation is due to the aspartic acid substitution has yet to be determined.

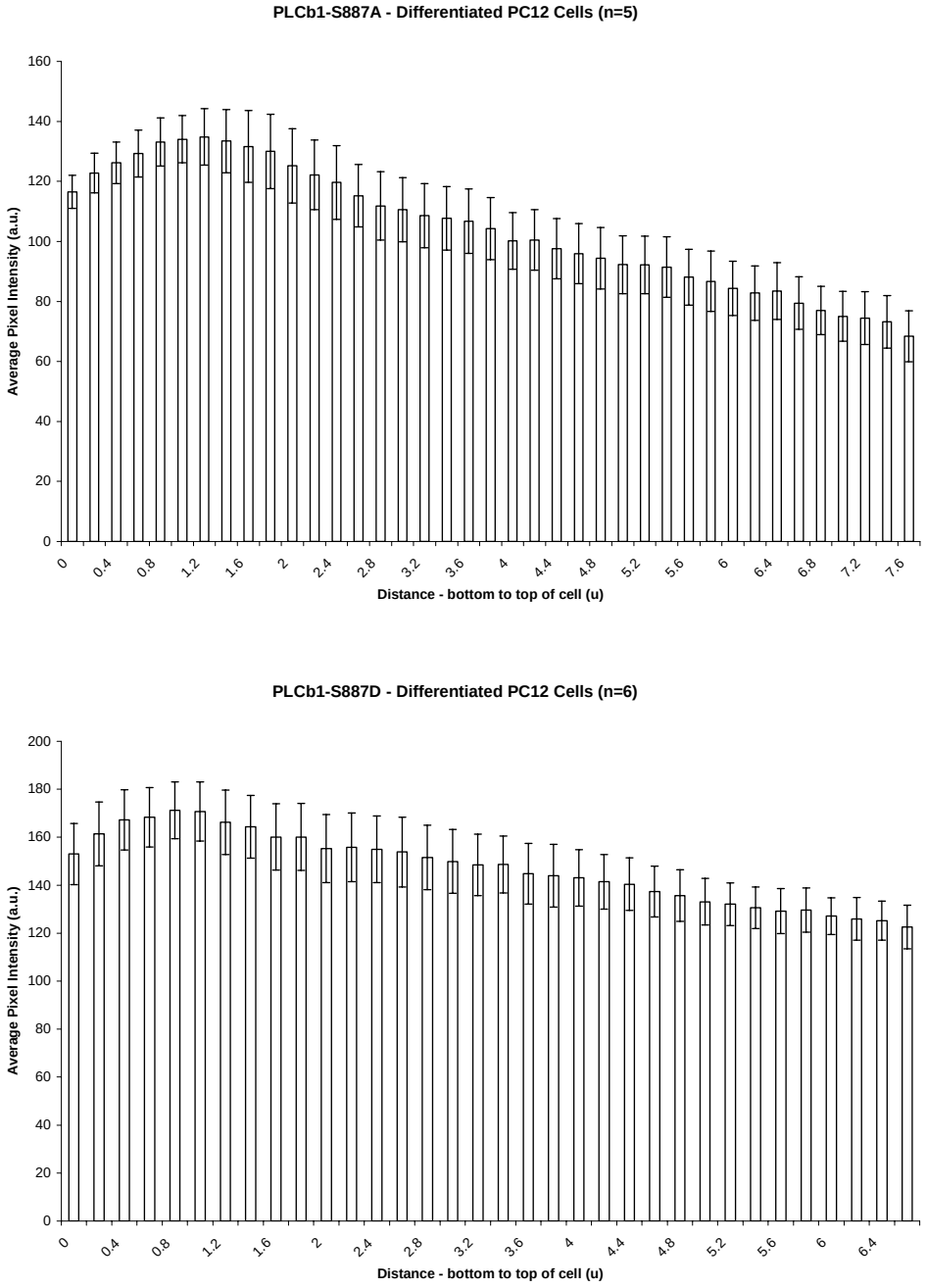


**Figure A.1:** Localization of eYFP-PLC$\beta_1$S887A (top panel) and eYFP-PLC$\beta_1$S887D (bottom panel) in differentiated PC12 cells. Shown are histographs of the average intensity of fluorescence collected from 5-6 cells on the z-axis from the bottom toward the top of the cells. Error is shown as standard error of the mean.

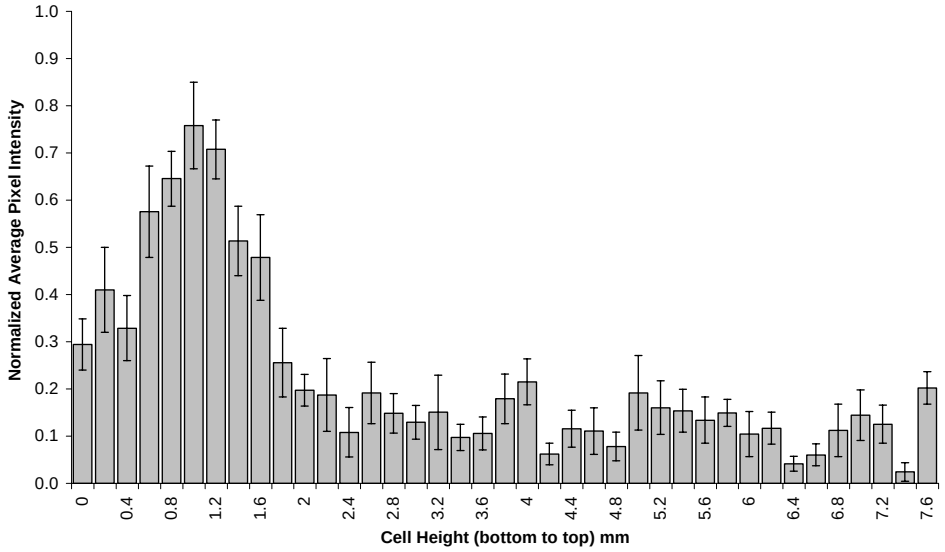


**Figure A.2:** Distribution of eYFP-PLC$\beta_1$ in a differentiated PC12 cell (16).

*PLC activity of cellular fractions*

The PLC activity of PC12 cell cytosolic and membrane fractions transfected with empty vector, eYFP-PLC$\beta_1$, eYFP-PLC$\beta_1$S887A, and eYFP-PLC$\beta_1$S887D was compared to assess whether the point mutations would have an effect on PI(4,5)$P_2$ hydrolysis. Due to background activity levels of other PLCs (most notably, PLC$\delta_1$) and possible variations in expression levels from transfection to transfection, it was difficult to assess whether or not mutation of residue 887 had an effect on activity as compared to the wild-type PLC$\beta_1$. Although it appeared that the S887A mutation resulted in an increase in this construct's activity over the others, for the membrane fraction, there was not a statistical significant difference between the transfection groups due to variations in the samples when comparing the raw data (counts/minute) which contributed to a large error (see figure A.3). The raw data is shown in lieu of fold activation over empty vector cellular

fractions to avoid misinterpretation of the results. In addition, there were not any differences in the PLC activity for the cytosolic fractions.

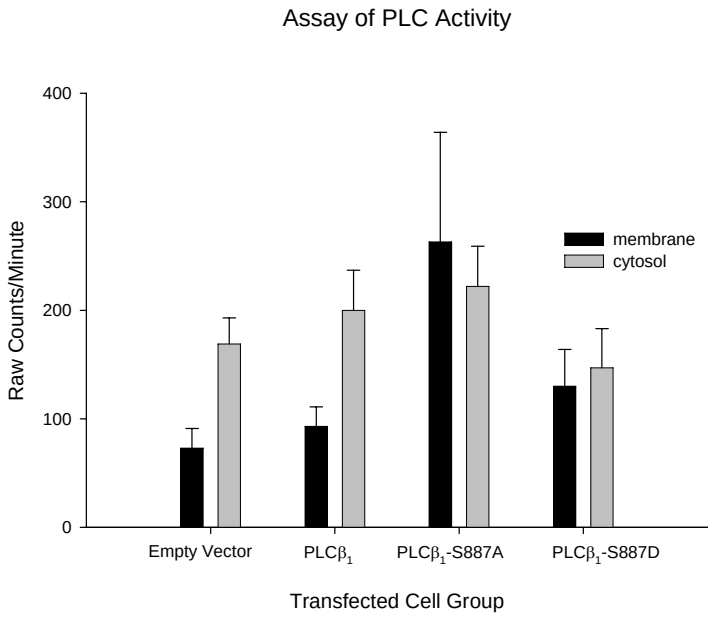


**Figure A.3:** PLC activity assay of cellular fractions from transfected PC12 cells. Shown is average data from 3 separate experiments, and error is reported as standard error of the mean.

*In vivo FRET between $G\alpha_q$-eCFP and eYFP-PLC$\beta_1$S887A and eYFP-PLC$\beta_1$S887D in the basal state in HEK293 cells*

Previously, we have shown a stable association between $G\alpha_q$ and PLC$\beta_1$ in PC12 cells in the basal and stimulated states (16). To study whether point mutations at residue 887 affected the interaction with $G\alpha_q$, we conducted similar, *in vivo* FRET experiments in HEK293 cells. We observe a similar FRET efficiency for the mutants and wild-type eYPF-PLC$\beta_1$ with eCFP-$G\alpha_q$ (about 40%). The level of FRET does not change over time (see figure A.4) indicating that these proteins are in a stable complex with the G protein in the basal state.

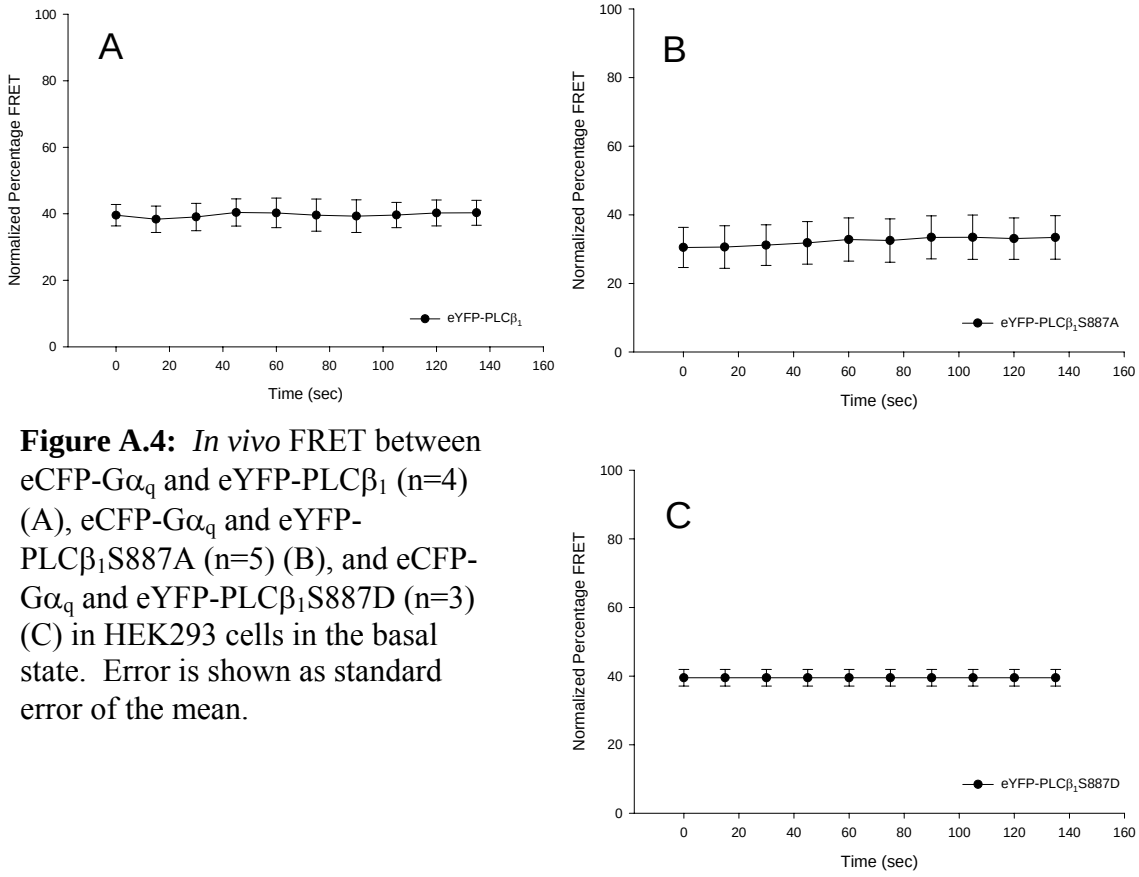


**Figure A.4:** *In vivo* FRET between eCFP-G$\alpha_q$ and eYFP-PLC$\beta_1$ (n=4) (A), eCFP-G$\alpha_q$ and eYFP-PLC$\beta_1$S887A (n=5) (B), and eCFP-G$\alpha_q$ and eYFP-PLC$\beta_1$S887D (n=3) (C) in HEK293 cells in the basal state. Error is shown as standard error of the mean.

Shown, in figures A.5-A.7, are examples of single cells from the above studies. From the FRET distribution graphs, it is clear that the FRET signal is not changing over time or moving into a higher or lower global FRET category. Again, this indicates that mutation of residue 887 does disrupt the interaction with G$\alpha_q$ in the basal state. Studies are underway to look at these interactions upon stimulation.

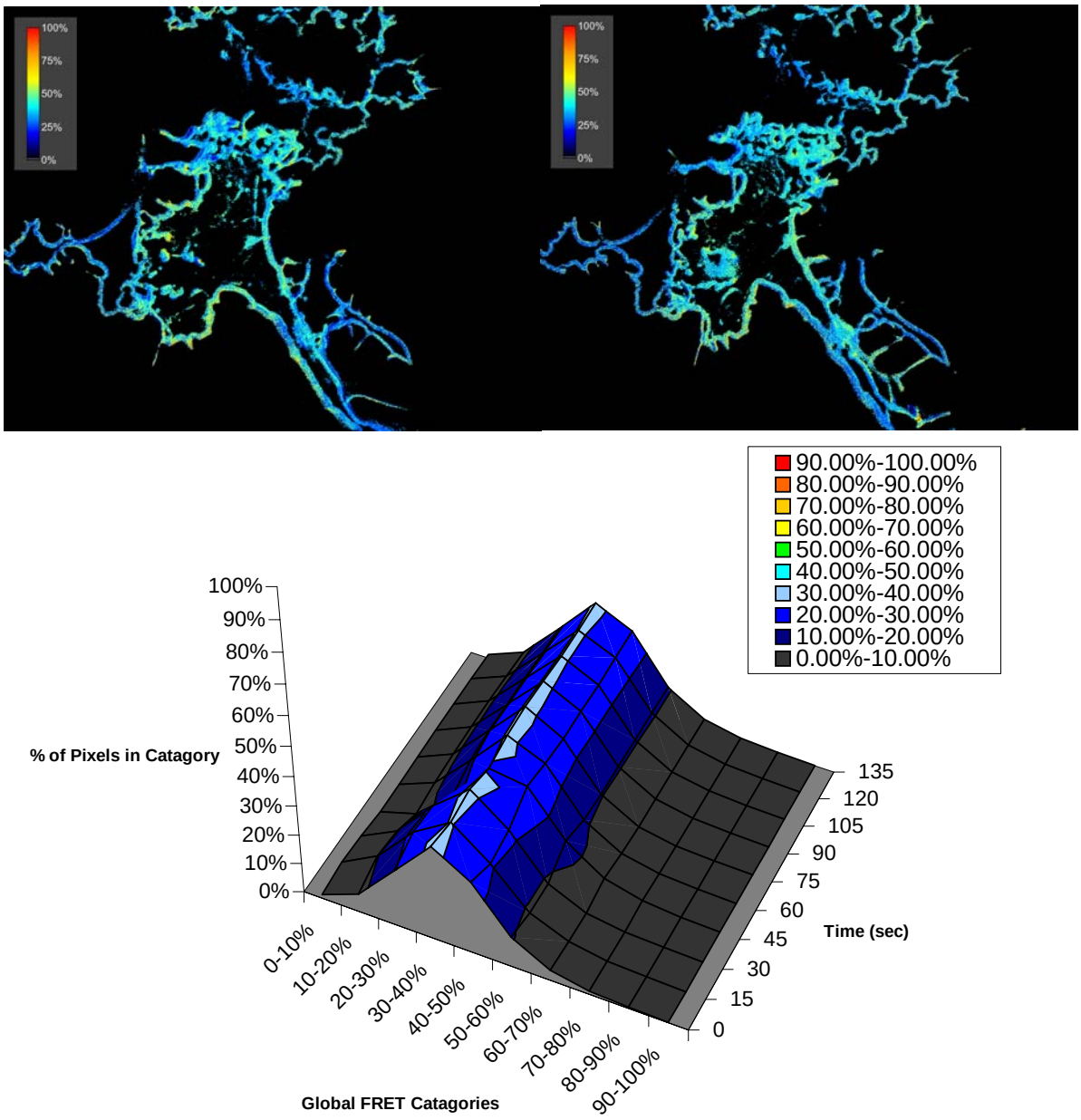


**Figure A.5:** Example of single cell FRET between eCFP-G$\alpha_q$ and eYFP-PLC$\beta_1$ in an HEK293 cell. Top two panels depict a pseudo-colored HEK293 cell at the beginning (left panel) and at the end (right panel) of the time study. Lower panel is a graph representing the percentage of pixels in each global FRET category and reflects the FRET distribution over time.

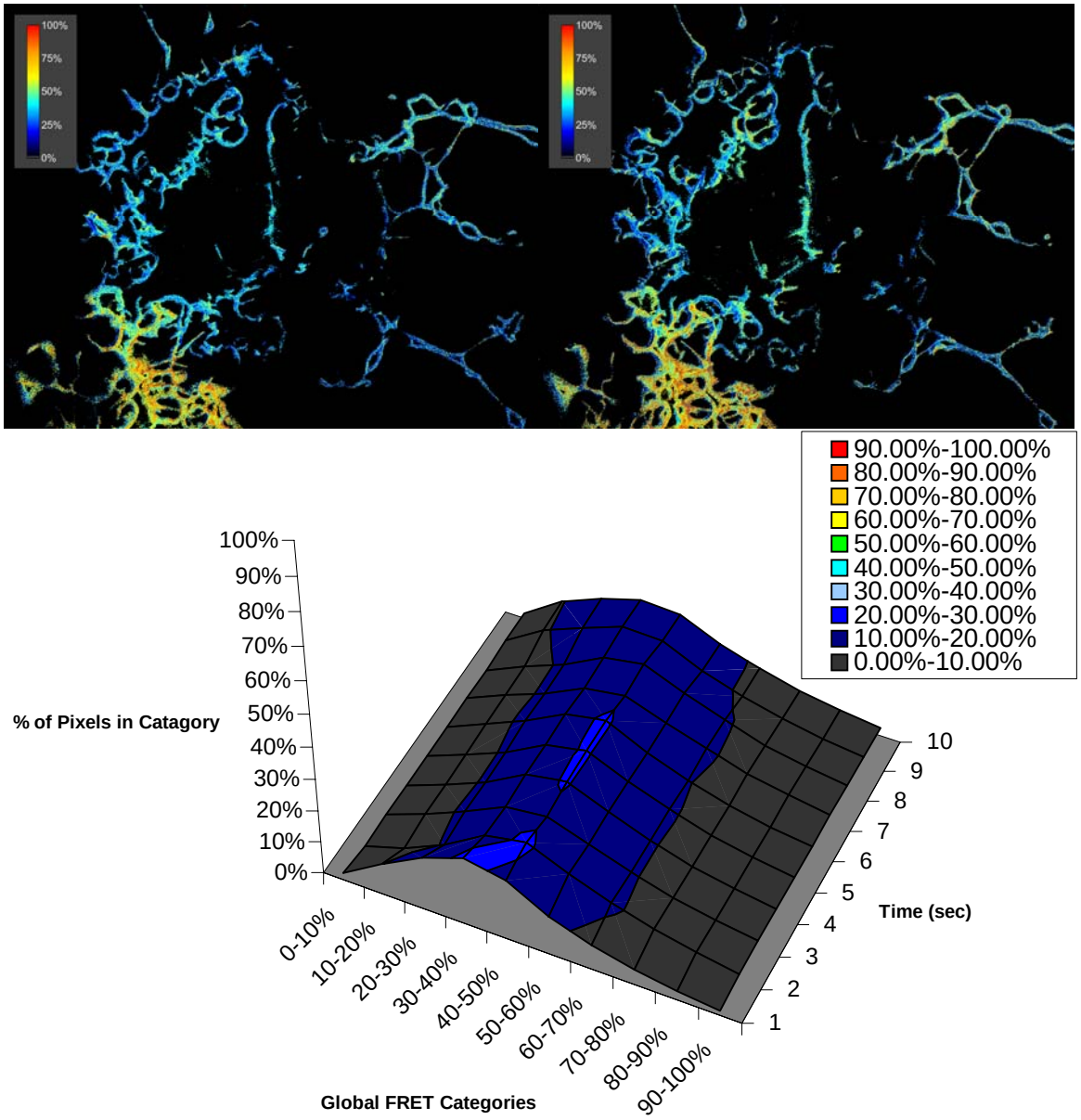


**Figure A.6:** Example of single cell FRET between eCFP-G$\alpha_q$ and eYFP-PLC$\beta_1$S887A in an HEK293 cell. Top two panels depict a pseudo-colored HEK293 cell at the begining (left panel) and at the end (right panel) of the time study. Lower panel is a graph representing the percentage of pixels in each global FRET category and reflects the FRET distribution over time.

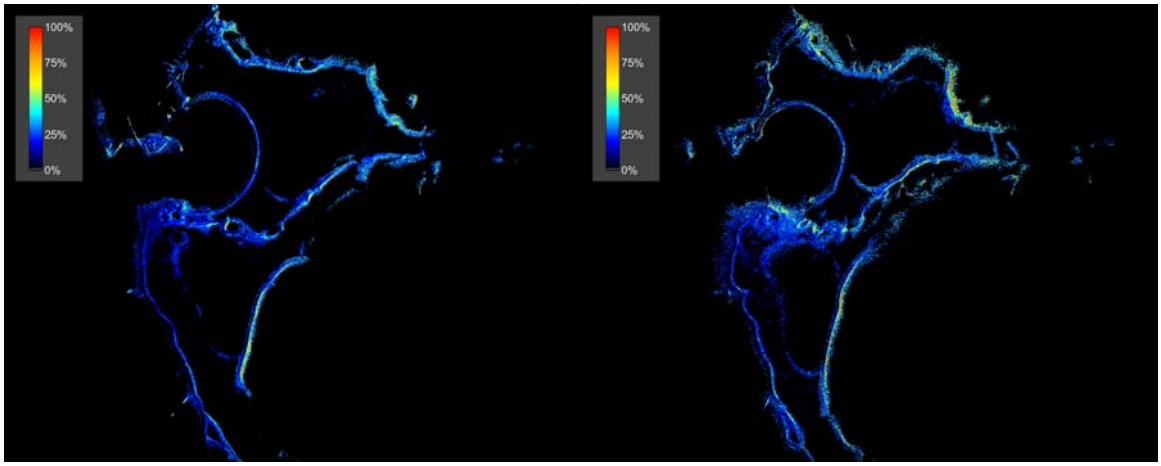


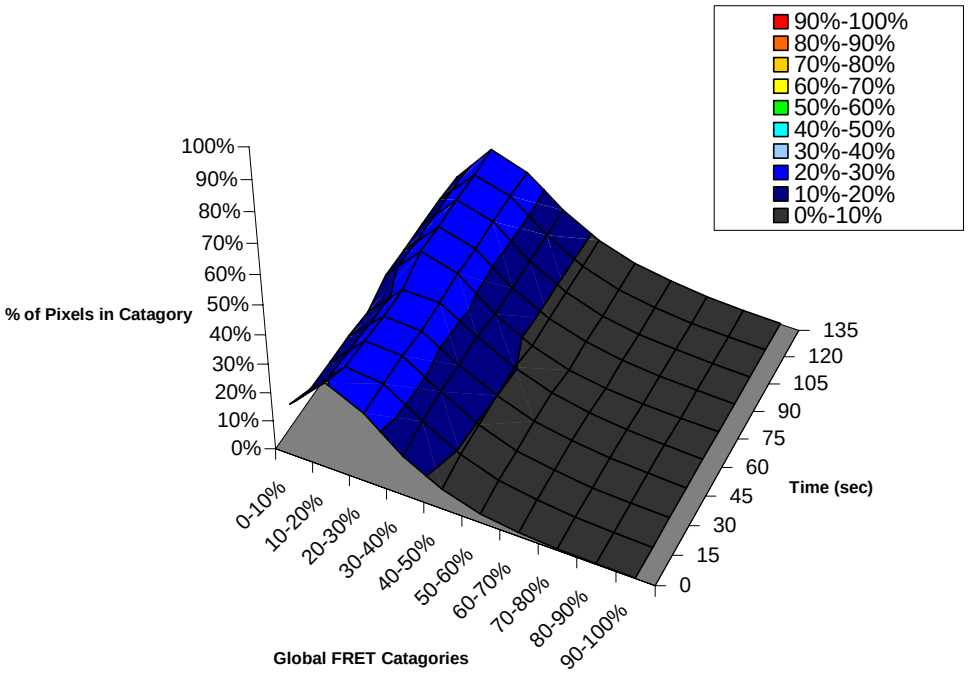


**Figure A.7:** Example of single cell FRET between eCFP-G$\alpha_q$ and eYFP-PLC$\beta_1$S887D in an HEK293 cell. Top two panels depict a pseudo-colored HEK293 cell at the begining (left panel) and at the end (right panel) of the time study. Lower panel is a graph representing the percentage of pixels in each global FRET category and reflects the FRET distribution over time.

*Comparison of wild-type eYFP-PLC$\beta_1$ mobile fraction and diffusion to eYFP-PLC$\beta_1$S887A and eYFP-PLC$\beta_1$S887D using FRAP*

If the point mutations at residue 887 disrupted interactions that normally hold PLC$\beta_1$ in a complex with other proteins, we might observe differences in the mobile fraction between wild-type eYFP-PLC$\beta_1$ and the mutants. By bleaching a spot on the plasma membrane and watching the recovery of the fluorescence over time in that spot, we can calculate the fraction of over-expressed protein that is mobile. FRAP experiments on wild-type and point mutant proteins demonstrated that the point mutants had a similar recovery pattern (see figure A.8) and a mobile fraction of about 60% (see table A.1) as compared to the wild-type.

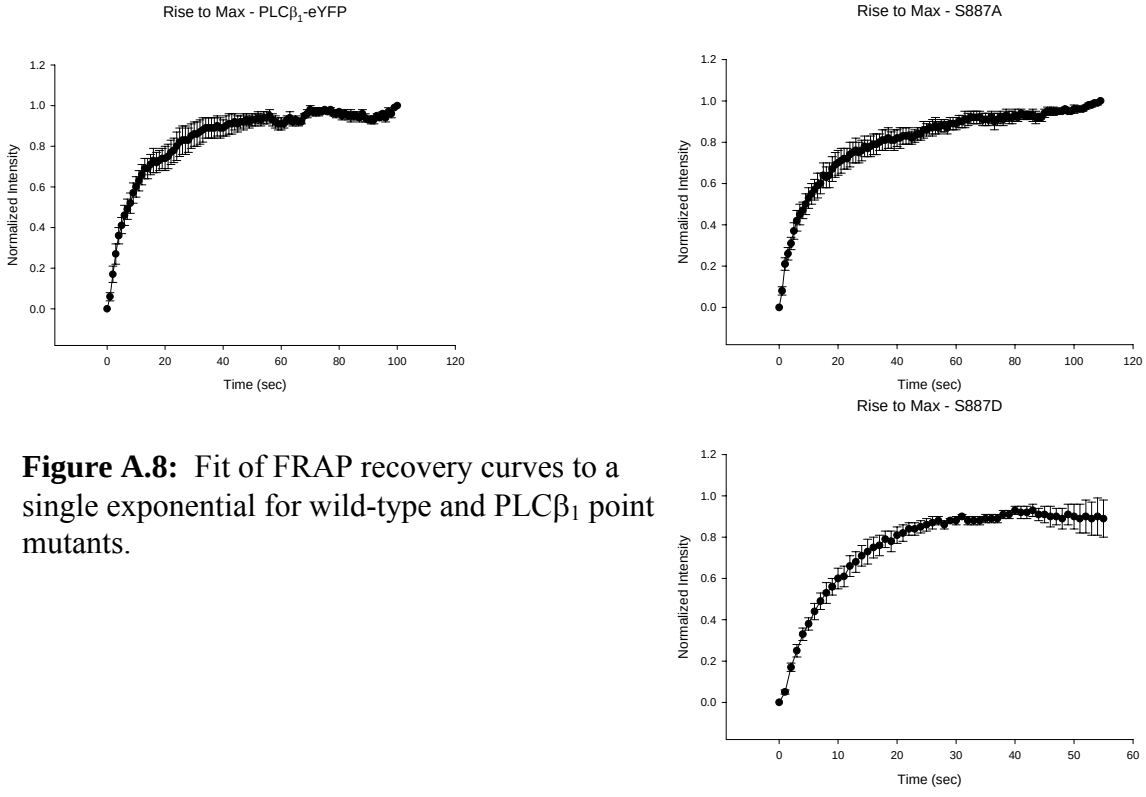


**Figure A.8:** Fit of FRAP recovery curves to a single exponential for wild-type and PLC$\beta_1$ point mutants.

**Table A.1:** Comparison of the Mobile Fraction, $Sec^{-1}$, and $t_{1/2}$ between eYFP-PLC$\beta_1$ and point mutants.

| | **Mobile Fraction** | **$Sec^{-1}$** | **$t_{1/2}$** | **n** |
|---|---|---|---|---|
| **eYFP-PLC$\beta_1$** | 69 ± 9% | 0.10 ± 0.02 | 8.5±1.8 | 5 |
| **eYFP-PLC$\beta_1$S887A** | 61 ± 8% | 0.08 ± 0.02 | 10.6±2.7 | 6 |
| **eYFP-PLC$\beta$1S887D** | 60 ± 9% | 0.08 ± 0.01 | 9.7±1.9 | 6 |

**Discussion**

Data, in the literature, suggest that phosphorylation of PLCβs could negatively regulate their enzymatic activity. The strongest evidence for regulation of PLC$\beta_1$ by phosphorylation comes from studies done on nuclear PLCβ1, although regulation of PLC$\beta_1$ in the nucleus would be expected to differ from that at the plasma membrane due to the fact that, to date, G proteins have not been observed in that cellular compartment. Therefore, additional mechanisms for regulating PLC activity in the nucleus would have to be employed. However, since an increase in DAG in the nucleus attracts PKCα, and since production of DAG that occurs in the plasma membrane also attracts PKC, we reasoned that PKC would have access to PLC$\beta_1$ in the plasma membrane and may phosphorylate it. Phosphorylation at residue 887, which is in the C-terminal portion of the protein that interacts with G$\alpha_q$, might interfere with the normal interaction between these two proteins and inhibit PLC$\beta_1$ activation by G$\alpha_q$.

Studies on the point mutations made at residue 887 of eYFP-PLC$\beta_1$ are still incomplete and whether or not this residue has physiological significance for regulation of the enzyme at the plasma membrane is still very much unclear. We do observe a

greater cytosolic localization for both point mutants compared to the wild-type protein, but whether the mutation is truly disrupting an interaction between other protein partners that normally aid in plasma membrane localization or is simply a reflection of over-expression is unknown.

Activity measurements do not indicate a difference in the activities of the point mutants and wild-type PLC$\beta_1$. Although these studies are difficult to carry out due to background contributions from endogenous PLCs, data in the literature, using purified proteins, suggest that phosphorylation of residue 887 does not reflect in a decrease in PLC$\beta_1$ activity (7).

Presumably, mutation of serine 887 to aspartic acid would mimic the phosphorylated state. And, if phosphorylation at this residue negatively regulates the enzyme and inactivates it, we would expect to see an interruption in the interaction between this point mutant and G$\alpha_q$. However, studies using *in vivo* FRET in the basal state do not suggest this as there is not a difference in the level of FRET between eYFP-PLC$\beta_1$S887D and eYFP-PLC$\beta_1$ and eCFP-G$\alpha_q$. The reasons why we do not observe less FRET between eYFP-PLCβ1S887D and eCFP-G$\alpha_q$ could be as follows: either phosphorylation does not significantly weaken the interaction between PLC$\beta_1$ and G$\alpha_q$ or it subtly changes the orientation of the proteins to one another but does not change the distance between the two probes meaning that we would not detect a change in FRET efficiency. Most likely, changes in the interaction between G$\alpha_q$ and eYFP-PLC$\beta_1$S887A would be observed upon stimulation since there would not be feed-back regulation due to its inability to be phosphorylated at that residue. However, results at this point with the alanine mutant are still too preliminary to be shown or discussed.

The point mutants demonstrate similar behavior as wild-type eYFP-PLC$\beta_1$ in the FRAP studies conducted. Most likely, mutation of residue 887 does not interrupt interactions that hold the wild-type enzyme in higher order signaling complexes. For all three proteins, a significant immobile fraction is observed (about 40%) indicating that the diffusion of the proteins through the plasma membrane is limited.

To demonstrate that the point mutants are functionally active, calcium release experiments were attempted. However, results were never obtained because the cells did not respond to stimulation and release calcium. Why, experiments that normally work reliably with good reproducibility in our lab, stopped working is unclear. At first, we thought it was due to problems with the PC12 cells and switched to HEK293 cells. Although empty vector HEK293 cells, did release calcium sometimes upon stimulation, they would not do this every time the experiment was attempted. Thus, studies to assess that the point mutants are functionally active and coupled to functional receptors were not able to be completed. If residue 887 is important in PLC$\beta_1$ regulation, upon stimulation, the alanine mutant might be expected to cause a sustained increase in intracellular calcium compared with wild-type and the aspartic acid mutant.

Finally, although phosphorylation at residue 887 of PLC$\beta_1$ by PKC$\alpha$ may occur, it might not be physiological relevant for control of the enzyme's activity at the plasma membrane. However, future studies to complete this chapter are underway and will be as follows.

First, since the mutants display a more cytosolic distribution than the wild-type protein, it would be important to do more rigorous characterization of their localization. Quantitative western blots of membrane and cytosolic fractions from HEK293 cells

overexpressing the point mutants would lend to the confirmation of a cytosolic population. Also, by taking additional z-stacks, using the CFM-MEM membrane marker as a reference for the plasma membrane, we would be able to get a better handle of what percentage of the over-expressed protein is in the cytoplasm and compare it to the distribution of the wild-type. In addition, z-stacks taken before and after stimulation would help resolve whether or not the cytoplasmic point mutant population translocates to the plasma membrane upon stimulation. Although we do not see movement to or away from the plasma membrane for wild-type eYFP-PLC$\beta_1$, the point mutants may behave differently upon stimulation. Data up to this point, certainly suggests that eYFP-PLC$\beta_1$S887D has a very large cytosolic population – larger than that of eYFP-PLC$\beta_1$S887A and wild-type.

Second, we plan to carry out *in vivo* FRET single cell studies to look at the interaction between the point mutants and eCFP-G$\alpha_q$ in the stimulated state. Very preliminary data, from one experiment, demonstrated an increase in the FRET efficiency between eCFP-G$\alpha_q$ and eYFP-PLC$\beta_1$S887A upon stimulation (n=3). Although this initial result was very exciting, careful experiments need to be repeated many more times to confirm that we are truly observing an increase in the FRET efficiency. If the alanine mutant is not able to be phosphorylated, an increase in the FRET efficiency between it and eCFP-G$\alpha_q$ might suggest that it is no longer subject to negative regulation by PKC$\alpha$ after initiation of the signaling cascade.

Thirdly, we need to demonstrate that the over-expressed point mutants are coupled to functional receptors. To do this, we need to look at calcium release upon stimulation. Hopefully, in time, these experiments will start to work again in our

laboratory. It is still unclear and disturbing why the HEK293 cells would sometimes release calcium and sometimes not.

By performing the above experiments, we will be able to begin to better define the role of phosphorylation of residue 887 in the regulation of PLC$\beta_1$ and whether it is an important modification for localization and regulation of the enzyme at the plasma membrane.

## Literature Cited


1. Hug, H., and Sarre, T. F. (1993) *Biochem J* **291 (Pt 2)**, 329-343
2. Nishizuka, Y. (1995) *Faseb J* **9**(7), 484-496
3. Martelli, A. M., Evangelisti, C., Nyakern, M., and Manzoli, F. A. (2006) *Biochim Biophys Acta* **1761**(5-6), 542-551
4. Hubbard, K. B., and Hepler, J. R. (2006) *Cell Signal* **18**(2), 135-150
5. Wettschureck, N., and Offermanns, S. (2005) *Physiol Rev* **85**(4), 1159-1204
6. Rebecchi, M. J., and Pentyala, S. N. (2000) *Physiol Rev* **80**(4), 1291-1335
7. Ryu, S. H., Kim, U. H., Wahl, M. I., Brown, A. B., Carpenter, G., Huang, K. P., and Rhee, S. G. (1990) *J Biol Chem* **265**(29), 17941-17945
8. Martelli, A. M., Manzoli, L., and Cocco, L. (2004) *Pharmacol Ther* **101**(1), 47-64
9. Cocco, L., Martelli, A. M., Fiume, R., Faenza, I., Billi, A. M., and Manzoli, F. A. (2006) *Adv Enzyme Regul* **46**, 2-11
10. Xu, A., Wang, Y., Xu, L. Y., and Gilmour, R. S. (2001) *J Biol Chem* **276**(18), 14980-14986
11. Ali, H., Fisher, I., Haribabu, B., Richardson, R. M., and Snyderman, R. (1997) *J Biol Chem* **272**(18), 11706-11709
12. Yue, C., Ku, C. Y., Liu, M., Simon, M. I., and Sanborn, B. M. (2000) *J Biol Chem* **275**(39), 30220-30225
13. Yue, C., Dodge, K. L., Weber, G., and Sanborn, B. M. (1998) *J Biol Chem* **273**(29), 18023-18027
14. Filtz, T. M., Cunningham, M. L., Stanig, K. J., Paterson, A., and Harden, T. K. (1999) *Biochem J* **338 (Pt 2)**, 257-264
15. Dowal, L., Elliott, J., Popov, S., Wilkie, T. M., and Scarlata, S. (2001) *Biochemistry* **40**(2), 414-421
16. Dowal, L., Provitera, P., and Scarlata, S. (2006) *J Biol Chem* **281**(33), 23999-24014
17. Hughes, T. E., Zhang, H., Logothetis, D. E., and Berlot, C. H. (2001) *J Biol Chem* **276**(6), 4227-4235

18. Sambrook, J., Fritsch, E. F., and Maniatis, T. (1989) Molecular Cloning: A Laboratory Manual. In: Irwin, N. (ed). Cold Spring Harbor Press, Inc., Plainview, NY
19. Runnels, L. W., and Scarlata, S. F. (1998) *Biochemistry* **37**(44), 15563-15574
20. Xia, Z., and Yuechueng, L. (2001) *Biophys.J.* **81**, 2395-2402